LBNL-40915
UC-2000

ERNEST ORLANDO LAWRENCE
BERKELEY NATIONAL LABORATORY

Ground Penetrating Radar Results at the Box Canyon Site

1996 Survey as Part of Infiltration Test

John E. Peterson, Jr. and Kenneth H. Williams

Earth Sciences Division

August 1997

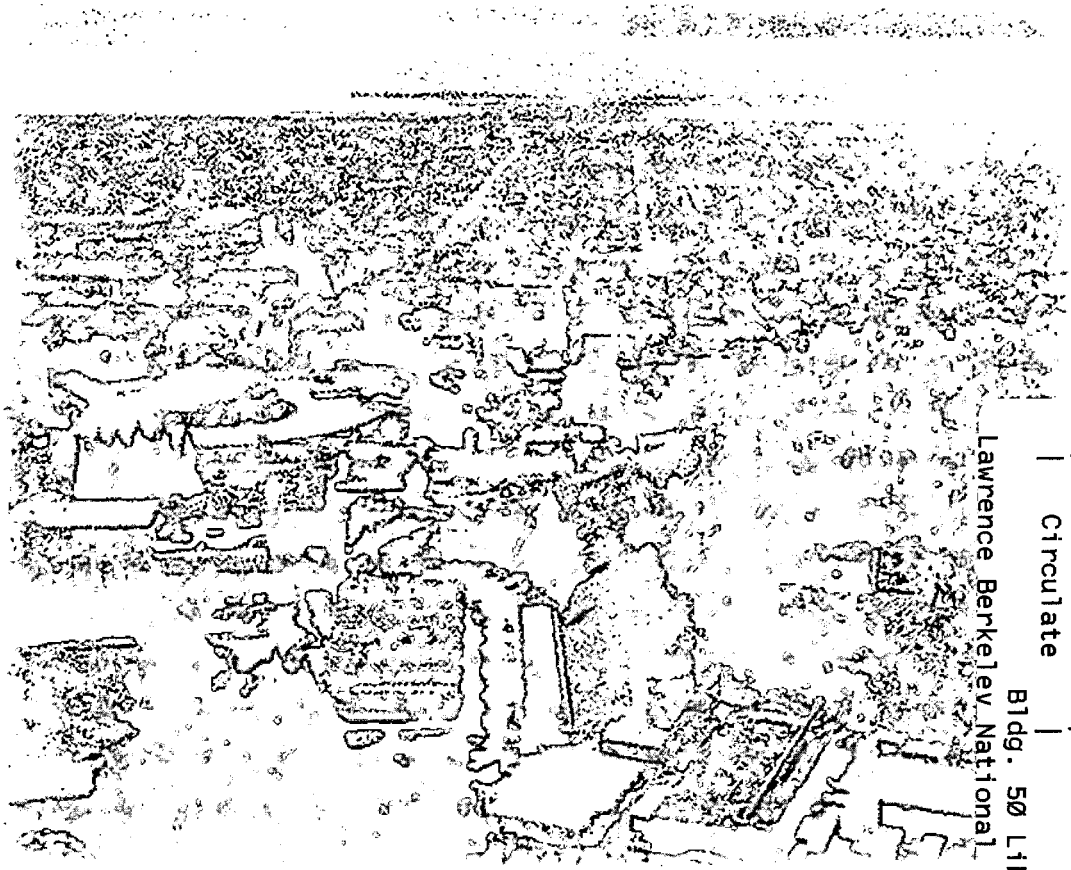

DISCLAIMER

LBNL-40915
UC-2000

GROUND PENETRATING RADAR RESULTS AT THE BOX CANYON SITE

1996 SURVEY AS PART OF INFILTRATION TEST

John E. Peterson, Jr. and Kenneth H. Williams
Earth Sciences Division
Ernest Orlando Lawrence Berkeley National Laboratory
Berkeley, CA 94720

August, 1997

This work was supported by the Assistant Secretary for Environmental Restoration and Waste Management, EM-50, Office of Technology Development, Characterization, Monitoring and Sensor Technology Program, of the US Department of Energy under Contract No. DE-AC03-76SF00098.

Introduction

This data report presents a discussion of the borehole radar tomography experiment conducted at Box Canyon, Idaho. Discussion concentrates on the survey methodology, data acquisition procedures, and the resulting tomographic images and interpretations.

The entire geophysics field effort for FY96 centered around the collection of the borehole radar data within the inclined boreholes R1, R2, R3 and R4 before, during, and after the ponded infiltration experiment. The well pairs R1-R2, R2-R4 and R3-R4 comprised the bulk of the field survey; however, additional data were collected between vertical boreholes within and around the infiltration basin. The intent of the inclined boreholes was to allow access beneath the infiltration basin and to enhance the ability of the radar method to image both vertical and horizontal features where flow may dominate. This data report will concentrate on the inclined borehole data and the resulting tomograms.

The borehole radar method is one in which modified ground penetrating radar antennas are lowered into boreholes and high frequency electromagnetic signals are transmitted through subsurface material to a receiving antenna. The transmitted signals may be represented as multiple raypaths crossing through the zone of interest. If sufficient raypaths are recorded, a tomographic image may be obtained through computer processing. The data normally recorded are signal amplitude versus time. The information extracted from such data includes the following: a) the transit time which depends on the wave velocity, b) the amplitude which depends on the wave attenuation, c) the dispersion which indicates a change in velocity and attenuation with frequency.

Instrumentation

All of the radar data collected at Box Canyon were acquired using the Sensors and Software pulseEKKO 100 ground penetrating radar system equipped with prototype 100 MHz center frequency borehole antennas. The bistatic design of the system (indicative of two separate antennas for transmitting and receiving) and the relativey low cost and flexibility led to its selection as the most desirable of the commercially available radar systems. A pulseEKKO system consists of six basic components; a pair of identical antennas, a transmitter electronics unit, a receiver electronics unit, a control console and a personal computer acting as a recording system and data storage unit.

The pulseEKKO 100 antennas are resistively damped dipolar antennas. The antenna radiation patterns are the pattern of a half wavelength dipole. Each antenna pair is designed to have a bandwidth to center frequency ratio of one. The borehole antennas used at Box Canyon have a center frequency of 100 MHz and therefore have usable energy over the frequency range 50 to 150 MHz.

The pulseEKKO system used at Box Canyon consisted of a 400V transmitter having a peak voltage of 400 volts with a rise time of 2.5 nanoseconds. The transmitter is powered by 12 volts and emits a pulse on command from the control console. The power actually radiated from the system is dependent on the subsurface conditions. The 400V transmitter used here delivers a peak power of 3.2 kilowatts into a 50 ohm load. Only a small fraction of the available power is actually transformed into radiated electromagnetic signals because the antennas are damped and are inefficient radiators.

The receiver electronics digitize the voltage at the receiver antenna connector to 16-bit resolution. The receiver design is such that it acquires the received waveform with very high fidelity. The receiver electronics typically clip the incoming voltage at a 50 mV level and the receiver noise level is nominally around 200 microvolts per stack. The present receiver resolution for a single bit after analog to digital conversion is 1.5

microvolts.

The control console provides the overall management of the transmitter and receiver operation. The control console is a microprocessor controlled unit which communicates with both the transmitter and receiver electronics and the external PC. The PC passes the system configuration information and the acquisition parameters to the control console which then manages all of the hardware functions of the radar system.

The operating principles are as follows: a) the user defines the time window, sampling interval and number of traces to be stacked via the PC user interface; b) the user selects the acquisition mode (here, transillumination); c) the PC configures the pulseEKKO console through the PC's standard RS232 port and the console takes over control of data acquisition; d) the pulseEKKO console commands the transmitter to fire; the transmitter generates a high voltage pulse which is shaped by the transmitting antenna into a radiated pulse; e) the console advises the receiver electronics to digitize the signal from the receiving antenna; the receiver digitizes the ambient electric field present at the receiving antenna after the band limiting characteristics of the antenna transfer function; the digital number representing the voltage at the time of acquisition is transferred to the control console; f) steps d) and e) are repeated until the desired waveform length and stack count are achieved; g) the console transmits the stacked waveform to the PC; h) the PC stores the data and displays the radar trace.

Acquisition

The borehole radar technique utilized at Box Canyon during the infiltration experiment was a crosshole radar profiling method in which the transmitter and receiver antennas were located in separate boreholes and data were collected with the antennas at various vertical offsets. The data collection at Box Canyon was performed using two acquisition modes. The first was a Zero Offset Profile (ZOP) in which the transmitter and receiver antennas were fixed such that there was no vertical offset. The second was a

Multiple Offset Profile (MOP) in which the receiving antenna remained at a fixed depth while the transmitter antenna was moved incrementally in the second borehole. A series of multiple offset profiles were used to acquire the raypaths necessary for tomographic processing.

Over the course of the infiltration experiment, the radar system was operated by using identical acquisition parameters for each of the three field surveys (before, during, and after filling the infiltration basin). The parameter values used were: a) Pulser Voltage - 400V; b) Antenna Frequency - 100 MHz; c) Sampling Interval - 800 picoseconds; d) Number of Stacks - 64; e) Shot Spacing - 0.25 meters.

All data are stored as acquired. No adjustments, filters or gains are recorded in the stored gathers. All subsequent data display is thus derived from raw data with no user controlled parameters between the time of acquisition and the time of processing. This is important to note because it illustrates the manner in which user dependence is removed from the system operation. Data acquisition and hence data repeatability is the same regardless of who operates the system and when - so long as the antenna configuration is the same. Due to the nature of the experiment conducted at Box Canyon, data repeatability is tantamount to successful tomographic differencing and interpretation (see following processing discussion).

The most important information to be obtained from radar data is the travel times, which are inverted for the velocity structure between boreholes. It is vital to know the precise time when the transmitter fires (known as time-zero), in order to determine accurate travel times between the transmitter and receiver antennas. The procedure used to determine time-zero for the surveys at Box Canyon consisted of taking direct air wave measurements (the signal from transmitter antenna to receiver antenna in air) with the antennas held together in air and at the boreholes in air. Additional measurements were taken with the antennae at their respective well heads. Four recordings of each were taken as a consistency check. After the time-zero data were collected, the

antennas were immediately moved into the boreholes and a ZOP data set was collected. Following this procedure, the MOP datasets were then collected with the locations determined before the start of the survey. In the case of the Box Canyon surveys, the transmitter and receiver intervals were 0.25 meters. As in all MOP gathers, the receiver antenna remained at a fixed location (1m, 1.25m, 1.5m, etc.) while the transmitter antenna occupied each of its possible locations down the borehole (e.g., 0-19m at 0.25m spacing). In this manner, all MOP gathers were collected and sorted as receiver gathers with filenames corresponding to the well pair being surveyed and the fixed receiver location (e.g., MOP10400 - an MOP gather collected for well pair #1 at receiver location 4m below ground surface). In this manner, each of the necessary ray-paths is collected and recorded for the subsequent tomographic processing.

Data gathering

Each of the wells used in the primary survey, R1, R2, R3 and R4 (Figure 1), had acrylic casing, with an internal diameter of 10 cm. The stand up of the casing was 0.5m for well R1, well R2, and well R4, and 0.33m for R3. In addition, other wells were used for ZOP data. These are given in Appendix IV. The coordinates and average drill angles for all wells are given in Table 1.

In addition to the three primary well pairs (R2-R1, R2-R4, and R3-R4), the well pair R3-R1 was surveyed in the preliminary data gathering trip. The well pairs surveyed for ZOP data in this preliminary trip were also different than those surveyed in subsequent trips (see Appendix IV).

A baseline data set was acquired before the infiltration test was performed and will henceforth be called the PRE surveys. Unfortunately, the data were acquired immediately after the drilling of the boreholes and the acrylic casing and foam grout were not yet in place. Data were acquired across well pair R2-R4 on July 24, 1996, R1-R3 on July 25, 1996, R2-R1 on July 26, 1996, and R3-R4 on July 27, 1996. In addition several ZOP data sets were taken from various well pairs on July 27 and 28, 1996 (see

Appendix IV). The zero point for depth was taken at the top of each casing for this preliminary survey only. The length of stand up should by subtracted from each source and receiver z-position to be consistent with the next two surveys. The observer logs in Appendix I provide comments on the data gathering process.

Data were next acquired during the infiltration test, which began on Aug. 27, 1996. These data will be called the DURING surveys. Data were acquired across well pair R2-R1 on Sep. 4, 1996, R2-R4 on Sep. 4 and 5, 1996, and R3-R4 on Sep. 5 and 6, 1996. (See observer logs for which sweeps were done on each day). In addition, several ZOP data sets were acquired from various well pairs on Sep. 6, 1996 (see Appendix IV). The zero point for depth was taken at ground surface for this survey. The observer logs are given in Appendix II.

Data were finally acquired two weeks after the infiltration test termination which occurred on Sep. 9, 1996. These data will be called the POST surveys. Data were acquired across well pair R2-R1 on Sep. 24, 1996, R2-R4 on Sep. 25, 1996, and R3-R4 on Sep. 26, 1996. In addition, several ZOP data sets were acquired from various well pairs on Sep 26, 1996 (see Appendix IV). The zero point for depth was taken at ground surface for this survey. The observer logs are given in Appendix III.

Processing

The data is written to the pulseEkko system in SEG-2 format. Each file contains one sweep of data, i.e. signals corresponding to one receiver point and all sources (one MOP). The pulseEkko software provides a conversion routine which converts the SEG-2 format to SEG-Y or ASCII format. The SEG-Y format was used in most cases; however, at times the SEG-Y conversion routine drops a byte somewhere and then the conversion to ASCII format is necessary. The data can then be directly downloaded to any machine with an ethernet connection. The present data set was written first to a 3 1/2" floppy, then another PC was used to ftp the data over to a UNIX machine

(ccs.lbl.gov). The conversion to SEG-Y format produces output that is in IBM binary. Therefore, a program **ch_oyster** was written to covert this to IEEE format. When an ASCII file is output from the pulseEkko system, the program **ch_asc** is used to convert the data into SEG-Y format.

At this point, the data still does not have any coordinates or station numbers in the headers. Therefore, another program, **chh_radar**, must be used to add the source/receiver information to the header. This program enters the information into the header using the station numbers and increments as input and correlating these with an input station file. The individual SEG-Y files are then combined into a single SEG-Y file for each well pair using **combsgyn_rad**.

We now have a SEG-Y file for each well pair in each phase of the experiment (PRE, DURING, and POST) are individually read into the PROMAX seismic processing package where the travel times are picked and finally output. The travel times are picked at the first peak. The absolute time is necessary for the inversion, so time must be subtracted from the picked time to correspond to the first zero crossing. Also, the zero time, as determined from the corresponding ZOP, must be subtracted from the travel time. This is done using the program **addtim**.

Determining the zero time

The zero time is defined as that instant the source emits a signal. The determination of this time is essential for the inversion of travel times for velocity and the accuracy critical for differencing of times between data sets. The determination of the zero time proved far more difficult than we had anticipated. We had hoped that taking a measurement with the source and receiver antennae together before each surveyed well pair would give an adequate value for the zero time throughout that survey. It was not anticipated that the zero time would shift after some time, or when the battery was recharged, or for various other reasons. Therefore, a different methodology had to be found to determine the zero time accurately. The zero time, as measured with the

antennae together, was subtracted from the ZOP data to find the absolute time for this data. An equivalent ZOP profile was extracted from the MOP data set that could be compared to the ZOP profile acquired from the field. The zero time was subtracted from this psuedo-ZOP profile and if the travel times match, then this is taken to be the zero time. When the times were offset, the average offset time was calculated and the MOP zero times were corrected for this value. This proved to provide an accurate measure of zero time throughout the surveys.

Well pair R2-R1

The wells R2 and R1 are approximately 5.4 meters apart at the surface. R2 is drilled at an angle of 41 degrees due west and R1 drilled at an angle of 28 degrees due west (see Table 1). The two wells are therefore in the same plane, but deviate apart from each other with depth. Accurate coordinates must be calculated for each source and receiver point before any processing can begin. This is done using the deviation logs. Specifically, we use the easting (edev.dev), northing (ndev.dev) and total depth (total.depth) deviation files, which give the actual x,y,z coordinates at 0.1 foot intervals down each well. The source and receiver coordinates, which are at 0.25 meter intervals, must be determined by interpolating between these 0.1 foot intervals. Since wells R2 and R1 are virtually in an east-west plane, the x (easting) and z (depth) coordinates can be used as coordinates for the 2-D tomographic inversions.

Figure 2 shows a typical receiver gather for the R2-R1 well pair. The frequency content of a trace at near-zero offset (Figure 3a) shows the energy peaking at 80 to 100 MHz and a steep roll off for higher frequencies. The higher frequencies appear to be attenuated for larger offset traces (Figure 3b). The energy peaks at a little less than 80 MHz and drops rapidly for higher frequencies. The greater attenuation is due to the greater distances traveled by these ray paths and the source radiation pattern producing lower transmitted energy at these higher incident angles (Figure 4). The steep roll-off of energy at higher frequencies is not typical. The roll-off is usually not so steep, even

in highly resistive media.

The data from each of the three field surveys (PRE, DURING, and POST) were processed using the procedure outlined above. After the travel times are picked for both the MOP and ZOP data, the zero time is determined using the methodology outlined above. The ZOP and MOP travel times vs. distance down source/receiver wells are shown in Figure 5. Figure 5a shows the curves for the PRE data, Figure 5b for the DURING data, and Figure 5c for the POST data. The DURING and POST ZOP and MOP/ZOP travel times matched without any corrections. The PRE MOP/ZOP travel times had to be corrected by about 4 ns to match the ZOP travel times. Figure 5d plots the PRE, DURING and POST ZOP values taken from the MOP data. The PRE travel times are consistently faster the the DURING and POST travel times, providing rough evidence that the infiltration produced lower overall velocities.

Characteristics of the travel time picks can be observed by plotting time-distance data (Figure 6a), velocity-incidence angle data (Figure 6b), and time-depth data for each gather (Figure 6c). The bulk of the travel times form a fairly tight line; the tighter the line the more homogeneous the medium. The group of anomalous times at greater distances are due to raypaths sampling the rubble zone (which is at about 12 meters depth). The velocity-incidence angle data also form a fairly flat, tight line at a velocity of 0.85 (m/ns); flatter values usually indicate less anisotropic medium. The anomalous data at slightly lower velocities again are produced by raypaths travelling through the rubble zone. Note that the x-scale goes from -30 deg to 90 deg, with positive angle taken as degrees below the horizontal. The greater positive angular coverage is due to the geometry of the boreholes. The time-depth curves for each gather (Figure 6c) indicate the smoothness of the picks and would show any systematic station anomalies. The curves in this case are quite smooth, again indicating a somewhat homogeneous geology.

The velocity inversion was performed using the picked travel times from each R2-R1 survey (PRE, DURING, and POST). An Algebraic Reconstruction Technique (ART), as described in Peterson (1986), is used for the inversion. The program name is **art3**, and the damping parameter used is 0.02. A 20.0 x 20.0 meter field in the plane of wells R2 and R1 is divided into a grid of 80x80 pixels producing a pixel dimension of 0.25x0.25 meters, which corresponds to the station spacing (Figure 7). The number of raypaths for which an arrival time was picked ranged between 2500 and 2800 for each survey. This creates a dense coverage of the area between wells (Figure 7).

The inverted times produce the velocity fields for the PRE, DURING, and POST surveys shown in Figure 8. The tomograms are all similar, with only subtle differences observable. Each tomogram clearly shows a very thin (less than 0.5 meter) low velocity layer at about 6 meters depth and the rubble zone at about 10 meters. The thickness of the rubble zone is undetermined because there are no raypaths below the rubble zone in R2. One change in velocity that can be easily observed occurs at the surface where the velocities are slightly higher for the PRE tomogram. The differences can be highlighted by inverting the differenced travel times. The travel times for each source-receiver pair from different surveys are subtracted, producing three travel time difference data sets: DURING-PRE, POST-PRE, and POST-DURING. These can be inverted for slowness. (The original travel times are also inverted for slowness, but velocity, the inverse of slowness, is shown in the tomograms. However, the inverse of the difference slowness does not produce the difference velocity.) The results are shown in Figure 9. Note that an increase in slowness (red) corresponds to a decrease in velocity.

These difference tomograms highlight the significant changes that occurred in the system. The average absolute slowness value is about $10x10^{-9}$s/m, so a difference value of $0.1x10^{-9}$s/m is about a 1% change in slowness (or velocity). There are several areas where the velocity decreases by over 5% in the DURING-PRE and POST-PRE

tomograms (Figure 9a and b). A decrease in velocity, with all other variables remaining constant, is assumed due to an increase in saturation. A large decrease in velocity is seen near the surface extending from the R2 wellhead diagonally to R1. Two thin horizontal layers of decreased velocity occur at about 6 to 7 meters depth. Another thin zone intersects this zone in R2 and angles toward R1 at about a 30° angle, intersecting the rubble zone. A general decrease in velocity exists above 5 meters.

The POST-DURING difference tomogram (Figure 9c) indicates primarily velocity increases, which is what one would expect if a region were drying. Note that the slowness changes are much smaller here than in the POST-PRE and DURING-PRE difference tomograms. Above the horizontal low velocity zone at 6 meters depth (seen in the velocity tomograms) there is a general increase in velocity, except for the very near surface. Below this depth, there is generally no change, except for some anomalous spots in the rubble zone itself.

The difference tomograms are consistent with an increase in water content during the infiltration test, then a decrease in water content two weeks after the termination of infiltration. This decrease is only observed above the intermediate fracture zone at 6 meters depth, while the increases in velocity below this zone may be due to inversion anomalies.

Well pair R3-R4

The wells R3 and R4 are approximately 5.6 meters apart at the surface. Both R3 and R4 are drilled at an angle of 28 degrees due west (see Table 1). The two wells are therefore parallel and in the same east-west bearing plane, which is ~5 meters away, and parallel to, the plane formed by the R2-R1 well pair (Figure 1). The source (R3) and receiver (R4) station coordinates, which are at 0.25 meter intervals, are determined in the same manner as for the R2-R1 well pair.

Figure 10 shows a typical receiver gather for the R3-R4 well pair. The frequency content of a trace at near-zero offset (Figure 11) shows the spectral energy is consistent with that of the R2-R1 data. The spectral amplitude is higher, most likely due to the smaller distance between wells.

The data from each of the three field surveys (PRE, DURING, and POST) were processed using the same procedure as for the R2-R1 data. The ZOP and MOP travel times vs. the distance down borehole curves are shown in Figures 12a-c for use in determining an accurate zero time. Figure 12a show the curves for the PRE data, Figure 12b for the DURING data, and Figure 12c for the POST data. Note that the DURING MOP curve has a few glitches in it; one at approximately 2.0 meters and one at approximately 11.0 meters. These correspond to a change in batteries and a halting of acquisition until the next day, respectively. Only the first glitch was corrected for since there also seemed to be a slight drift in zero time so that the correcting the second glitch would not improve the fit to the ZOP curve (Figure 12d). Also note that the fit between the MOP and ZOP curve for each survey is poor at about 15.0 meters, above which the travel time is very slow, then suddenly decreases. An interface is assumed at this point which produces diffractions, making it difficult to pick a consistent travel time (Figure 13). Figure 12e plots the PRE, DURING and POST ZOP values taken from the MOP data. The PRE travel times are consistently faster the the DURING and POST travel times, providing rough evidence that the infiltration produced lower overall velocities.

The plots of the time-distance data (Figure 14a), velocity-incidence angle data (Figure 14b), and time-depth data for each gather (Figure 14c) show slightly different characteristics than the R2-R1 plots. The time-distance data are much more scattered than for the R2-R1 data. Most of the scatter is due to more rays passing through the rubble zone, since the boreholes are deeper than the R2-R1 well pair. This scatter is also seen in the velocity-incidence angle data. The time-depth curves for each gather (Figure

14c) indicate several deviations from a smooth structure, the greatest being below 15 meters where other data has indicated a high velocity contrast. Some gaps in the curves may indicate inaccuracies or glitches in the zero time or possible inaccurate anttenae locations.

Velocity inversions were performed using the picked travel times from each R3-R4 survey (PRE, DURING, and POST). The inversion parameters are the same as for the R2-R1 well pair; a 20.0 x 20.0 meter field in the plane of the wells R3 and R4 is divided into a grid of 80x80 pixels producing a pixel dimension of 0.25x0.25 meters. The number of raypaths for which an arrival time was picked was about 3500 for each survey creating a dense coverage of the area between wells (Figure 15).

The inverted times produce the velocity fields for the PRE, DURING, and POST surveys shown in Figure 16. The tomograms are all similar, with only subtle differences observable. Each clearly show a very thin low velocity layer (less than 0.5 meters, similar in thickness and location as the layer observed in the R2-R1 velocity field) centered at about 6 meters depth and the rubble zone at about 12 meters. The thickness of the rubble zone can be determined because there are raypaths below the rubble zone in both R3 and R4. There is also a second intermediate low velocity layer two meters below the low velocity layer at 6 meters depth. This layer appears to pinch out a few meters away from R4. One change in velocity that can be easily observed occurs at the surface where there are decreases in velocity from the surface to the top of the low velocity zone at 5 meters. Other differences include the area below the rubble zone below 15 meters. This corresponds to the zone in Figure 12 which shows large changes in travel time and diffracted radar energy (Figure 13). The difficulty in picking travel times suggests that the velocities in this region are less reliable.

The differences can be highlighted by inverting the differenced travel times. The travel times for each source-receiver pair from different surveys are subtracted, producing three travel time difference data sets: DURING-PRE, POST-PRE, and POST-DURING.

These can be inverted for slowness, as for the R2-R1 data set. The results are shown in Figure 17. Note that an increase in slowness (red) corresponds to an decrease in velocity.

These difference tomograms show that some changes occurred to the system. However, the zero times for this well pair are less accurate than for the R2-R1 well pair, creating many inversion artifacts which show up more strongly on the difference plots. There are several areas where the velocity decreases by almost 10% in the DURING-PRE and POST-PRE tomograms (Figure 17a and b). A decrease in velocity, with all other variables remaining constant, is assumed due to an increase in saturation. However these decreases are at the surface where the inversion and picks are less reliable, and near the rubble zone where the picks are much less reliable. Two thin horizontal decreases in velocity occur in the region of the intermediate fracture zones; one at 6.0 meters and one at 8.0 meters. The velocity appears to increase below this, in the region from 11 to 15 meters. The rubble zone (at 13 to 15 meters depth) also produces a decrease in velocity after infiltration.

The POST-DURING difference tomogram (Figure 17c) indicates primarily velocity increases, which is what one would expect if a region were drying. Note that the slowness changes are much smaller here than in the POST-PRE and DURING-PRE difference tomograms. Above 12 meters there almost no change in velocity, with a slight decrease below this level. There is a decrease in velocity in the zone above 4 meters near R4 as seen in the DURING-PRE and POST-PRE difference tomogram. There is also a slight velocity increase in the zone from 12 to 15 meters, as seen in the DURING-PRE and POST-PRE difference tomograms. The anomalies below 15 meters are most likely artifacts of the inaccurate picks due to the diffracted arrivals.

The R3-R4 results are consistent with the R2-R1 results, but appear to contain more inversion artifacts. The difference tomograms suggest an increase in water content during the infiltration test, then a decrease in water content two weeks after the termination

of infiltration. In the R3-R4 well pair this decrease is observed throughout the imaged region.

Well pair R2-R4

The wells R2 and R4 are approximately 4.8 meters apart at the surface. R2 is drilled at an angle of 41 degrees due west and R4 are drilled at an angle of 28 degrees due west (see Table 1). The two wells are not parallel and in fact are quite skewed out of plane. The source (R2) and receiver (R4) station coordinates, which are at 0.25 meter intervals, are determined in the same manner as for the R2-R1 well pair.

Figure 18 shows a typical receiver gather for the R2-R4 well pair. The frequency content of a trace at near-zero offset (Figure 19) shows the spectral energy is consistent with that of the R2-R1 and R3-R4 data. The spectral amplitude is similar to that of the R3-R4 data, most likely due to similar distance between wells.

The data from each of the three field surveys (PRE, DURING, and POST) were processed using the same procedure as for the R2-R1 data. The ZOP and MOP travel time vs. the distance down borehole curve are shown in Figures 20a-c for use in determining an accurate zero time. Figure 20a show the curves for the PRE data, Figure 20b for the DURING data, and Figure 20c for the POST data. In each case, the pair of curve do not match well, showing that either the zero times drifted significantly, or the anttenae did not occupy the same location between surveys. This indicates that the difference tomograms may not be very reliable. The low velocity rubble zone can be easily seen at about 15 meters. Figure 20d plots the PRE, DURING and POST ZOP values taken from the MOP data. The PRE travel times are consistently faster the the DURING and POST travel times, providing rough evidence that the infiltration produced lower overall velocities. However, there are many glitches, and other evidence shows that the zero times may not be reliable.

The plots of the time-distance data (Figure 21a), velocity-incidence angle data (Figure 21b), and time-depth data for each gather (Figure 21c) show slightly different characteristics than the plots for the other well pairs. The time-distance data and the velocity-incident angle data are much less scattered than for the R2-R1 data. The time-depth curves for each gather (Figure 21c) indicate several deviations from a smooth structure, the greatest being below 15 meters where other data has indicated a high velocity contrast.

The velocity inversion was performed using the picked travel times from each R2-R4 survey (PRE, DURING, and POST). The inversion technique used in this case is slightly different than that used for the other well pairs, because the wells are so skewed. In this case the inversion grid is not just 2-D, but extends in an east-west direction, parallel to the ground surface. A 5.0 x 20.0 meter field in a north-south vertical plane is divided into a grid of 20x80 pixels producing a pixel dimension of 0.25x0.25 meters. The number of raypaths for which an arrival time was picked ranged between 3300 and 3700 for each survey creating a dense coverage of the area between wells (Figure 22).

The inverted times produce the velocity fields for the PRE, DURING, and POST surveys shown in Figure 23. The tomograms are all similar, with only subtle differences observable. Each clearly show a very thin low velocity layer (less than 0.5 meters, similar in thickness and location as the layer observed in the R2-R1 velocity field) centered at about 6 meters depth and the rubble zone at about 12 meters. The thickness of the rubble zone can be determined because there are raypaths below the rubble zone in both R2 and R4. There is also a second intermediate low velocity layer two meters below the low velocity layer at a 6 meter depth. Both intermediate low velocity layers correspond to similar zones in the R2-R1 and R3-R4 tomograms. The second is at the same depth as the pinched out layer observed in the R3-R4 velocity tomogram, indicating that it is continuous between R2 and R4, pinches out toward R3 and R1.. The

surface shows a low velocity zone near R2 and a corresponding high velocity zone near R4. This pattern is indicative of slight errors in station location, probably in depth. There are many changes in velocity that can be readily observed, but their locations are scattered. The zero time analysis suggests that the velocities in some regions may be less reliable.

The differences can be highlighted by inverting the differenced travel times. The travel times for each source-receiver pair from different surveys are subtracted, producing three travel time difference data sets: DURING-PRE, POST-PRE, and POST-DURING. These can be inverted for slowness, as for the R2-R1 data set. The results are shown in Figure 24. Note that an increase in slowness (red) corresponds to an decrease in velocity. These difference tomograms show that some changes may have occurred to the system, but because of the zero time and/or station location inaccuracies the tomograms appear totally unreliable.

The R2-R4 velocity tomgrams are consistent with the R2-R1 and R3-R4 tomograms. However, the difference tomograms contain too many artifacts to be reliable.

Conclusions

The radar velocity tomograms taken before infiltration, during infiltration, and after infiltration, show significant differences. The absolute velocity values appear be consistent between all three well pairs, R2-R1, R3-R4, and R2-R4. Each show an extensive half-meter thick low velocity layer at six meters depth. Another thin low velocity zone at eight meters depth pinches out toward the east (wells R1 and R3). The rubble zone is easily identified at about 12 meters depth, but this depth is probably quite variable. A thin high velocity layer occurs beneath the rubble zone.

The differences in the PRE, DURING, and POST tomograms may be attributed to changes in saturation due to infiltration from the pond. The velocity changes in two of the well pairs studied, R2-R1 and R3-R4, are consistent with each other, but there

appears to be slightly different geology between the two well pairs. The changes include a decrease in velocity in the intermediate low velocity zone and a slight decrease in velocity above this zone. These results are consistent with increased water content propagating from the surface.

Acknowledgement

This work was supported by the Assistant Secretary for Environmental Restoration and Waste Management, EM-50, Office of Technology Development, Characterization, Monitoring and Sensor Technology Program, of the US Department of Energy under Contract No. DE-AC03-76SF00098.

References

Peterson, J. E., 1986. The application of algebraic reconstruction techniques to geophysical problems. Ph.D. Thesis, LBL-21498, 188 pp.

APPENDIX I

BOREHOLE RADAR OBSERVER SHEET

Date: 7/24/96 Location: Box Canyon Test Site

Operator: K. Williams, S. Casey Type of System: S and S (PE100)

Antenna Freq.: 50 (100) 200 Antenna Separation: _____

Start Position: _____ End Position: _____ Step Size: 0.25m

Zero Adjust: _____ _____ Sampling Interval: 800ps No. of Stacks: _____

Type of GPR survey (ZOP) MOP

RECEIVER

Borehole name: R4 Casing I.D.: 4" Type: uncased

Height of stand up: _____ Type of protective well casing: metal standpipe

Depth of hole: 19.75m (from top of standpipe) Start Position: 0m End Position: 19.25m

---

TRANSMITTER

Borehole name: R2 Casing I.D.: 4" Type: uncased

Height of stand up: _____ Type of protective well casing: metal standpipe

Depth of hole: 20m (from top standpipe) Start Position: 0m End Position: 19.25m

---

Distance between boreholes: 16'9" _____

Distance from RX box to TX borehole: _____

Distance from TX box to RX borehole: _____

Distance from RX box to TX box: _____

Name of File: ZOP1

COMMENTS:

BOREHOLE RADAR OBSERVER SHEET

Date: 7/24/96 Location: Box Canyon Test Site

Operator: KWilliams, SCesarz Type of System: PE100

Antenna Freq.: 50 (100) 200 Antenna Separation: N/A

Start Position: N/A End Position: N/A Step Size: 0.25 m

Zero Adjust: ____ ____ Sampling Interval: 800 ps No. of Stacks: 64

Type of GPR survey ZOP (MOP)

RECEIVER

Borehole name: R4 Casing I.D.: 4" Type: uncased

Height of stand up: 1'8.5" (0.52m) Type of protective well casing: metal standpipe

Depth of hole: 19.75m (top of standpipe) Start Position: 1m End Position: 19.25m

---

TRANSMITTER

Borehole name: R2 Casing I.D.: 4" Type: uncased

Height of stand up: 1'6" (0.46m) Type of protective well casing: metal standpipe

Depth of hole: 20m (top of standpipe) Start Position: 0m End Position: 19.5m

---

Distance between boreholes: 16'9"

Distance from RX box to TX borehole: 33'0"

Distance from TX box to RX borehole: 40'3"

Distance from RX box to TX box: 54'6"

Name of File: MOP10100 - MOP11925

COMMENTS:

MOP11000 : Changed Rx/Tx batteries

MOP11075 - MOP11125 : Noisy records (RF?) early in the record / several traces of noise

BOREHOLE RADAR OBSERVER SHEET

Date: 7/25/96 Location: Box Canyon Test Site

Operator: KWilliams SGosnay J.Grenick Type of System: PE100

Antenna Freq.: 50 (100) 200 Antenna Separation: 17'

Start Position: 0m End Position: 19.5m Step Size: 0.25

Zero Adjust: ____ ____ Sampling Interval: 800ps No. of Stacks: 64

Type of GPR survey (ZOP) MOP

RECEIVER

Borehole name: R1 Casing I.D.: 4" Type: uncased

Height of stand up: 1'5" Type of protective well casing: metal standpipe

Depth of hole: 20m Start Position: 0 End Position: 19.5

TRANSMITTER

Borehole name: R3 Casing I.D.: 4" Type: uncased

Height of stand up: 1'2" Type of protective well casing: metal standpipe

Depth of hole: 24m Start Position: 0 End Position: 19.5

Distance between boreholes: 17' (surface)

Distance from RX box to TX borehole: 35'2"

Distance from TX box to RX borehole: 26'6"

Distance from RX box to TX box: 44'7"

Name of File: ZOP2

COMMENTS:

BOREHOLE RADAR OBSERVER SHEET

Date: 7/25/96 Location: Box Canyon Test Site

Operator: KWilliams SCosway J. Breznick Type of System: PE100

Antenna Freq.: 50 (100) 200 Antenna Separation: N/A

Start Position: N/A End Position: N/A Step Size: 0.25

Zero Adjust: ____ ____ Sampling Interval: 800ps No. of Stacks: 64

Type of GPR survey ZOP (MOP)

RECEIVER

Borehole name: R1 Casing I.D.: 4" Type: uncased

Height of stand up: 1'5" (0.50m) Type of protective well casing: metal standpipe

Depth of hole: 20m Start Position: 0 End Position: 19.5m

TRANSMITTER

Borehole name: R3 Casing I.D.: 4" Type: uncased

Height of stand up: 1'2" (0.33m) Type of protective well casing: metal standpipe

Depth of hole: 24m Start Position: 0 End Position: 23.5m

Distance between boreholes: 17' (surface)

Distance from RX box to TX borehole: 35'2"

Distance from TX box to RX borehole: 26'6"

Distance from RX box to TX box: 44'7"

Name of File: MOP20100 - MOP21950

COMMENTS:

MOP21100 : changed Tx & Rx batteries

MOP21595-1675 ? : noted polarity change / phase reversal at approx. 16m depth
Question: does this correspond to source matching Rx position then moving past it? → appears to be no.

Note: between MOP21600 and 1950, receiver was mislocated ⇒ N/A!

BOREHOLE RADAR OBSERVER SHEET

Date: 7/26/96 Location: Box Canyon Test Site

Operator: L Williams J. Breard Type of System: PE100

Antenna Freq.: 50 (100) 200 Antenna Separation: _____

Start Position: 0 End Position: 19.5 m Step Size: 0.25

Zero Adjust: -250ns Sampling Interval: 800 ps No. of Stacks: 64

Type of GPR survey (ZOP) MOP

RECEIVER

Borehole name: R1 Casing I.D.: 4" Type: uncased

Height of stand up: 1'5" Type of protective well casing: _____

Depth of hole: 20m Start Position: 0 End Position: 19.5 m

TRANSMITTER

Borehole name: R2 Casing I.D.: 4" Type: uncased

Height of stand up: 1'6" Type of protective well casing: _____

Depth of hole: 20m Start Position: 0 End Position: 19.5

Distance between boreholes: _____

Distance from RX box to TX borehole: _____

Distance from TX box to RX borehole: _____

Distance from RX box to TX box: _____

Name of File: 2093

COMMENTS:

BOREHOLE RADAR OBSERVER SHEET

Date: 7/26/96 Location: Box Canyon Test Site

Operator: KWilliams & Breymith Type of System: PE100

Antenna Freq.: 50 (100) 200 Antenna Separation: N/A

Start Position: N/A End Position: N/A Step Size: 0.25

Zero Adjust: -250ns Sampling Interval: 800ps No. of Stacks: 64

Type of GPR survey ZOP (MOP)

RECEIVER

Borehole name: R1 Casing I.D.: 4" Type: uncased

Height of stand up: 1'6" (.5m) Type of protective well casing:

Depth of hole: 20m Start Position: 1m End Position: 19.5m

TRANSMITTER

Borehole name: R2 Casing I.D.: 4" Type: uncased

Height of stand up: 1'6" (.5m) Type of protective well casing:

Depth of hole: 20m Start Position: 0 End Position: 19.5m

Distance between boreholes: 16'6"

Distance from RX box to TX borehole: 29'

Distance from TX box to RX borehole: 32'

Distance from RX box to TX box: 26'

Name of File: MOP30100 - MOP31950

COMMENTS: Note: Timezero position reset due to system collapse! Timezero adjusted to -250ns.

MOP31100: Rx and Tx batteries changed

BOREHOLE RADAR OBSERVER SHEET

Date: 7/27/96 Location: Box Canyon Test Site

Operator: KWilliams / J Breznick Type of System: PE100

Antenna Freq.: 50 (100) 200 Antenna Separation: N/A

Start Position: N/A End Position: N/A Step Size: 0.25m

Zero Adjust: -250ns Sampling Interval: 800ps No. of Stacks: 64

Type of GPR survey ZOP (MOP)

RECEIVER

Borehole name: R4 Casing I.D.: 4" Type: uncased

Height of stand up: 1'8.5" (0.52m) Type of protective well casing: metal standpipe

Depth of hole: 19.75 top of standpipe Start Position: @ 1m End Position: 19.25m

TRANSMITTER

Borehole name: R3 Casing I.D.: 4" Type: uncased

Height of stand up: 1'2" (0.33m) Type of protective well casing: metal standpipe

Depth of hole: 24m top of standpipe Start Position: 0m End Position: 23.5m

Distance between boreholes: 19'

Distance from RX box to TX borehole: 34'8"

Distance from TX box to RX borehole: 16'

Distance from RX box to TX box: 29'

Name of File: MOP40100 - MOP41925

COMMENTS: MOP40275 - obstruction @ approx 22 m bgs (no signal at this depth) mislocated thereafter by ~ 0.5m

*MOP0800 = MOP40800 (7/27/96)

BOREHOLE RADAR OBSERVER SHEET

Date: 7/27/96 Location: Box Canyon Test Site

Operator: KWilliams J. Breznick Type of System: PE100

Antenna Freq.: 50 (100) 200 Antenna Separation: 19'

Start Position: 0 End Position: 1925m Step Size: 0.25

Zero Adjust: -250ns Sampling Interval: 800PS No. of Stacks: 64

Type of GPR survey (ZOP) MOP

RECEIVER

Borehole name: R4 Casing I.D.: 4" Type: uncased

Height of stand up: 1'8.5" Type of protective well casing:

Depth of hole: 19.75m top of standpipe Start Position: 0 End Position: 19.25m

---

TRANSMITTER

Borehole name: R3 Casing I.D.: 4" Type: uncased

Height of stand up: 1'2" Type of protective well casing:

Depth of hole: 24m top of standpipe Start Position: 0 End Position: 19.25m

---

Distance between boreholes: 19'

Distance from RX box to TX borehole:

Distance from TX box to RX borehole:

Distance from RX box to TX box:

Name of File: ZOP4

COMMENTS:

APPENDIX II

BOREHOLE RADAR OBSERVER SHEET

Date: 9/5/96 Location: Box Canyon

Operator: K Williams Type of System: Sensors & Software PE100

Antenna Freq.: 50 (100) 200 Antenna Separation: N/A

Start Position: _____ End Position: _____ Step Size: 0.25 m

Zero Adjust: -290 ns Sampling Interval: 800ps No. of Stacks: 64

Type of GPR survey: (CMP / WARR) ZOP (MOP)

RECEIVER

Borehole name: R4 Casing I.D.: 5.7 cm Type: acrylic

Height of stand up: 0 m Type of protective well casing: _____

Depth of hole: 19.5 m Start Position: 1 End Position: 19 m

TRANSMITTER

Borehole name: R3 Casing I.D.: 5.7 cm Type: acrylic

Height of stand up: 0.50 m Type of protective well casing: _____

Depth of hole: 23.25 m Start Position: 0 End Position: 22.75 m

---

Distance between boreholes: 5.9 m @ surface

Distance from RX box to TX borehole: _____

Distance from TX box to RX borehole: _____

Distance from RX box to TX box: _____

Name of File: MOP30100 - MOP31900
ZOP3

COMMENTS: MOP30100 - MOP31075 → 9/5/96
MOP31075 - MOP31900 → 9/6/96
Battery changed after MOP30150

132
22.75
4
91.00 + 1 = 92 MOP
+ 8 = 100 ZOP

BOREHOLE RADAR OBSERVER SHEET

Date: 9/4/96 Location: Box Canyon

Operator: K Williams Type of System: Sensor & Software PE100

Antenna Freq.: 50 (100) 200 Antenna Separation: N/A

Start Position: ____ End Position: ____ Step Size: 0.25m

Zero Adjust: -360 ns Sampling Interval: 800ps No. of Stacks: 64

Type of GPR survey: (CMP / WARR) ZOP (MOP)

RECEIVER

Borehole name: R4 Casing I.D.: 5.7cm Type: acrylic

Height of stand up: 0 m Type of protective well casing: ____

Depth of hole: 19.5m Start Position: 1 End Position: 19 m
from ground

TRANSMITTER

Borehole name: R2 Casing I.D.: 5.7cm Type: acrylic

Height of stand up: 0.75m Type of protective well casing: ____

Depth of hole: 19.5 Start Position: 0 End Position: 19m
from ground

Distance between boreholes: 5.0m @ surface

Distance from RX box to TX borehole: ____

Distance from TX box to RX borehole: ____

Distance from RX box to TX box: ____

Name of File: MOP20100 - MOP21850
ZOP2 (Rx: 0 - 19.0m Tx: 0 - 19m) → Note: Start position not -2 as usual but 0 ∴ can reset in edit.

COMMENTS:

ZOP2
MOP20100 - MOP20675 → 9/4/96

MOP20700 - MOP21900 → 9/5/96

BOREHOLE RADAR OBSERVER SHEET

Date: 9/4/96 Location: Box Canyon

Operator: K Williams Type of System: Sensors & Software PE100

Antenna Freq.: 50 (100) 200 Antenna Separation: N/A

Start Position: _____ End Position: _____ Step Size: 0.25

Zero Adjust: -360 ns Sampling Interval: 800ps No. of Stacks: 64

Type of GPR survey: (CMP / WARR) ZOP (MOP)

RECEIVER

Borehole name: R1 Casing I.D.: 5.7 cm Type: acrylic

Height of stand up: 0.5m Type of protective well casing: acrylic

Depth of hole: 18.0 m from ground Start Position: 1 m End Position: 17.5 m

---

TRANSMITTER

Borehole name: R2 Casing I.D.: 5.7 cm Type: _____

Height of stand up: 0.75m Type of protective well casing: _____

Depth of hole: 19.5 m from ground Start Position: 0 m ground surface End Position: 19 m

Distance between boreholes: 5.1m @ surface

Distance from RX box to TX borehole: _____

Distance from TX box to RX borehole: _____

Distance from RX box to TX box: _____

Name of File: MOP10100 - MOP11750

ZOP1 (Rx: 0-17.5m Tx: 0-19m)

COMMENTS:

Rx Tx Batteries changed @ MOP11425

BOREHOLE RADAR OBSERVER SHEET

Date: 9/26/96 Location: Box Canyon

Operator: K Williams, A Pearson Type of System: Sensors & Software PE100

Antenna Freq.: 50 (100) 200 Antenna Separation: N/A

Start Position: _____ End Position: _____ Step Size: 0.25 m

Zero Adjust: _____ _____ Sampling Interval: 800ps No. of Stacks: 64

Type of GPR survey: (CMP / WARR) ZOP (MOP)

RECEIVER

Borehole name: R4 Casing I.D.: 5.7 cm Type: acrylic

Height of stand up: 0m Type of protective well casing: " "

Depth of hole: 19.5 m (from ground) Start Position: 1m End Position: 19 m

---

TRANSMITTER

Borehole name: R3 Casing I.D.: 5.7cm Type: acrylic

Height of stand up: 0.5m Type of protective well casing: " "

Depth of hole: 23.25 Start Position: 0 End Position: 22.75m

Distance between boreholes: 5.8 m @ surface

Distance from RX box to TX borehole: _____

Distance from TX box to RX borehole: _____

Distance from RX box to TX box: _____

Name of File: MOP3 0 100 - ~~ZOP3 0 100~~ MOP3 1900
ZOP3

COMMENTS:

BOREHOLE RADAR OBSERVER SHEET

Date: 9-25-96 Location: Box Canyon

Operator: K Williams, A Pearson Type of System: Sensors & Software PE100

Antenna Freq.: 50 (100) 200 Antenna Separation: N/A

Start Position: _____ End Position: _____ Step Size: 0.25m

Zero Adjust: ~280ns Sampling Interval: 800ps No. of Stacks: 64

Type of GPR survey: (CMP / WARR) ZOP (MOP)

RECEIVER

Borehole name: R4 Casing I.D.: 5.7cm Type: acrylic

Height of stand up: 0 m Type of protective well casing: " "

Depth of hole: 19.5m Start Position: 1m End Position: 19m
from ground surface

TRANSMITTER

Borehole name: R2 Casing I.D.: 5.7cm Type: acrylic

Height of stand up: 0.75m Type of protective well casing: " "

Depth of hole: 19.5m Start Position: 0 m End Position: 19 m
from ground (surface)

Distance between boreholes: 5.0 m @ surface

Distance from RX box to TX borehole: _____

Distance from TX box to RX borehole: _____

Distance from RX box to TX box: _____

Name of File: MOP20100 - MOP21900
ZOP2 (Rx, Tx : 0 - 19m)

COMMENTS:

BOREHOLE RADAR OBSERVER SHEET

Date: 9-24-96 Location: Box Canyon

Operator: JC Williams A Pearson Type of System: Sensors & Software PE100

Antenna Freq.: 50 (100) 200 Antenna Separation: N/A

Start Position: _____ End Position: _____ Step Size: 0.25

Zero Adjust: -280 ns Sampling Interval: 800ps No. of Stacks: 64

Type of GPR survey: (CMP / WARR) ZOP (MOP)

RECEIVER

Borehole name: R1 Casing I.D.: 5.7 cm Type: acrylic

Height of stand up: 0.5 m Type of protective well casing: _____

Depth of hole: 18.0m from ground Start Position: 1 m End Position: 17.5m

---

TRANSMITTER

Borehole name: R2 Casing I.D.: 5.7cm Type: _____

Height of stand up: 0.75 m Type of protective well casing: _____

Depth of hole: 19.5 m from ground Start Position: 0m ground surface End Position: 19 m

---

Distance between boreholes: 5.1 m @ surface

Distance from RX box to TX borehole: _____

Distance from TX box to RX borehole: _____

Distance from RX box to TX box: _____

Name of File: MOP10100 - MOP11750

ZOP1 (Tx: 0 - 19 m Rx: 0 - 17.5m)

COMMENTS:

BOREHOLE RADAR OBSERVER SHEET

Date: 7/28/96 Location: Box Canyon Test Site

Operator: K. Williams, T. Breznick Type of System: PE100

Antenna Freq.: 50 (100) 200 Antenna Separation: ____

Start Position: ____ End Position: ____ Step Size: 0.25

Zero Adjust: -250 ns Sampling Interval: 800 ps No. of Stacks: 64

Type of GPR survey (ZOP) MOP

RECEIVER

Borehole name: R4 / R2 Casing I.D.: 4" Type: uncased

Height of stand up: 1'8.5" / 1'6" Type of protective well casing: ____

Depth of hole: 18.75m / 20m Start Position: 0m / 0m End Position: 19.25m / 19.5m

---

TRANSMITTER

Borehole name: II-3 Casing I.D.: 5 7/8" Type: uncased

Height of stand up: 0.25m Type of protective well casing: metal standpipe

Depth of hole: 17.75 Start Position: 0m End Position: 17.25m

Distance between boreholes: ____

Distance from RX box to TX borehole: ____

Distance from TX box to RX borehole: ____

Distance from RX box to TX box: ____

Name of File: ZOP11 - ZOP12
(R4) (R2)

COMMENTS: ZOP11-12 are between R2/R4 and II-3

BOREHOLE RADAR OBSERVER SHEET

Date: 7/28/96 Location: Box Canyon Test Site

Operator: K. Williams, T. Brennick Type of System: PE100

Antenna Freq.: 50 (100) 200 Antenna Separation: _____

Start Position: 0 End Position: _____ Step Size: 0.25

Zero Adjust: -250ns Sampling Interval: 800 ps No. of Stacks: 64

Type of GPR survey (ZOP) MOP

RECEIVER

Borehole name: _____ Casing I.D.: 4" Type: uncased

Height of stand up: _____ Type of protective well casing: metal standpipe

Depth of hole: _____ Start Position: 0 m End Position: _____

TRANSMITTER

Borehole name: _____ Casing I.D.: 4" Type: uncased

Height of stand up: _____ Type of protective well casing: metal standpipe

Depth of hole: _____ Start Position: 0 m End Position: _____

Distance between boreholes: _____

Distance from RX box to TX borehole: _____

Distance from TX box to RX borehole: _____

Distance from RX box to TX box: _____

Name of File: ZOP5 - ZOP10
ZOP13-14. (Core hole)

Note: ZOP10 → delete last 4 traces

COMMENTS: all ZOP5-10 are between "T" holes

"5"	"7"	"6"	"10"	"9"	"8"
(Tx) (Rx)	(Rx) (Tx)	(Rx) (Tx)	(Rx) (Tx)	(Tx) (Rx)	(Tx) (Rx)
T1-T2	T3-T4	T2-T4	T1-T4	T2-T3	T1-T3
6.75m 7m	7m 7m	7m 7m	6.75m 7m	7m 7m	6.75m 7m
pth:					
? :					
tions:					
End: 0-6.25	0-6.5m	0-6.5m	0-6.25m	0-6.5m	0-6.25m

Box

ZOP

T1/T2	ZOP5	(7/27/96)
T4/T2	ZOP6	(7/27/96)
T4/T3	ZOP7	(7/27/96)
T1/T3	ZOP8	(7/27/96)
T2/T3	ZOP9	(7/27/96)
T4/T1	ZOP10	(7/27/96)
11-3/R4	ZOP 11	(7/27/96)
11-3/R2	ZOP12	(7/27/96)
T1/T2	ZOP13	(7/27/96) * 0.125 m step
T4/T3	ZOP 14	(7/27/96) * 0.125 m step.

BOX 2 & BOX 3

ZOP Shallows 0.125m spacing

(Tx) (Rx)
II-6 → T-8a TD (antenna) 5.875 → 0m

moving from bottom up.

∴ 48 traces

ZOP4

10.4m well separation

time zero adjust = -290 ns

(Tx) (Rx)
I-4 → T-8a

moving from top down

ZOP5

48 traces 5.875 m bgs

9m separation

(Tx)
II-4 → T-8a

moving from top down

ZOP6

48 traces

8.9m separation

(Tx) (Rx)
T-1 → T-8a

ZOP7

48 traces moving down hole

2.9 m separation

(Tx) (Rx)
II-3 → T-8a

ZOP8

48 traces moving down hole

4.45 m separation

(Tx) (Rx)
T-10 T-8a

ZOP9

23 traces moving down

2.7 m

(Tx)
II-1 → T-8a

48 traces 5.6 m separation

ZOP10

BOREHOLE PARAMETERS				
WELL	EASTING	NORTHING	ELEVATION	ANGLE
R-1	72.79	62.84	1.91	28.0
R-2	67.36	63.04	1.62	41.0
R-3	71.8	67.89	1.94	27.0
R-4	66.16	67.6	1.66	30.0

Table 1. Radar well parameters. All distances are in meters; angle is in degrees from vertical.

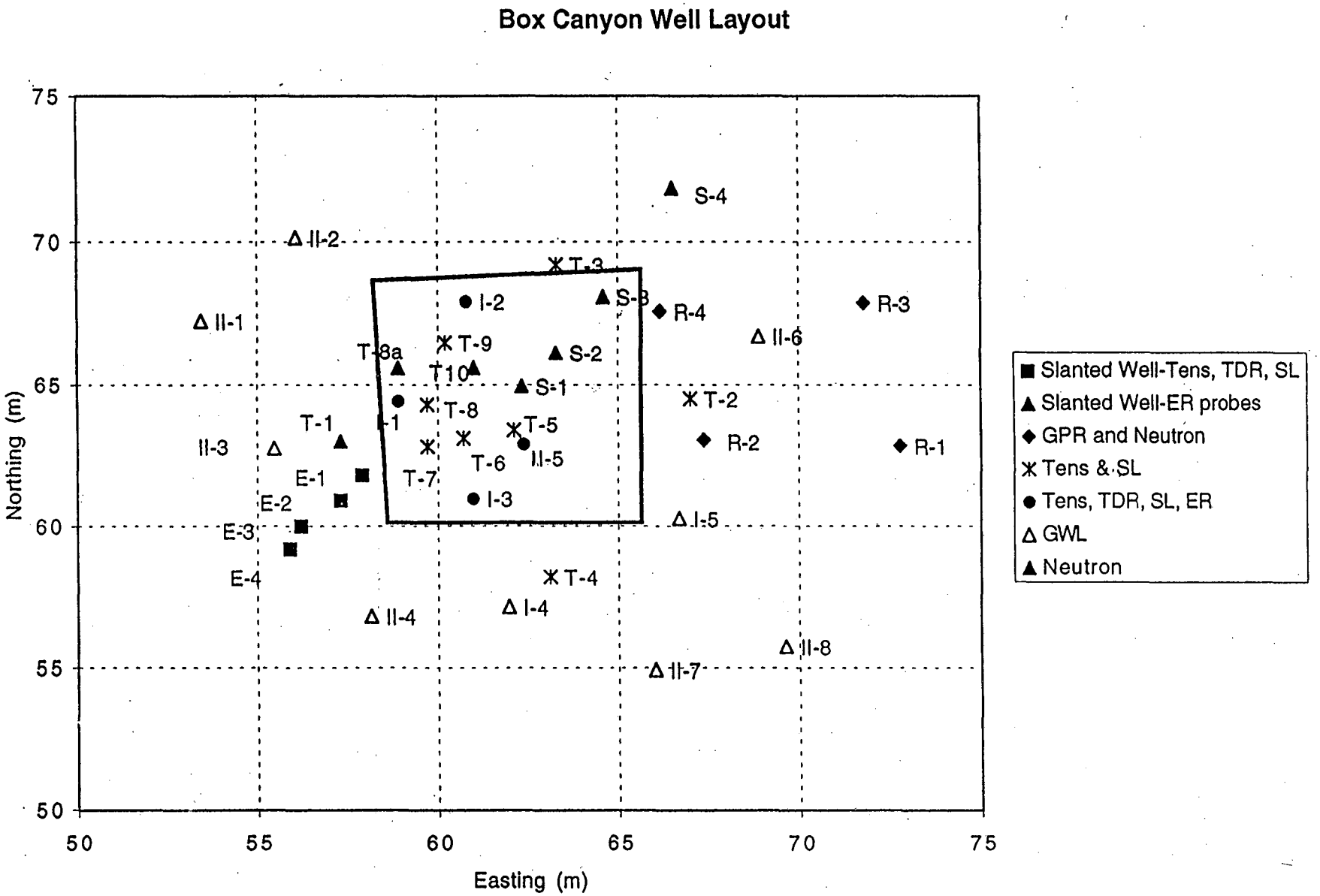

Figure 1. Layout of the wells at the Box Canyon site with approximate pond boundary given as the solid line. The radar wells are R-1, R-2, R-3, and R-4.

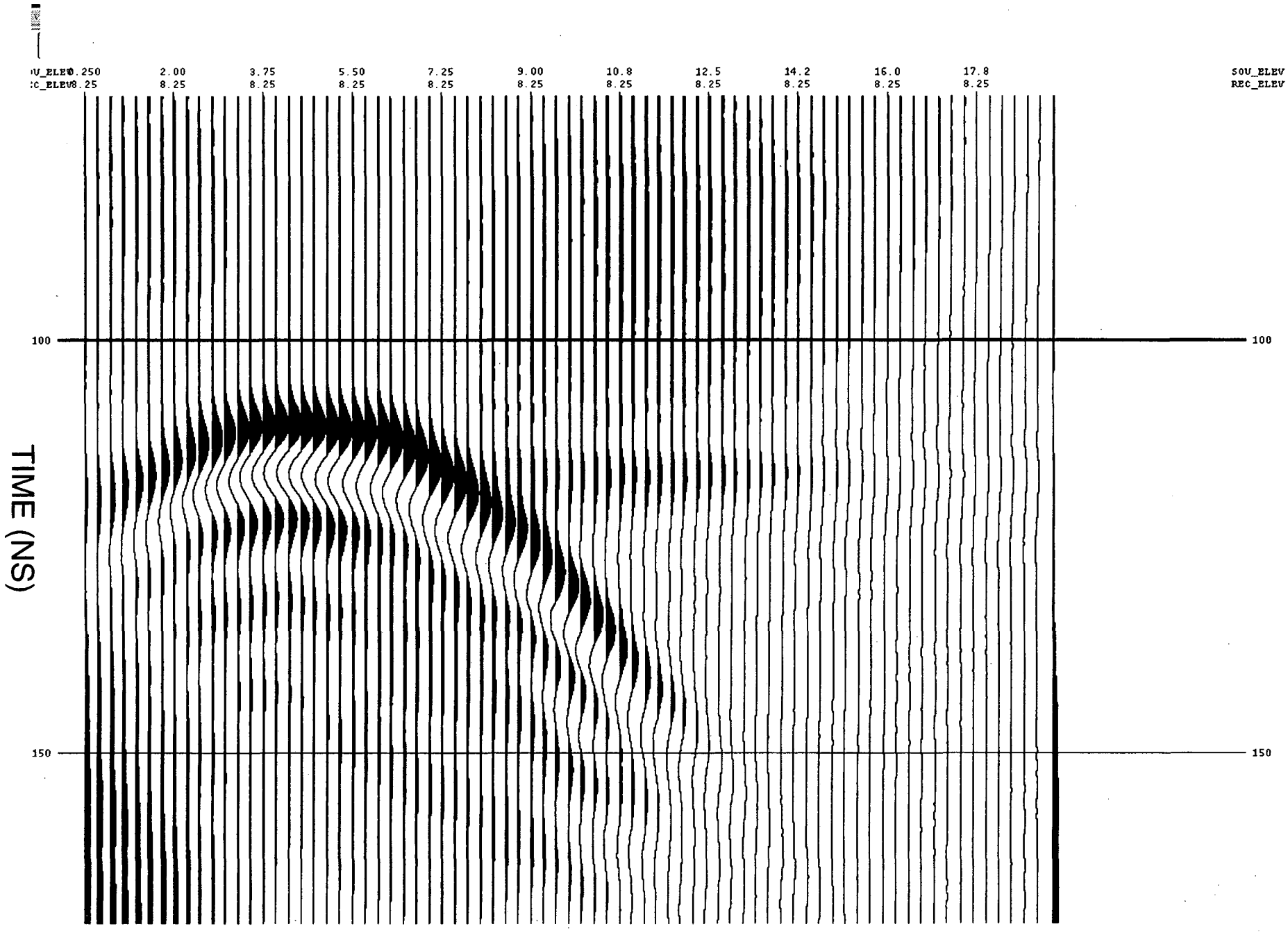

Figure 2. Typical receiver gather for R2-R1 with the receiver held at 8.25 meters down R-1

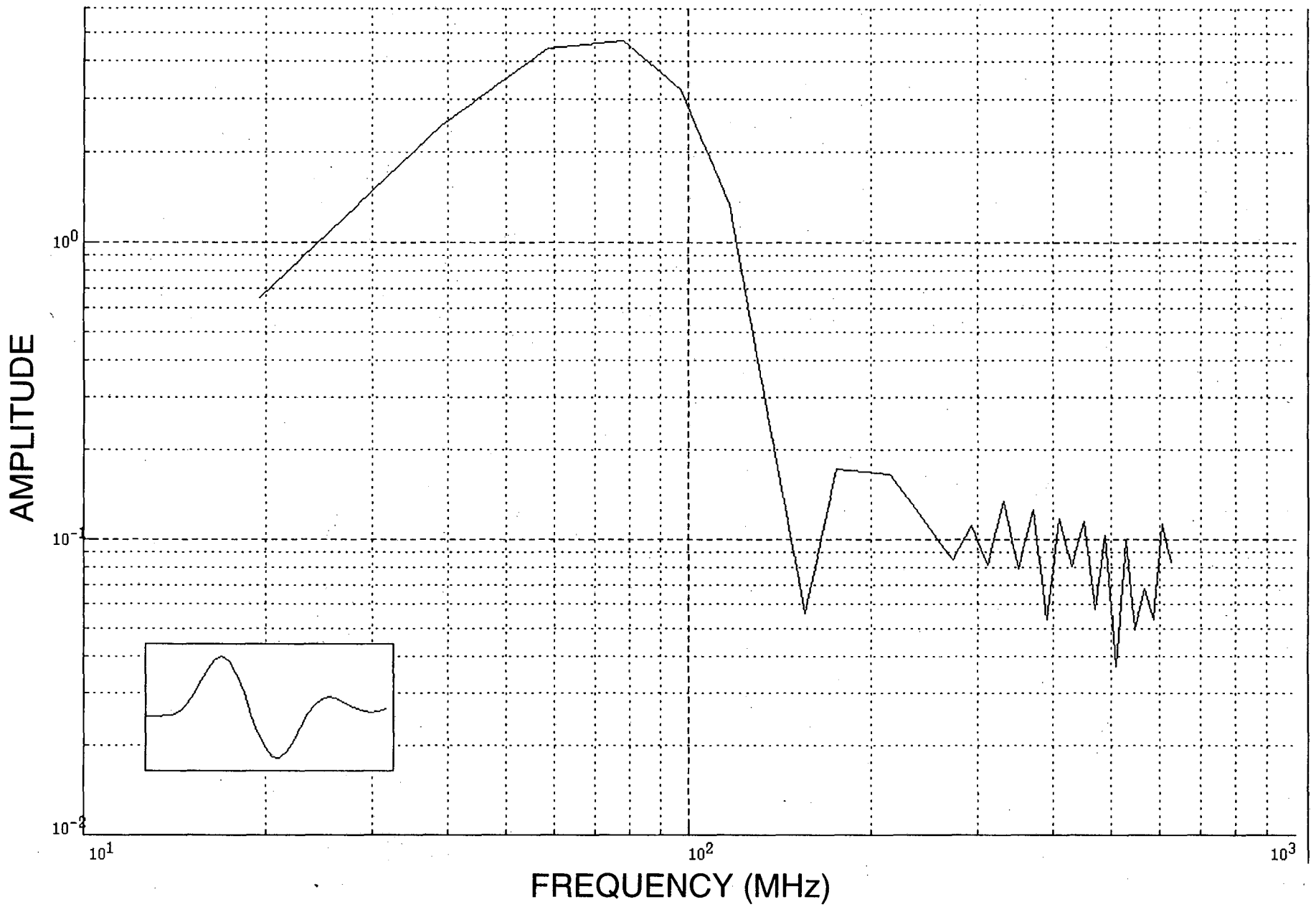

Figure 3a. Spectra for a trace at near zero offset (Receiver at 10 meters down R-1).

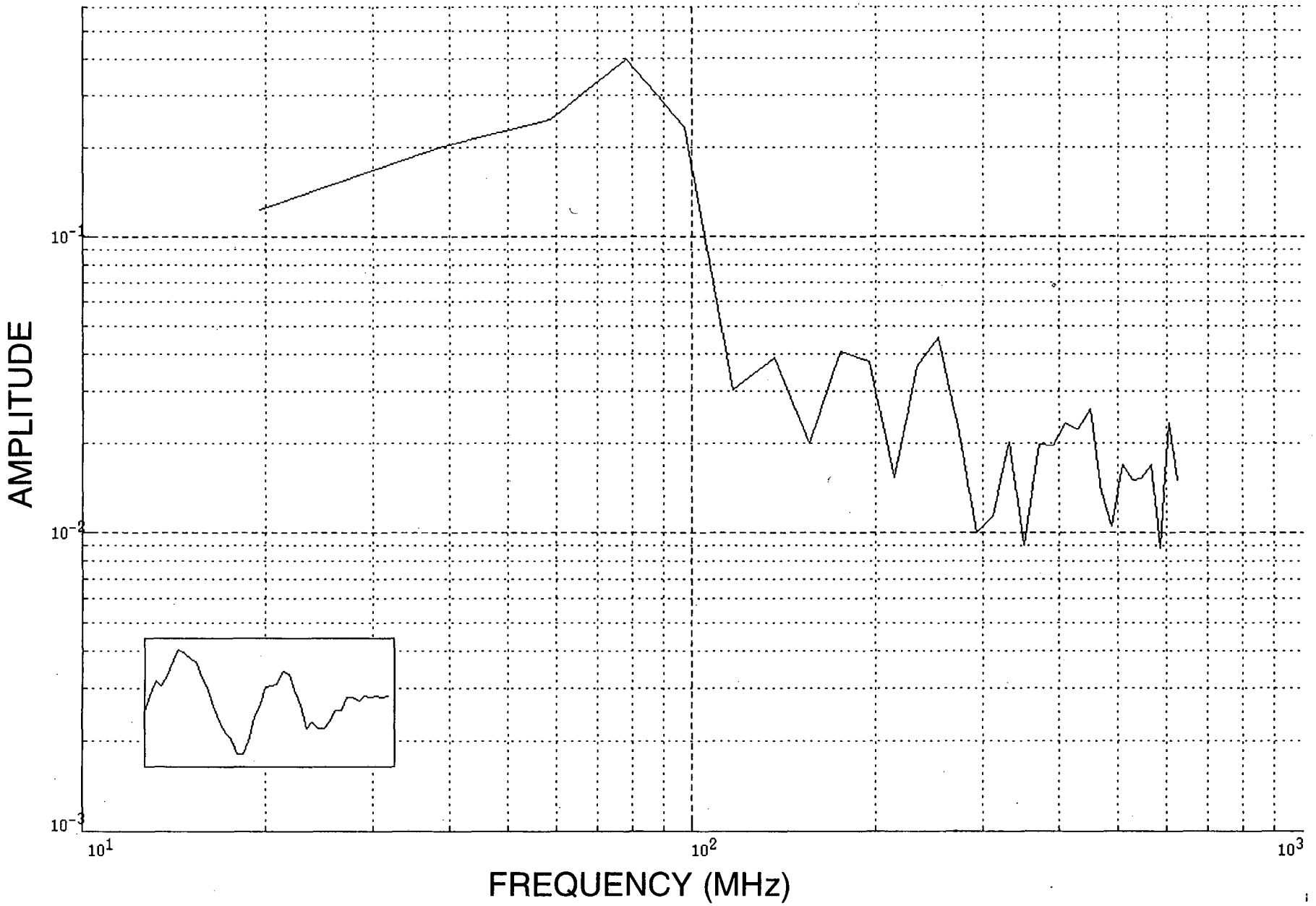

Figure 3b. Spectra for a trace at a large offset source-receiver pair (receiver 10 meters down R-1).

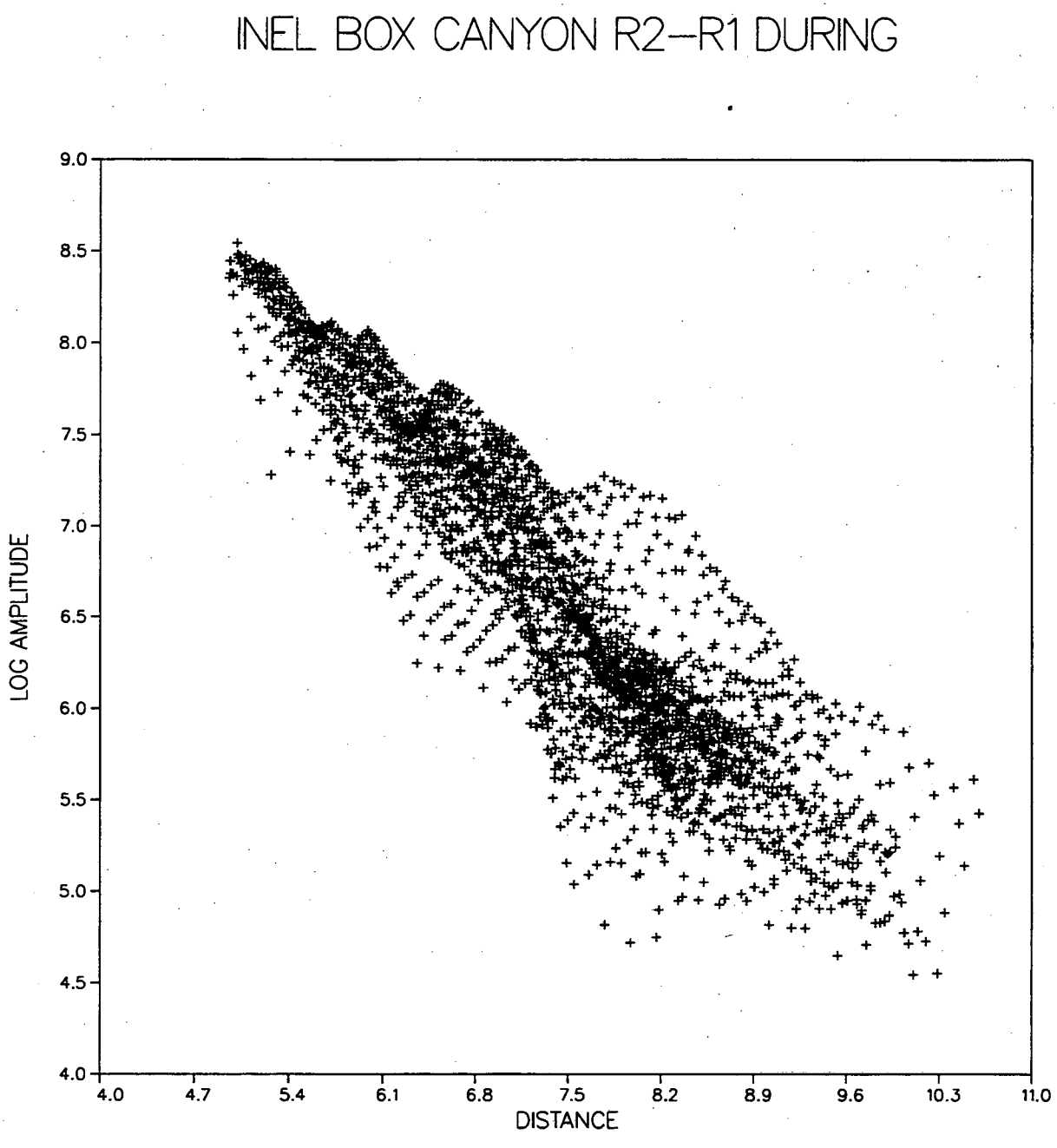

Figure 4. Distance versus log amplitude plot showing logrithmic loss of energy over distance.

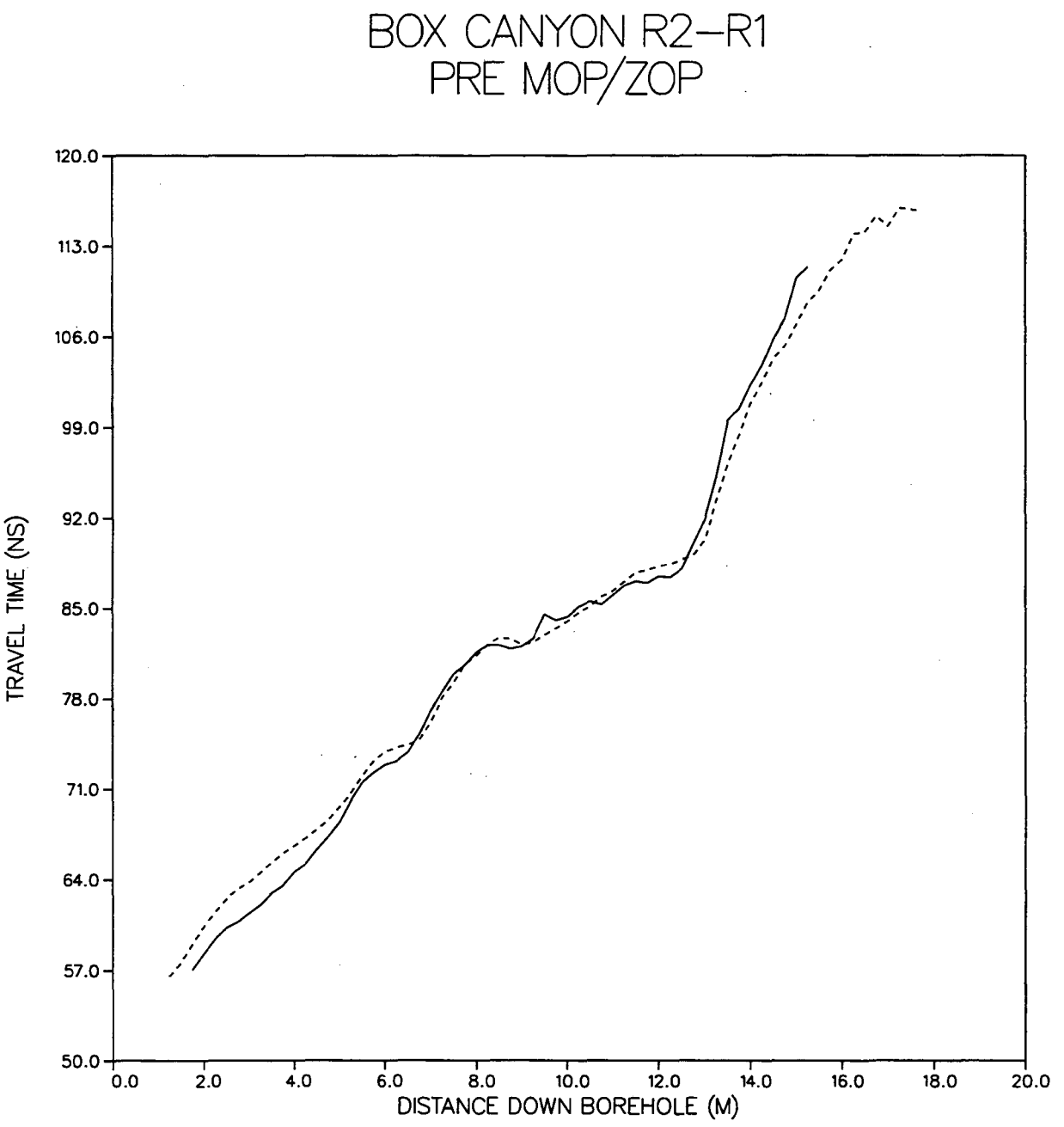

Figure 5a. Travel time vs. distance down source/receiver wells for the PRE data set. The solid line is the MOP values; dashed is ZOP values.

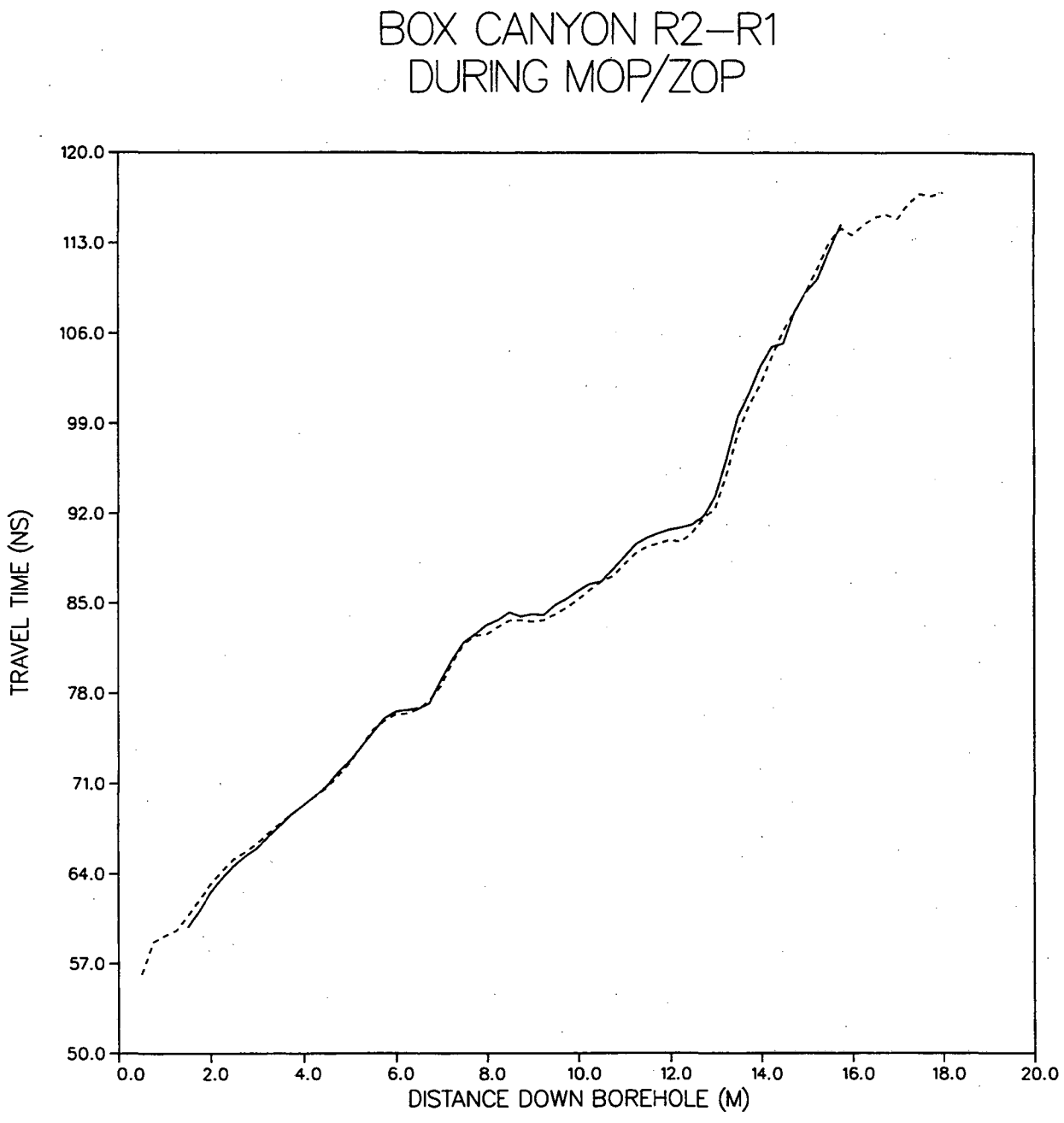

Figure 5b. Same as Figure 5a, but for the DURING values.

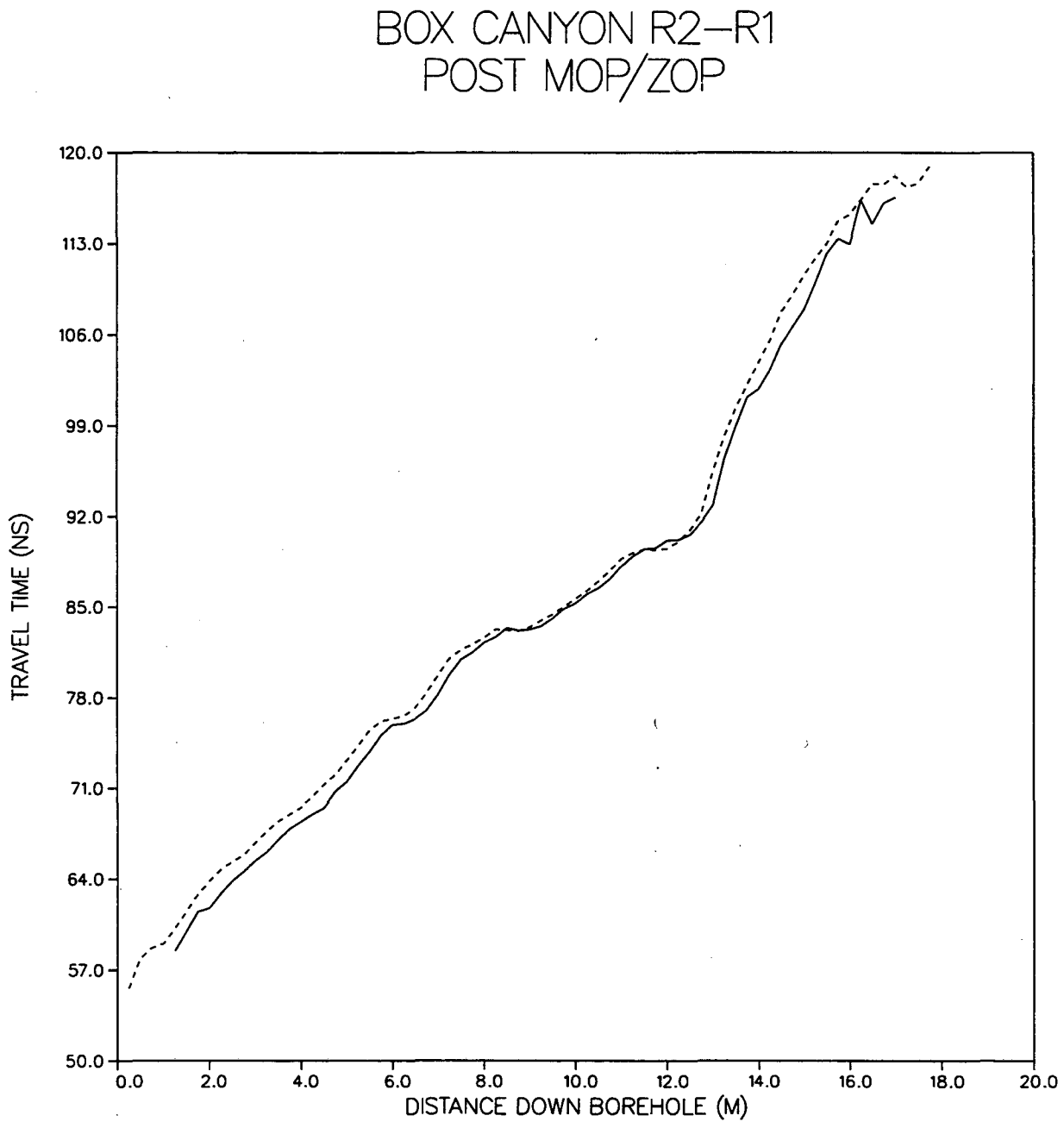

Figure 5c. Same as Figure 5a, but for the POST values.

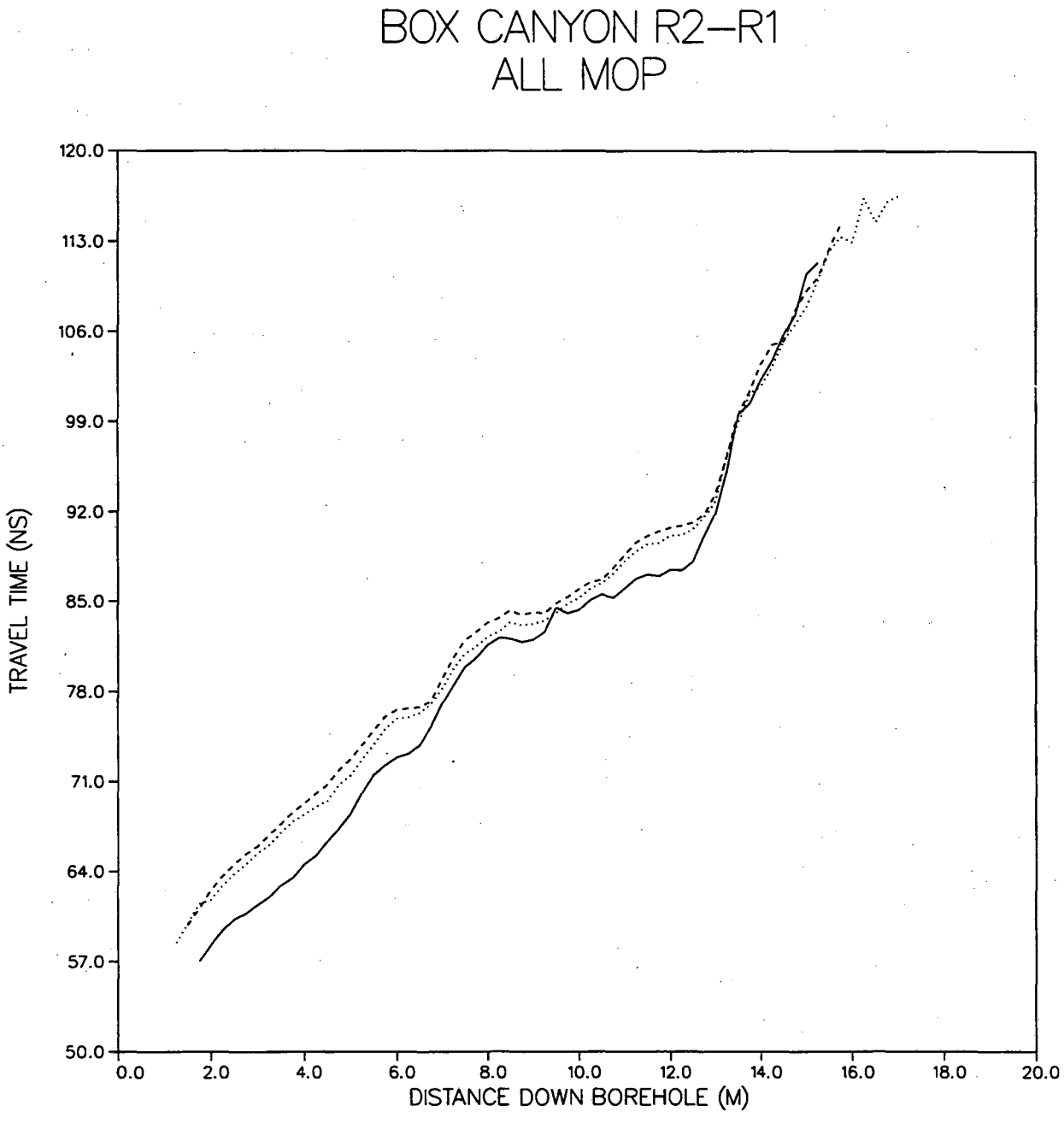

Figure 5d. Travel time vs. distance down source/receiver wells for the MOP values for the PRE (solid), DURING (dashed), and POST (dotted) data sets.

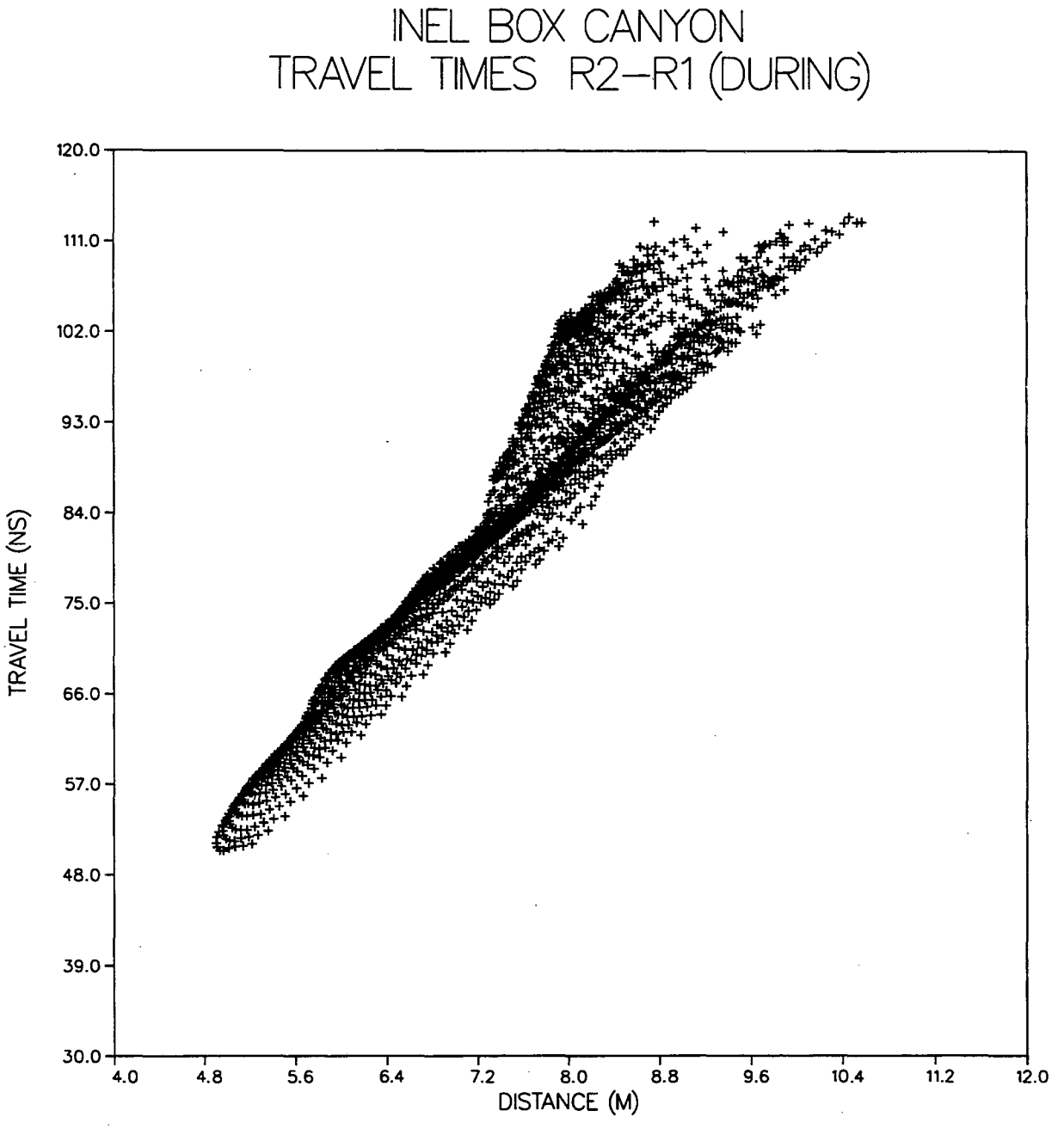

Figure 6a.Travel time versus distance values for the DURING data set. The difference in travel time values between data sets is relatively small.

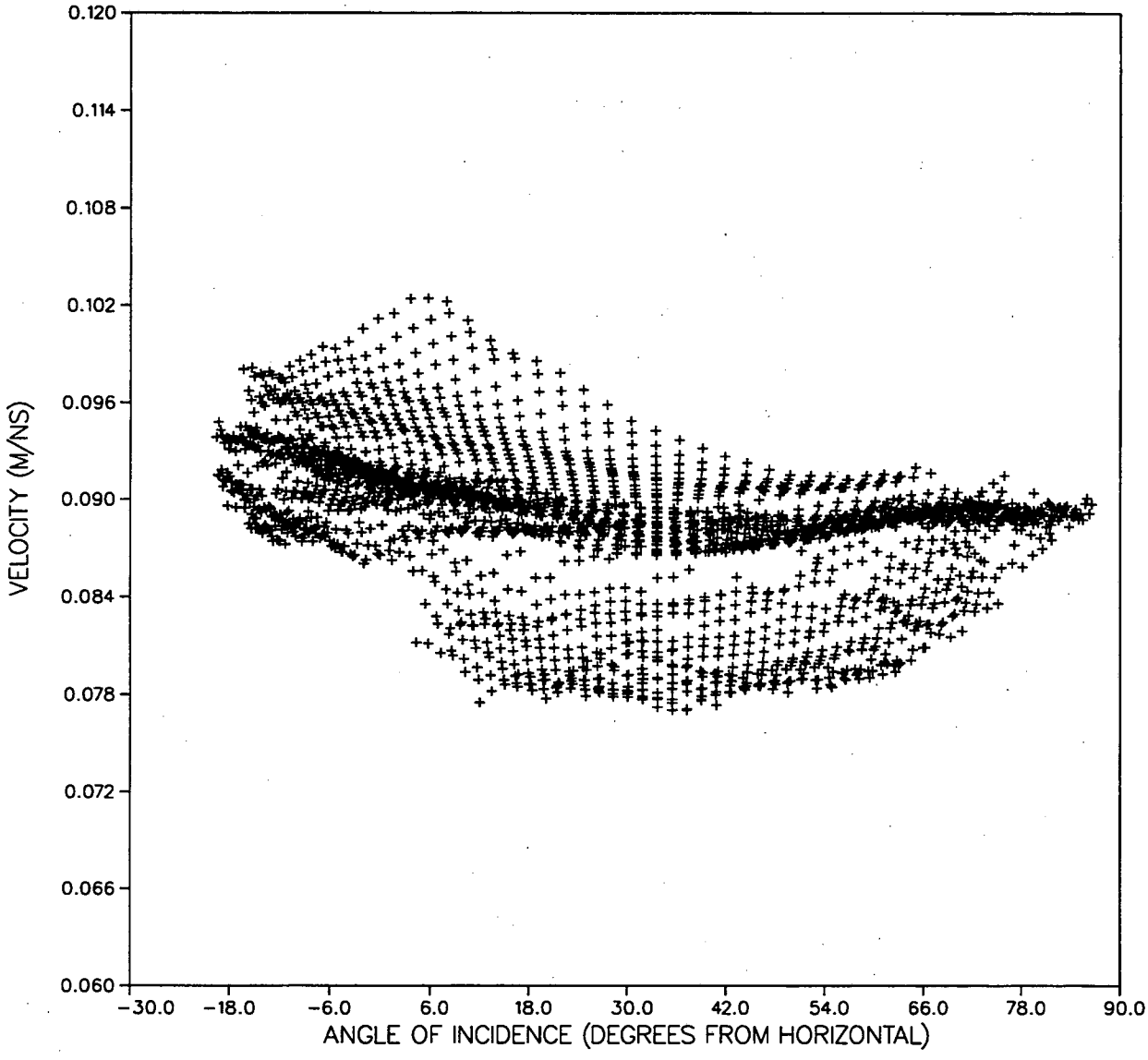

Figure 6b. Same as Figure 6a, but the velocity versus angle of incident values are plotted.

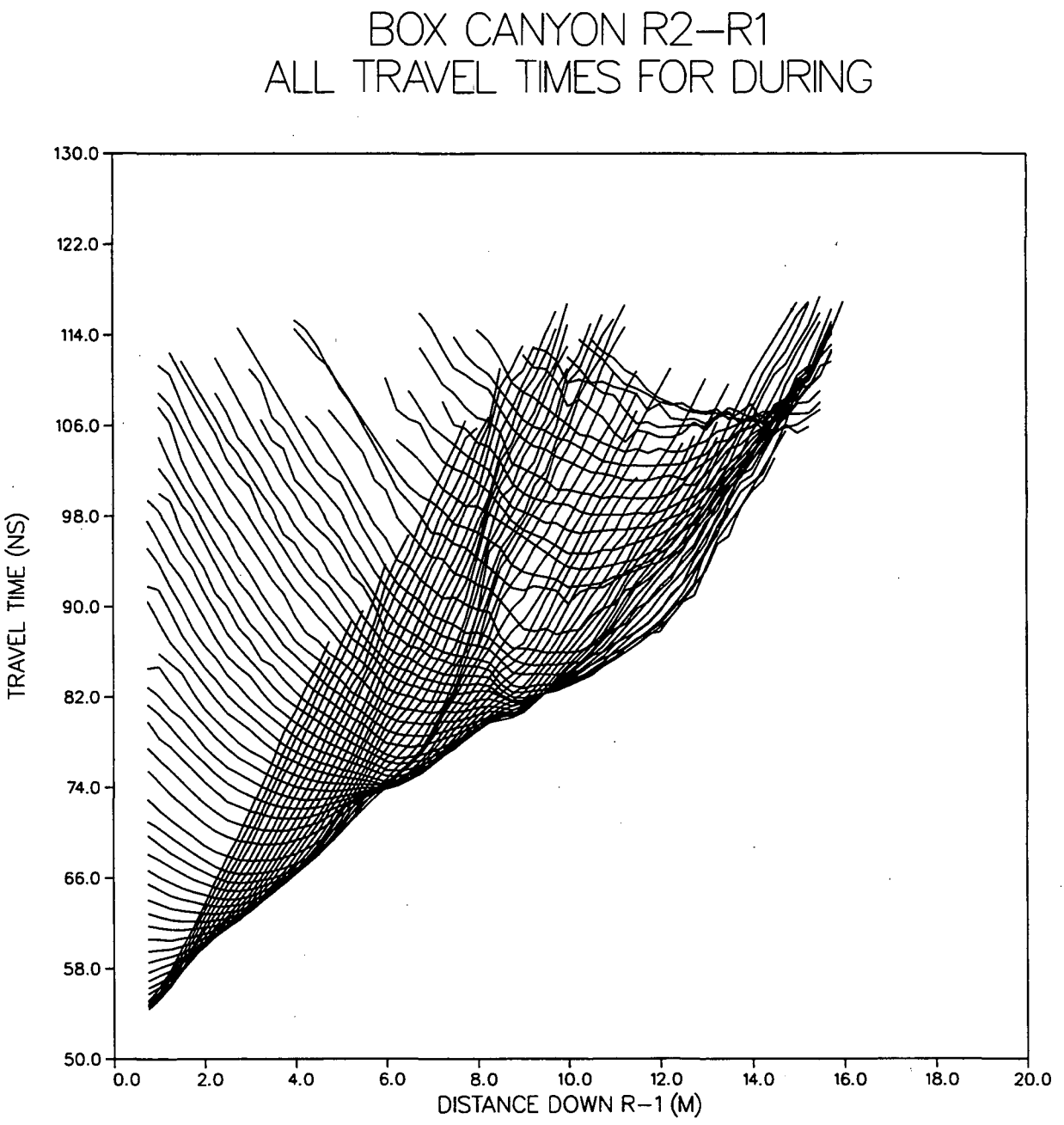

Figure 6c. Travel times for each receiver gather are shown by a single solid line. Values for the DURING data set.

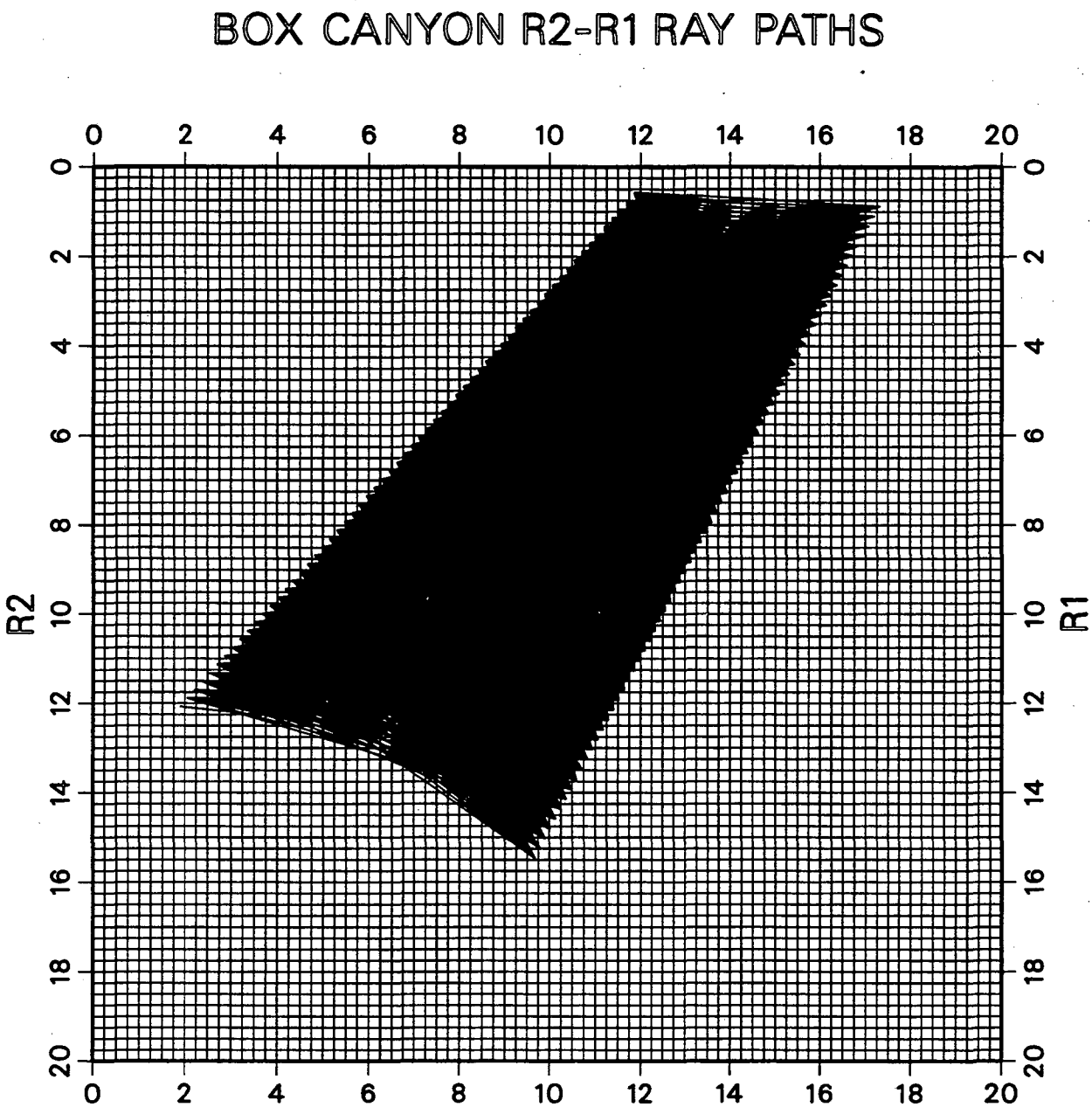

Figure 7. Ray coverage for the DURING travel times superimposed on the inversion grid.

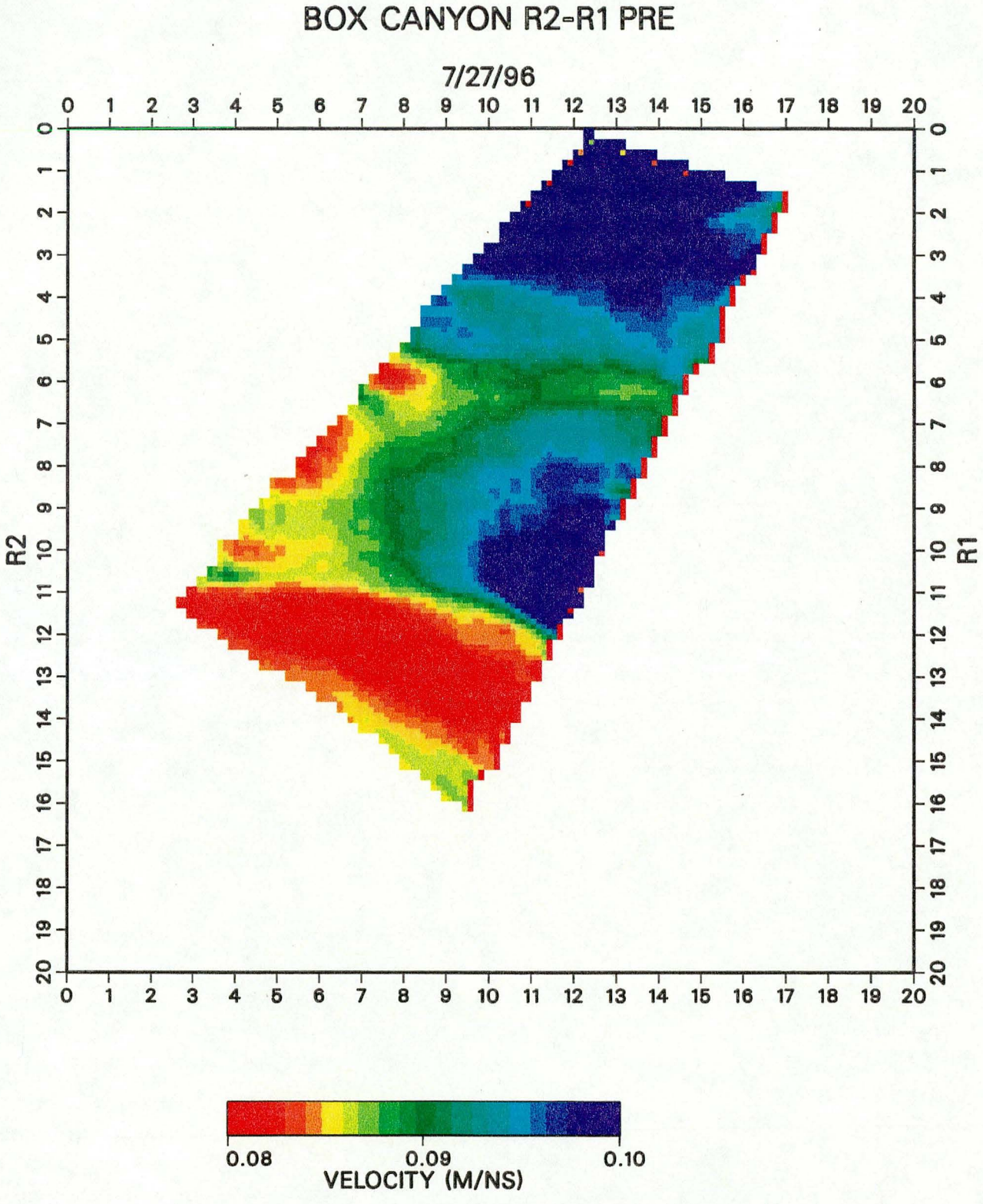

Figure 8a. Velocity tomogram inverted from the PRE R2-R1 travel times.

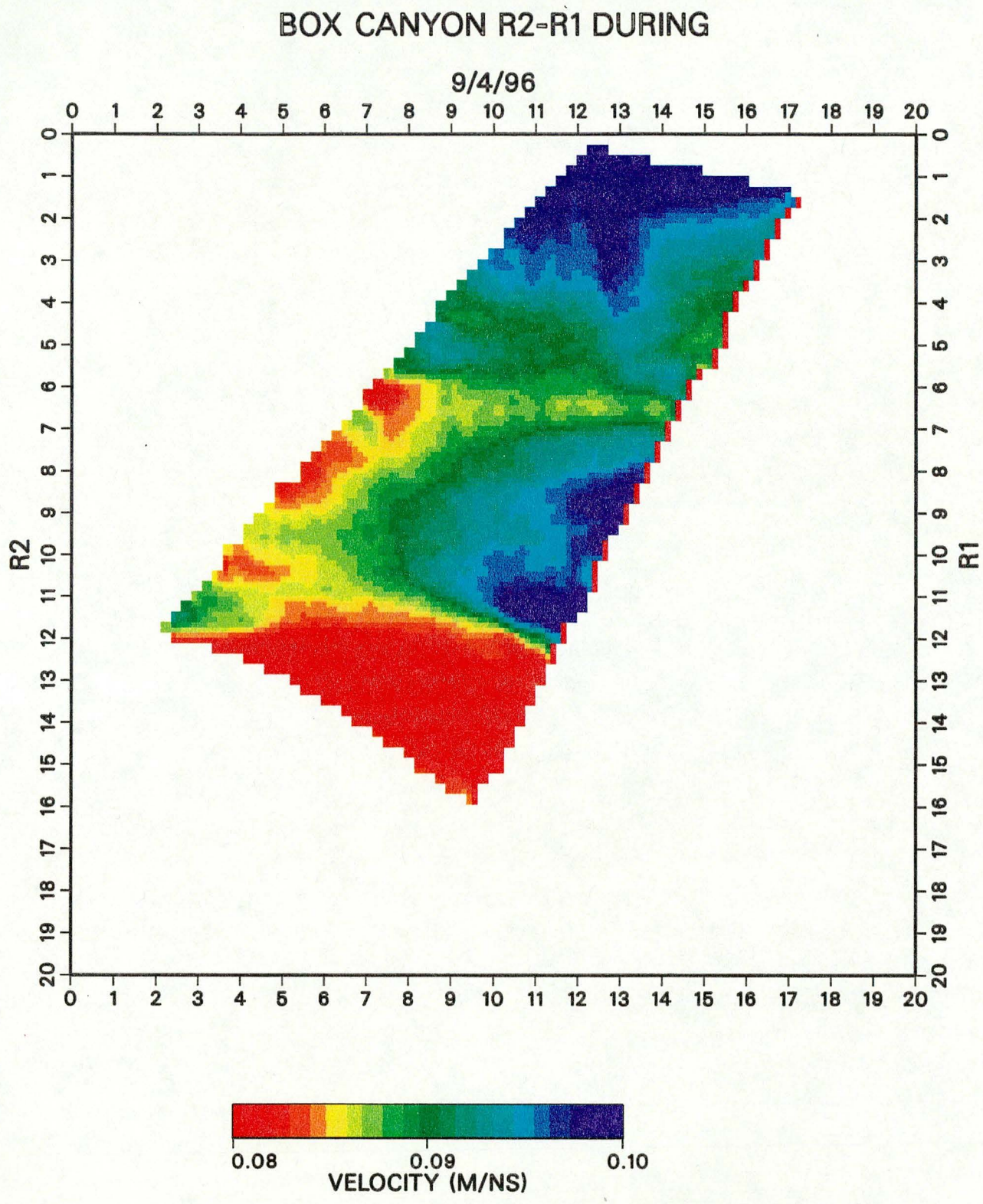

Figure 8b. Velocity tomogram inverted from the DURING R2-R1 travel times.

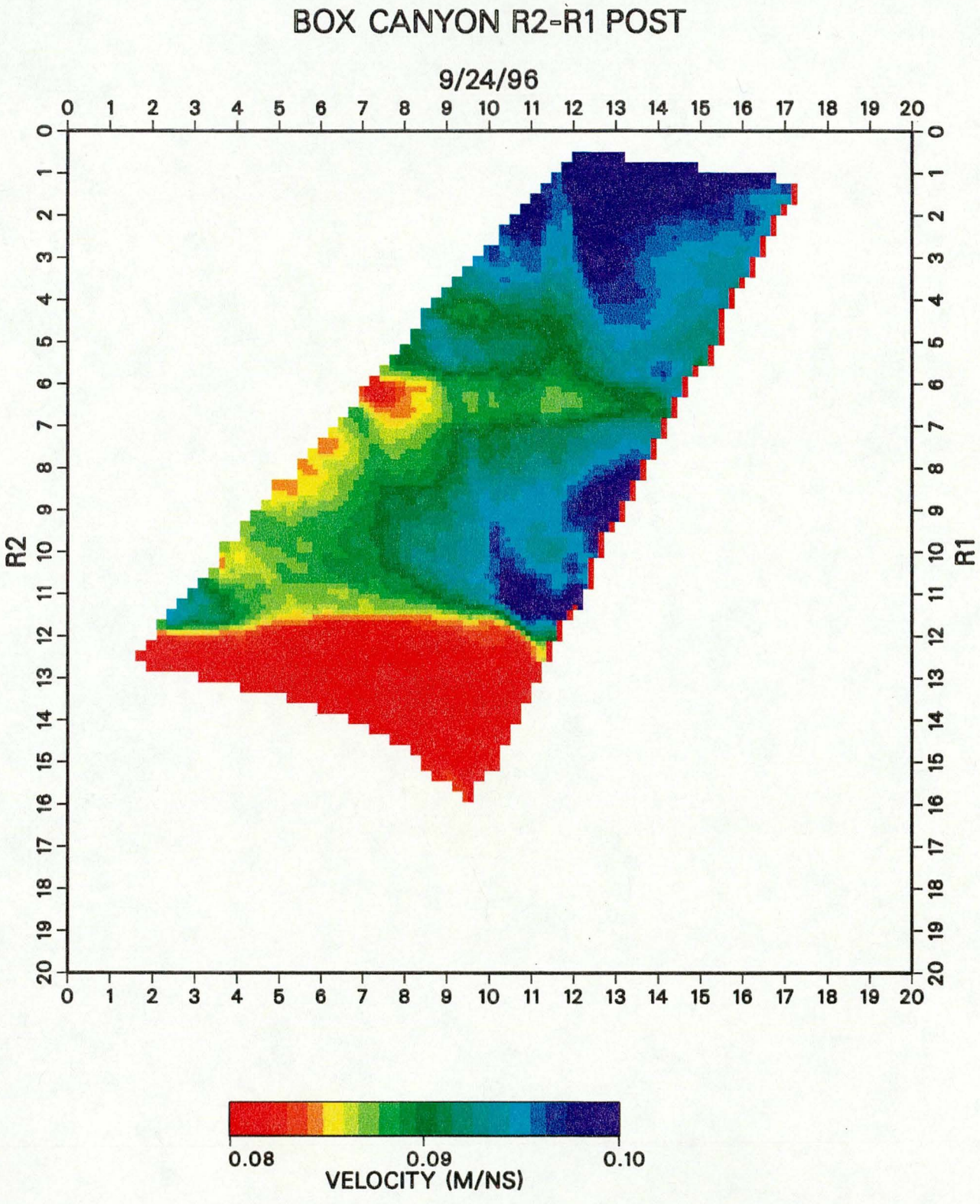

Figure 8c. Velocity tomogram inverted from the POST R2-R1 travel times.

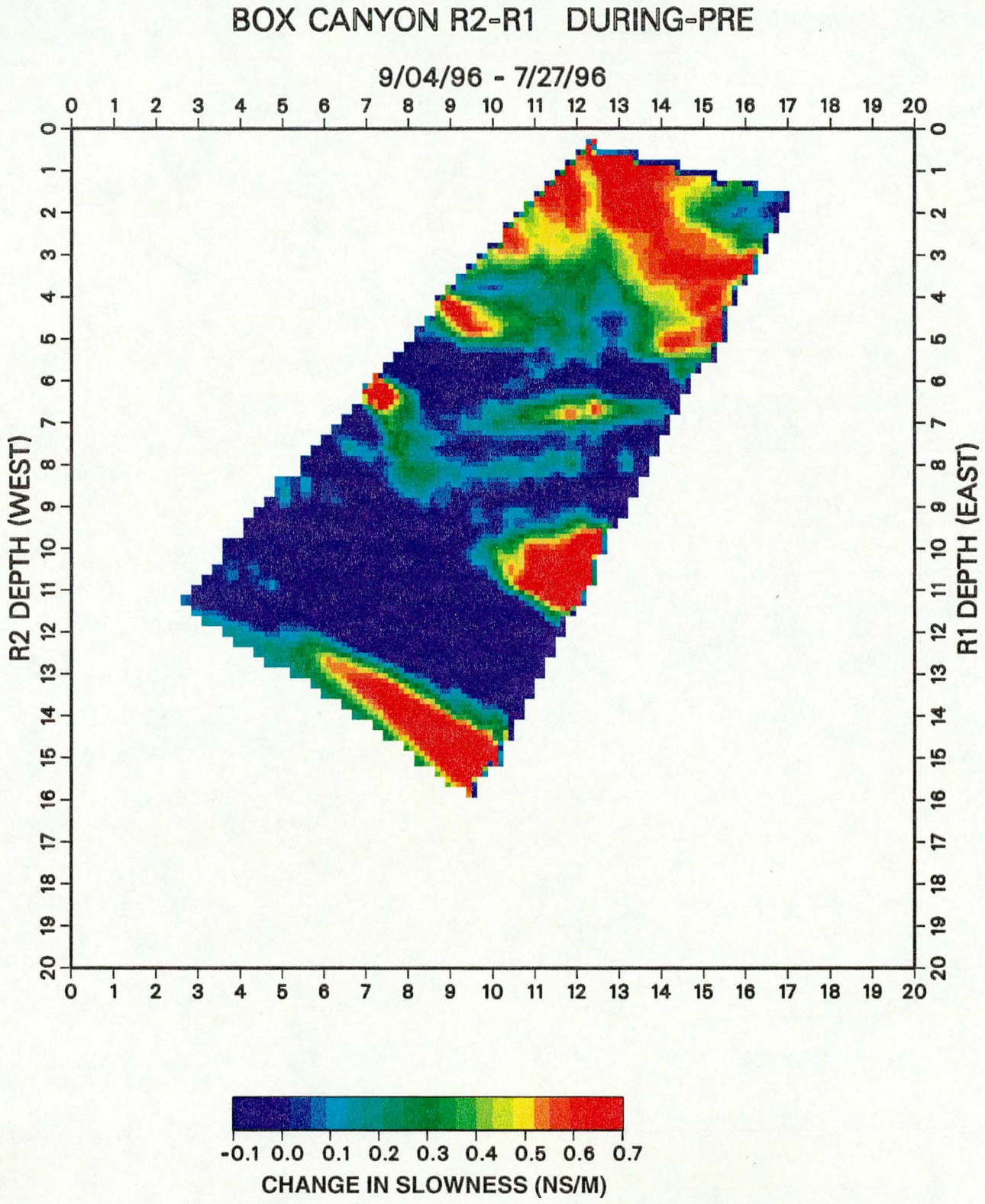

Figure 9a. Slowness difference tomogram determined by inverting the differences in the DURING minus PRE travel times. Note that an increase in slowness corresponds to a decrease in velocity.

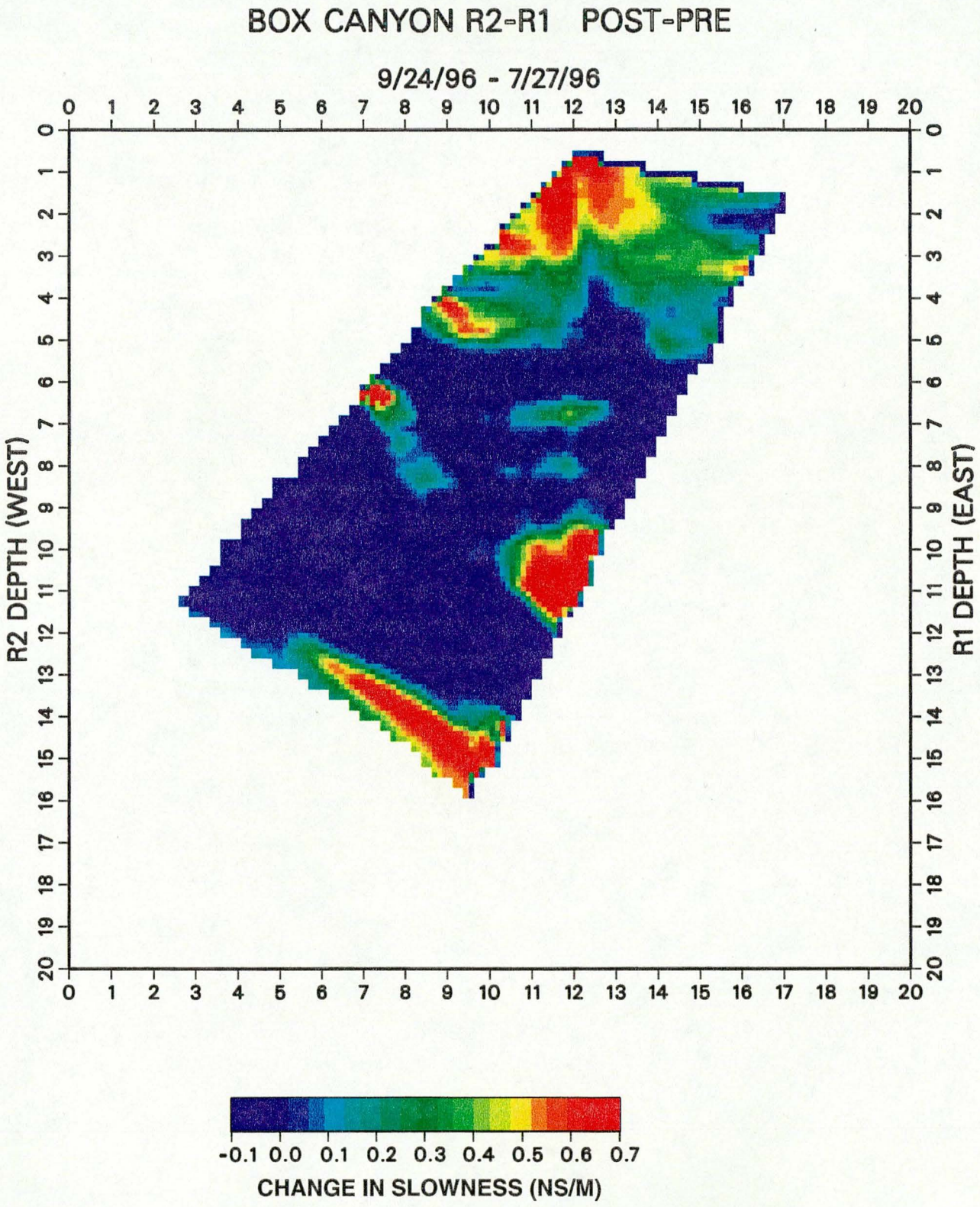

Figure 9b. Slowness difference tomogram determined by inverting the differences in the POST minus PRE travel times. Note that an increase in slowness corresponds to a decrease in velocity.

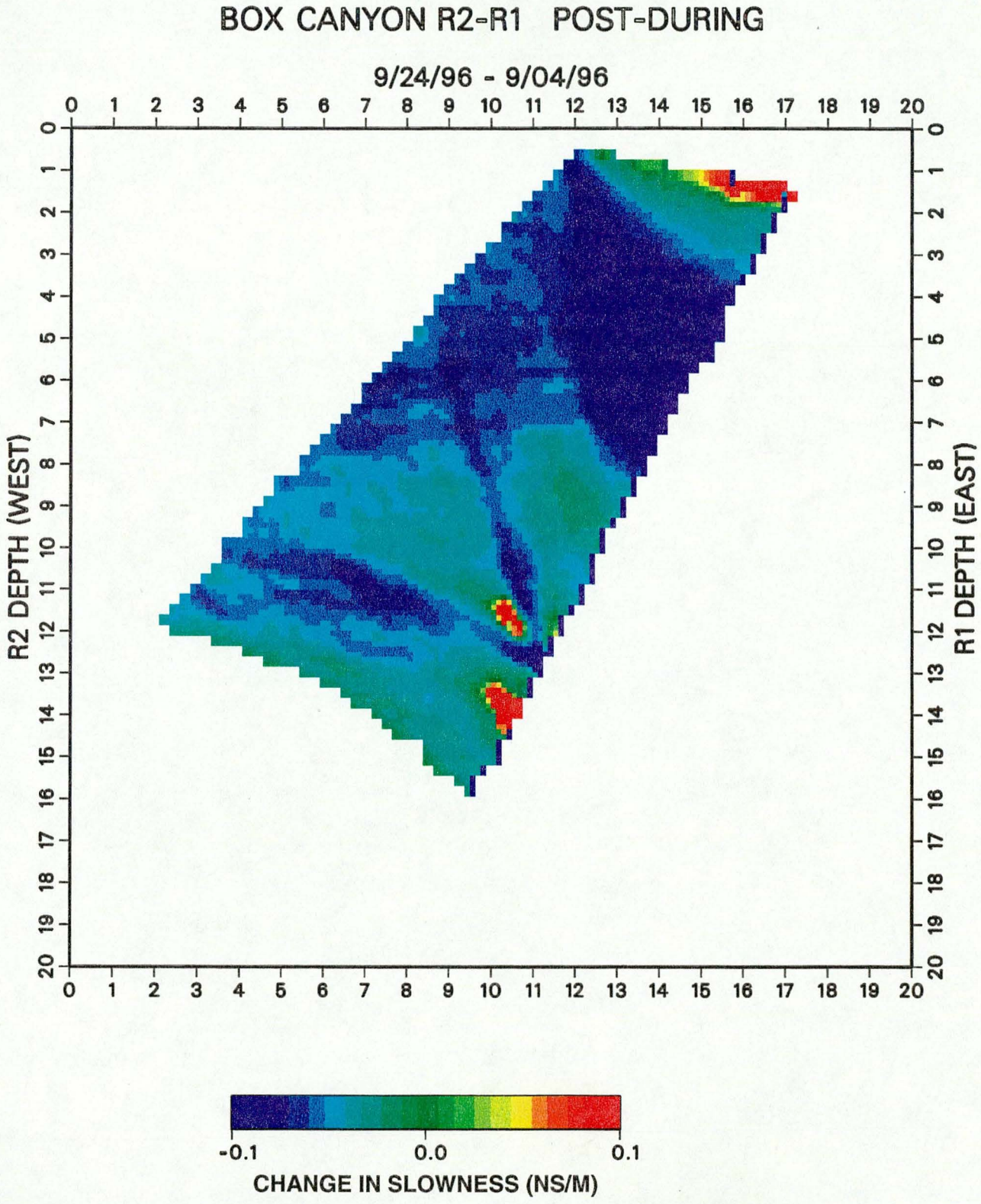

Figure 9c. Slowness difference tomogram determined by inverting the differences in the POST minus DURING travel times. Note that an increase in slowness corresponds to a decrease in velocity. Note change in scale from previous two figures.

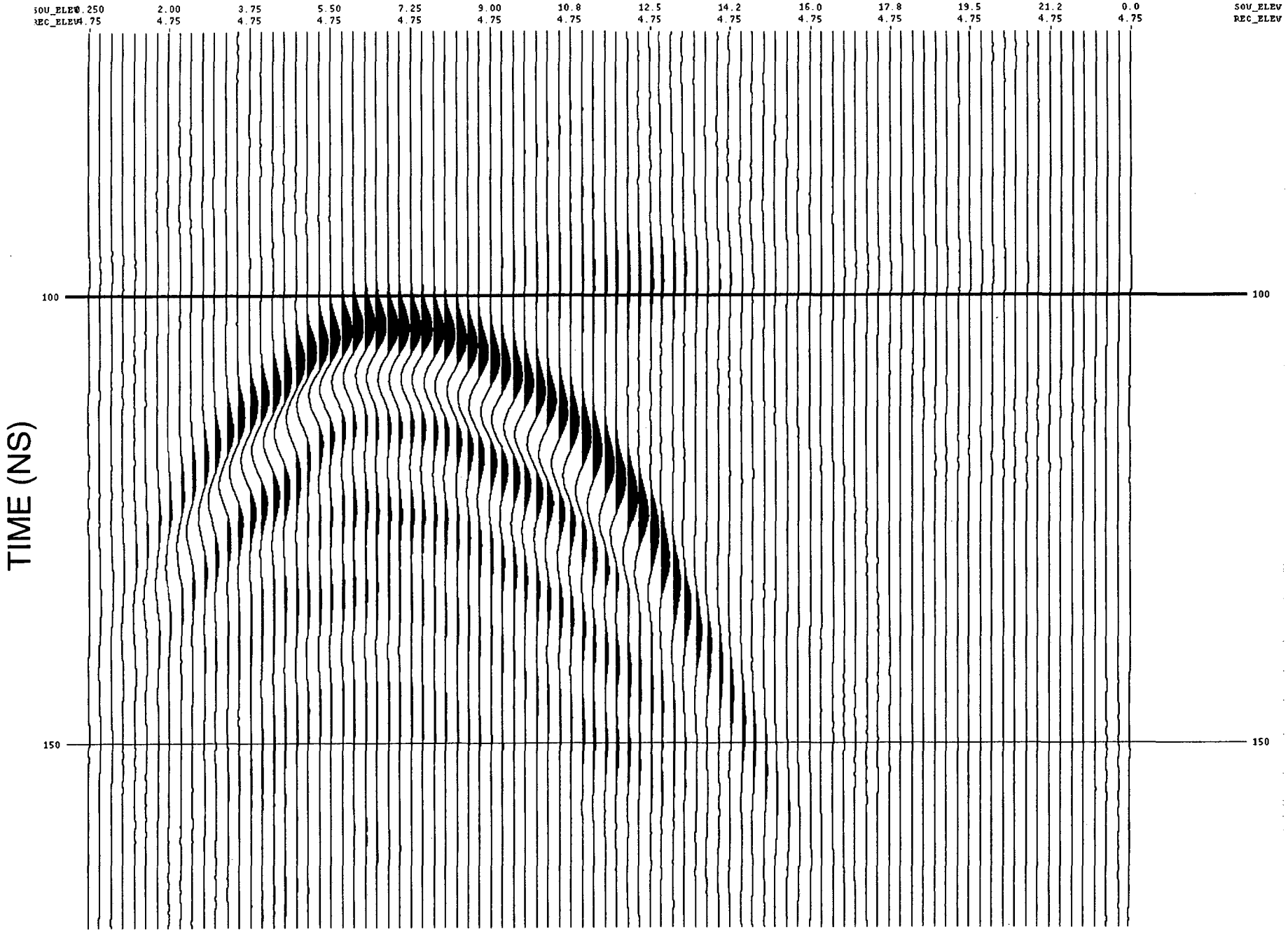

Figure 10. Typical receiver gather for R3-R4 with the receiver held at 4.75 meters down R4.

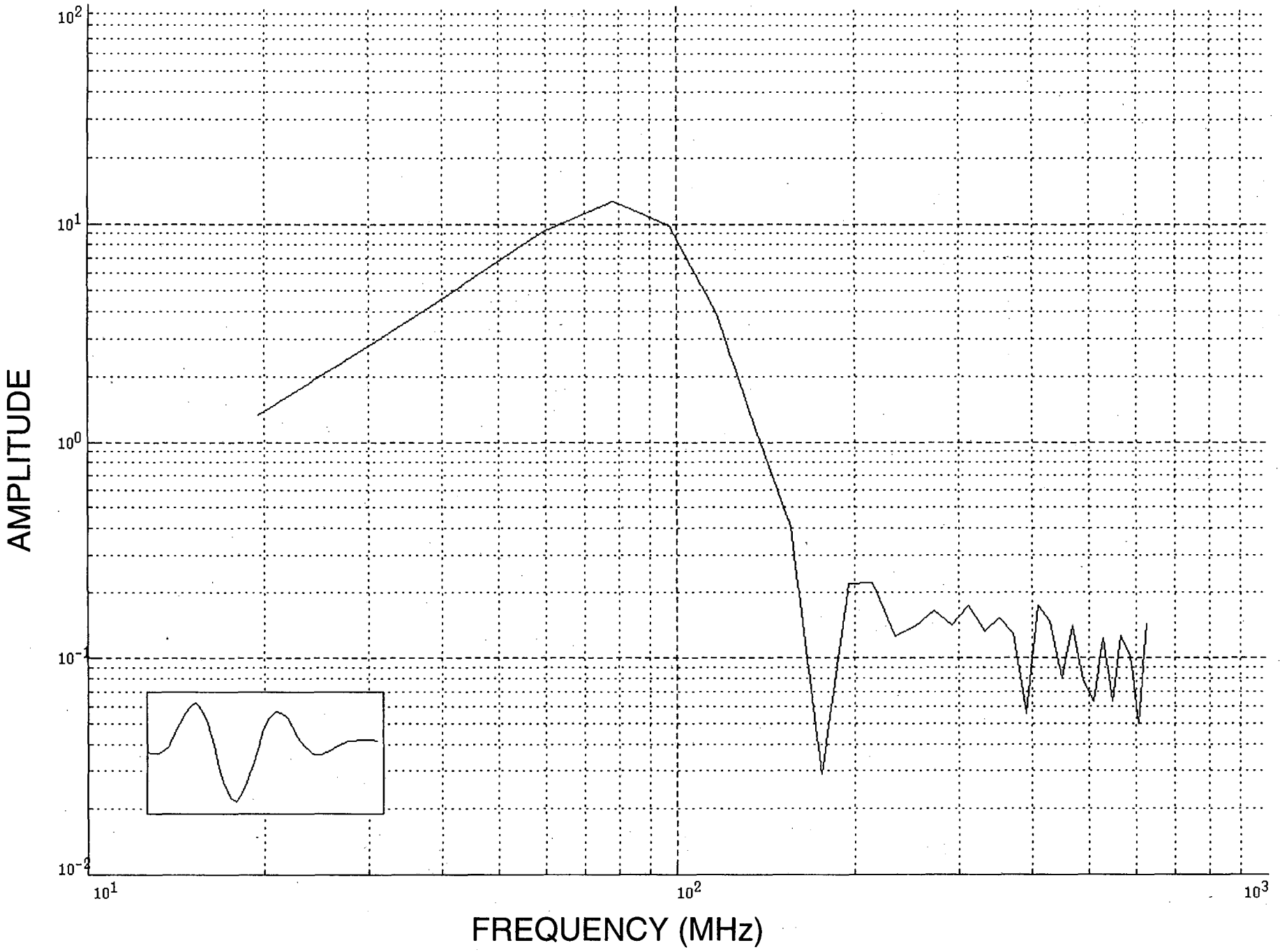

Figure 11. Spectra of a representative trace, 11 meters down R-4, 13 meters down R-3.

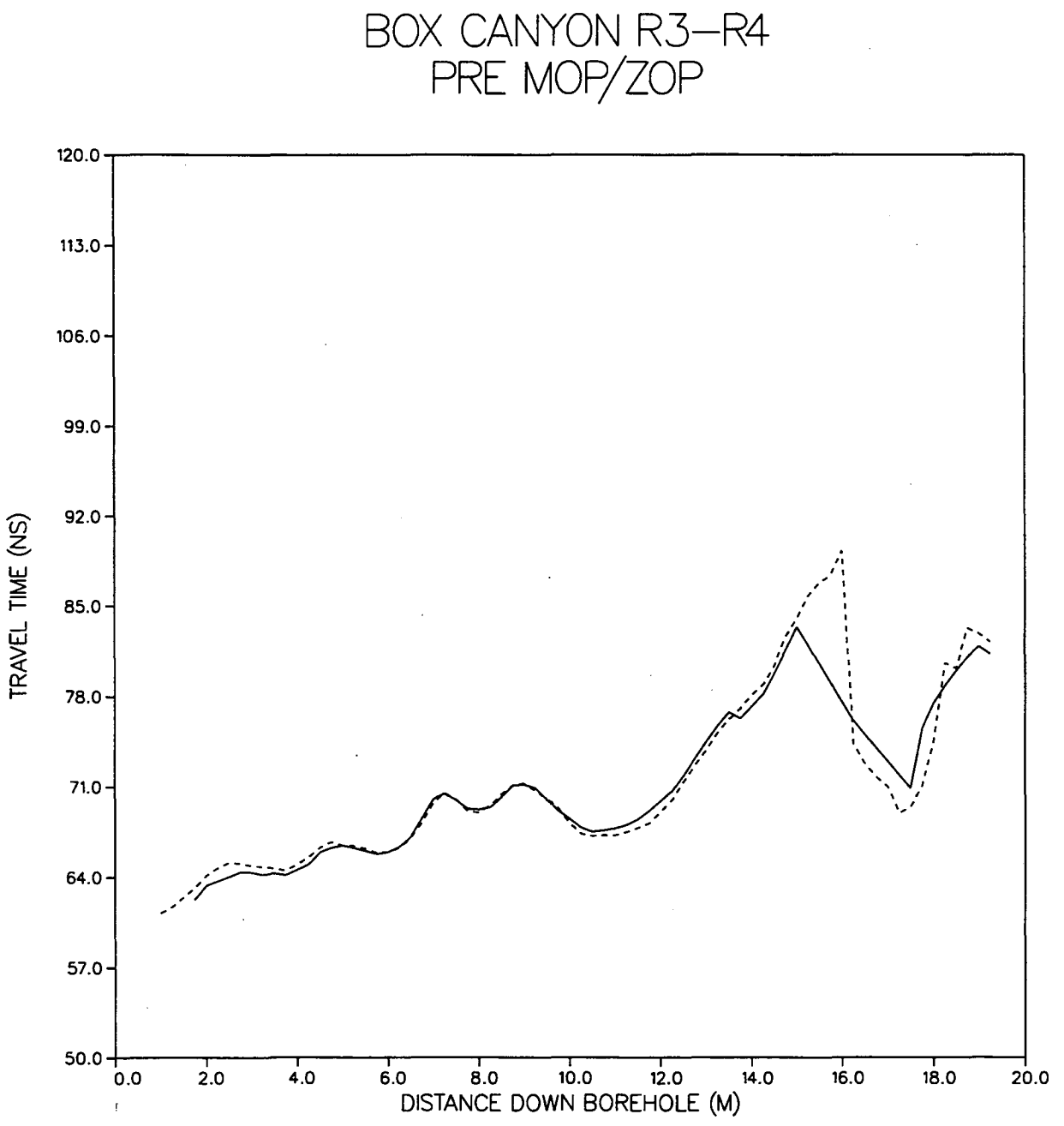

Figure 12a. Zero-offset travel times vs. distance down source/receiver wells for the PRE data set. The solid line is for the zero-offset MOP values; dashed is for ZOP values.

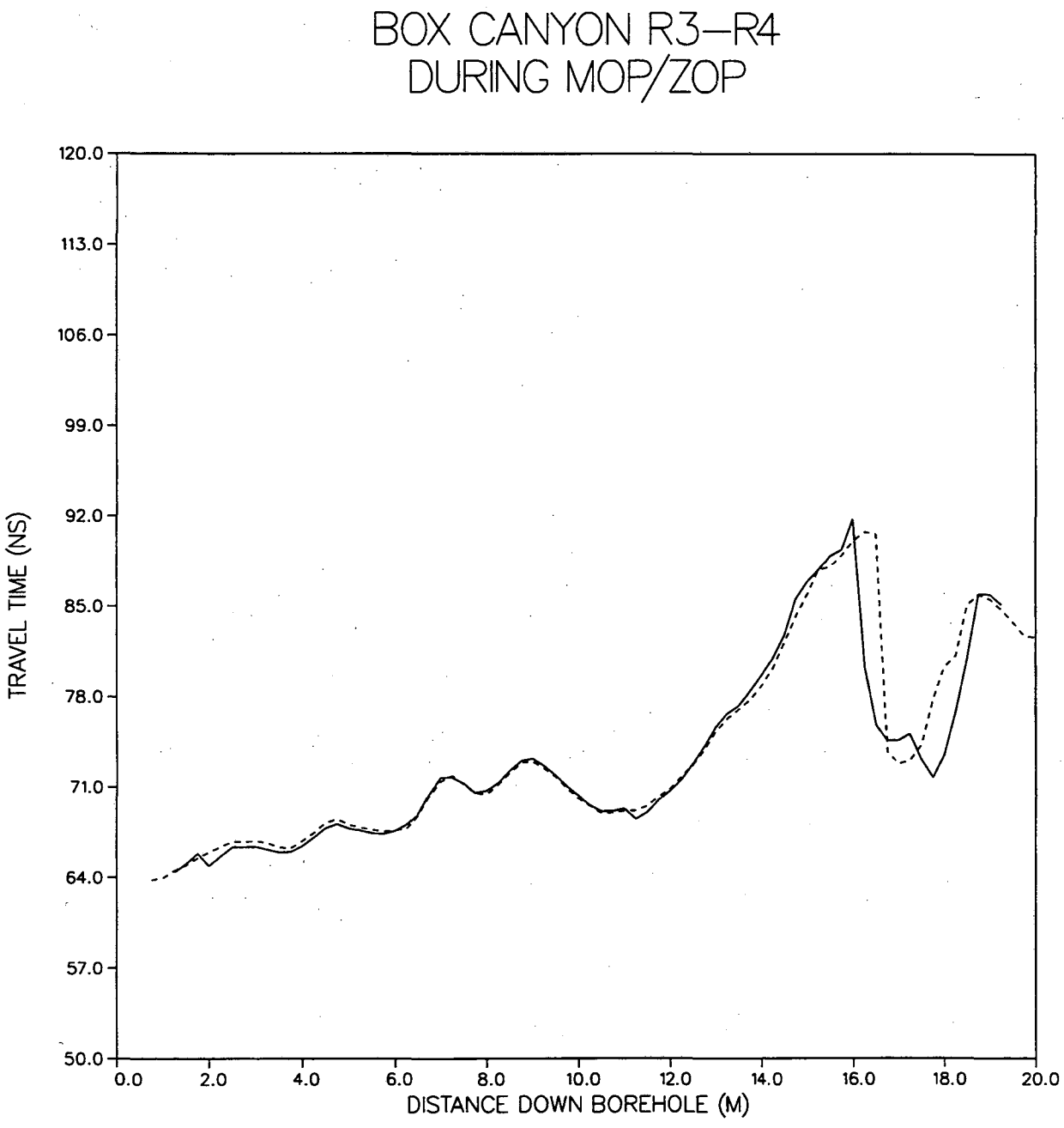

Figure 12b. Same as Figure 12a, but for the DURING data set values.

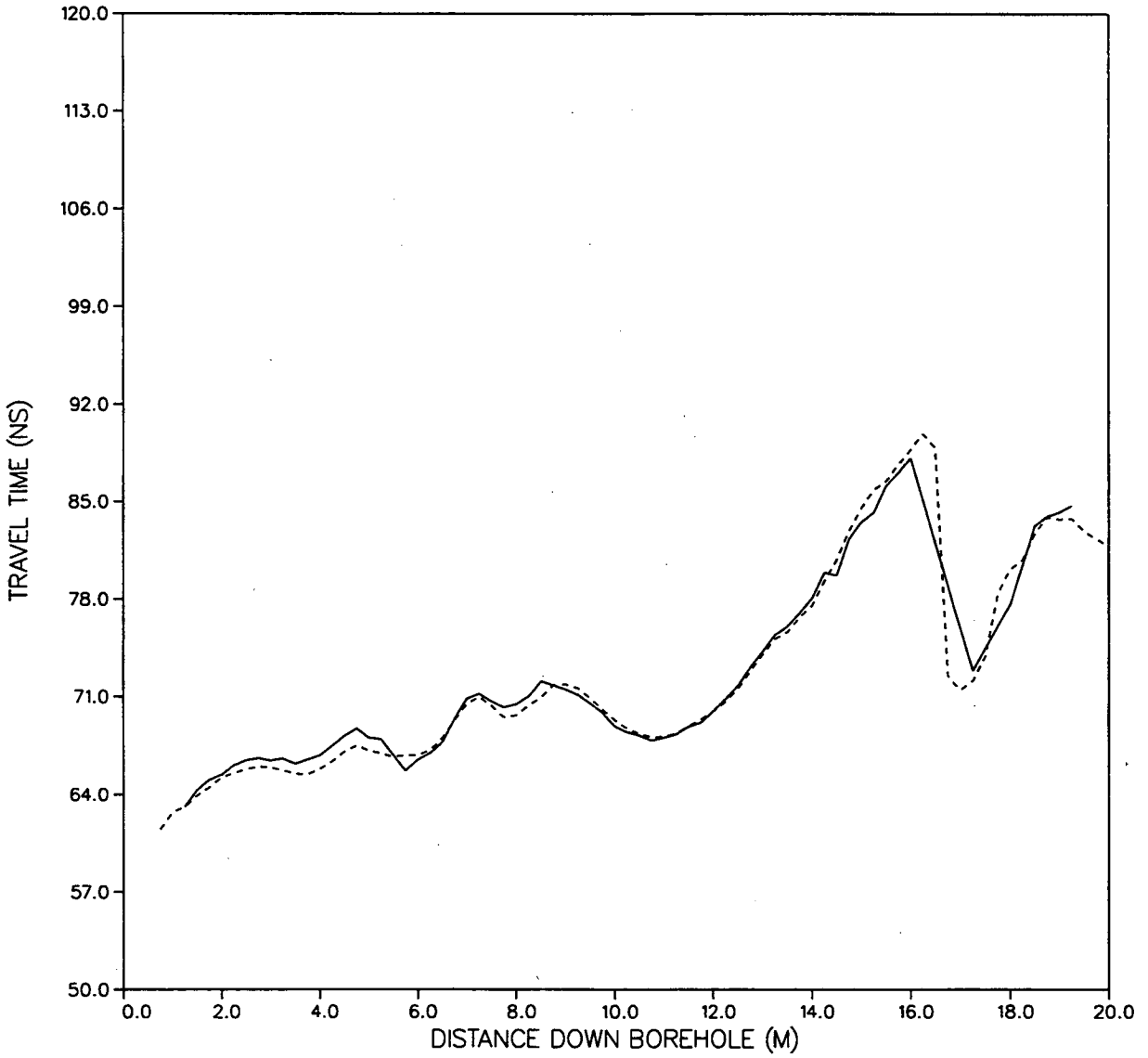

Figure 12c. Same as Figure 12a, but for the POST data set values.

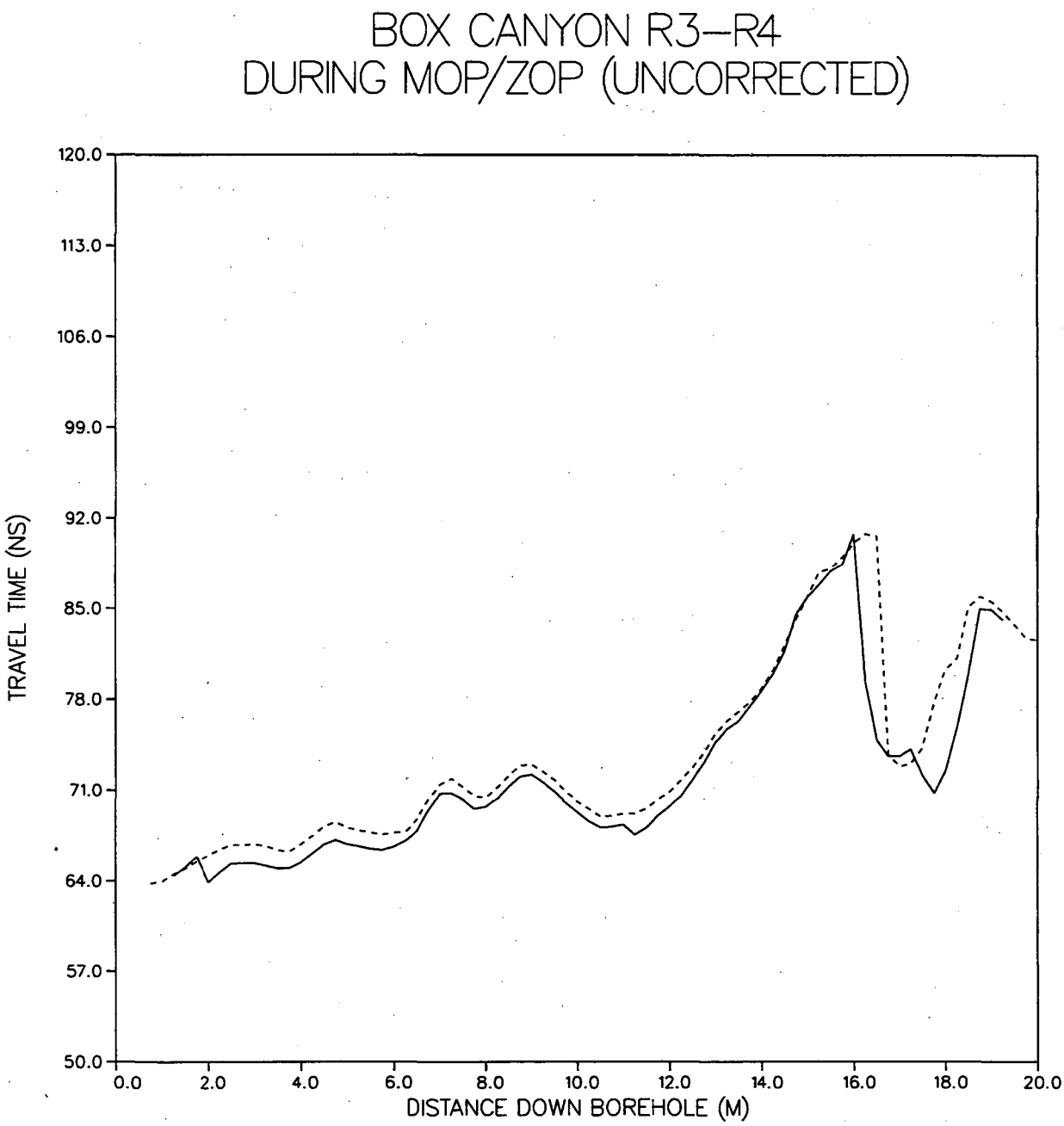

Figure 12d. Same as Figure 12b, but the times have not been corrected for zero-time glitches.

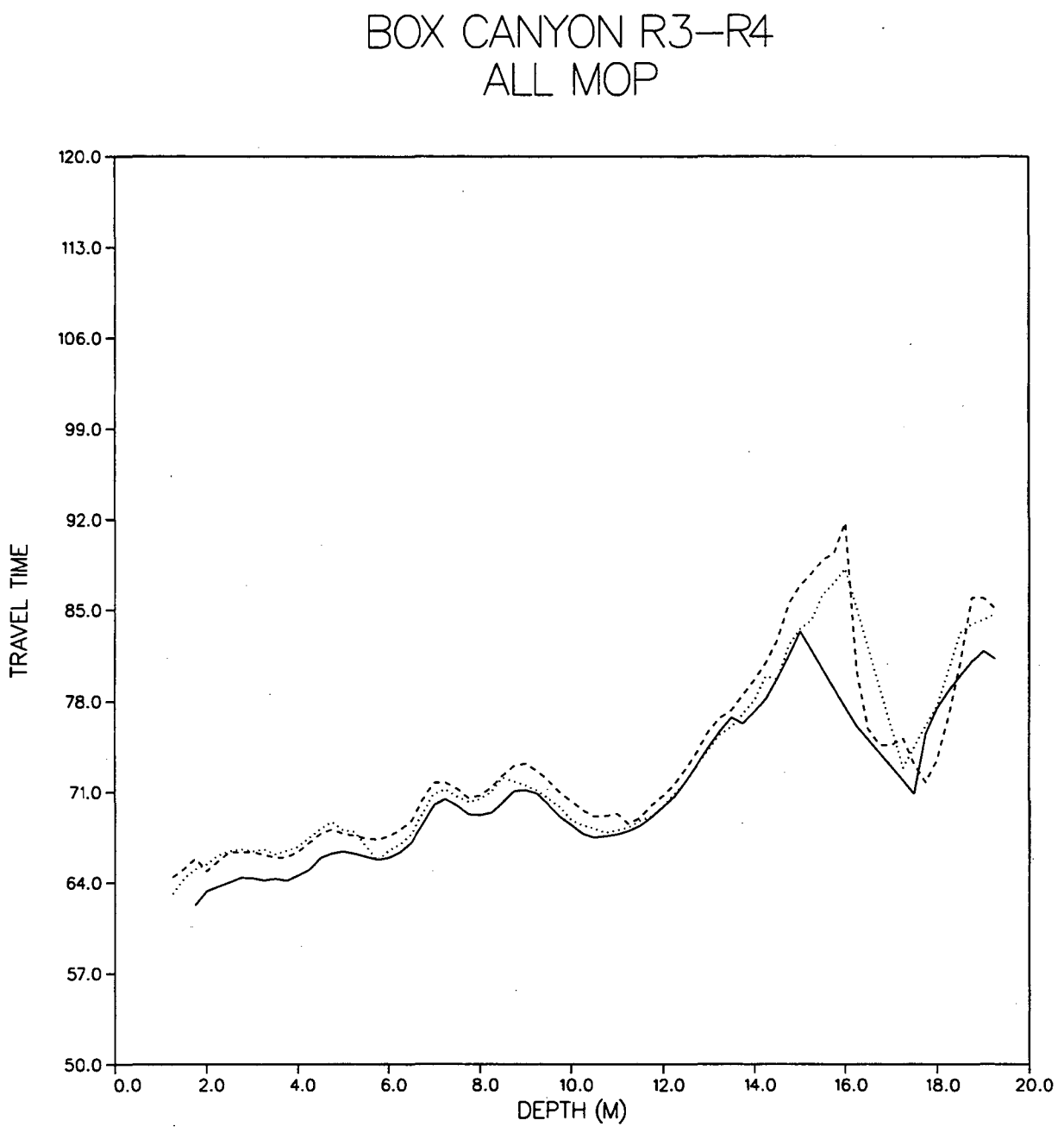

Figure 12e. Zero-offset travel time vs. distance down source/receiver wells for the zero-offset MOP values for the PRE (solid), DURING (dashed), and POST (dotted) data set.

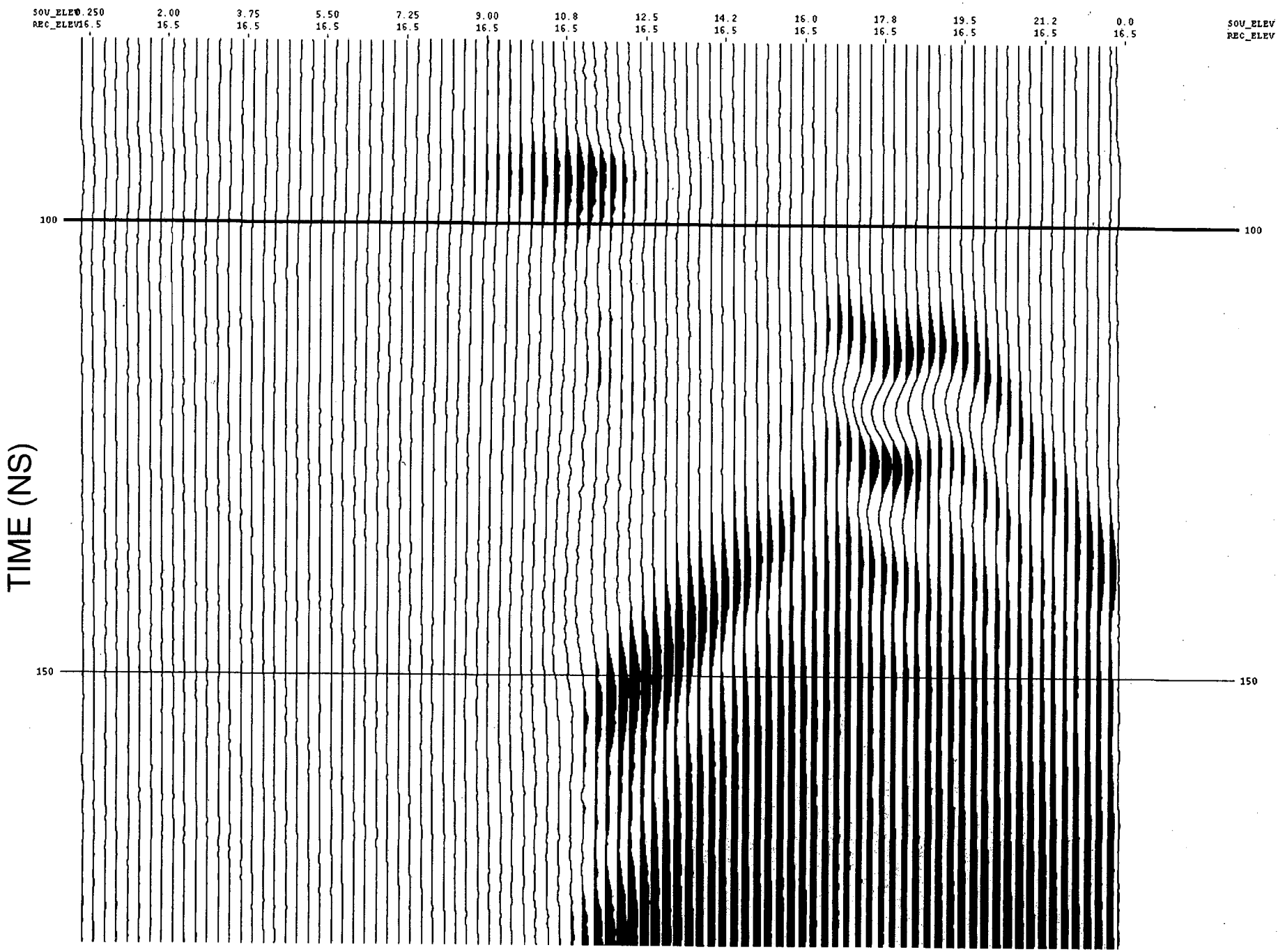

Figure 13. Receiver gather for receiver 16.5 meters down R-4 showing large change in travel time at about 16 meters down R-3.

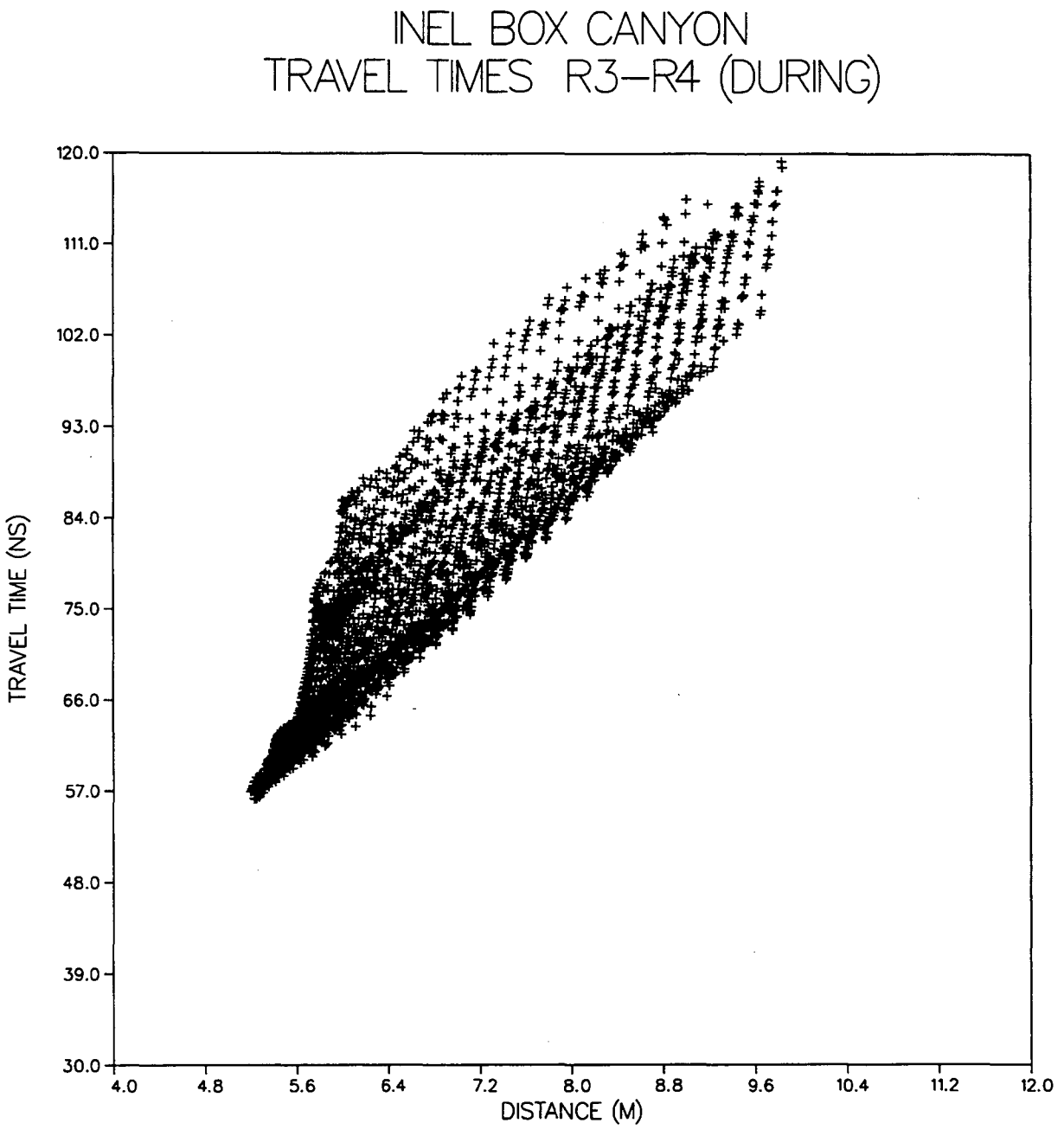

Figure 14a. Travel time vs. distance values for the DURING data set. The difference in travel time values between data sets is relatively small.

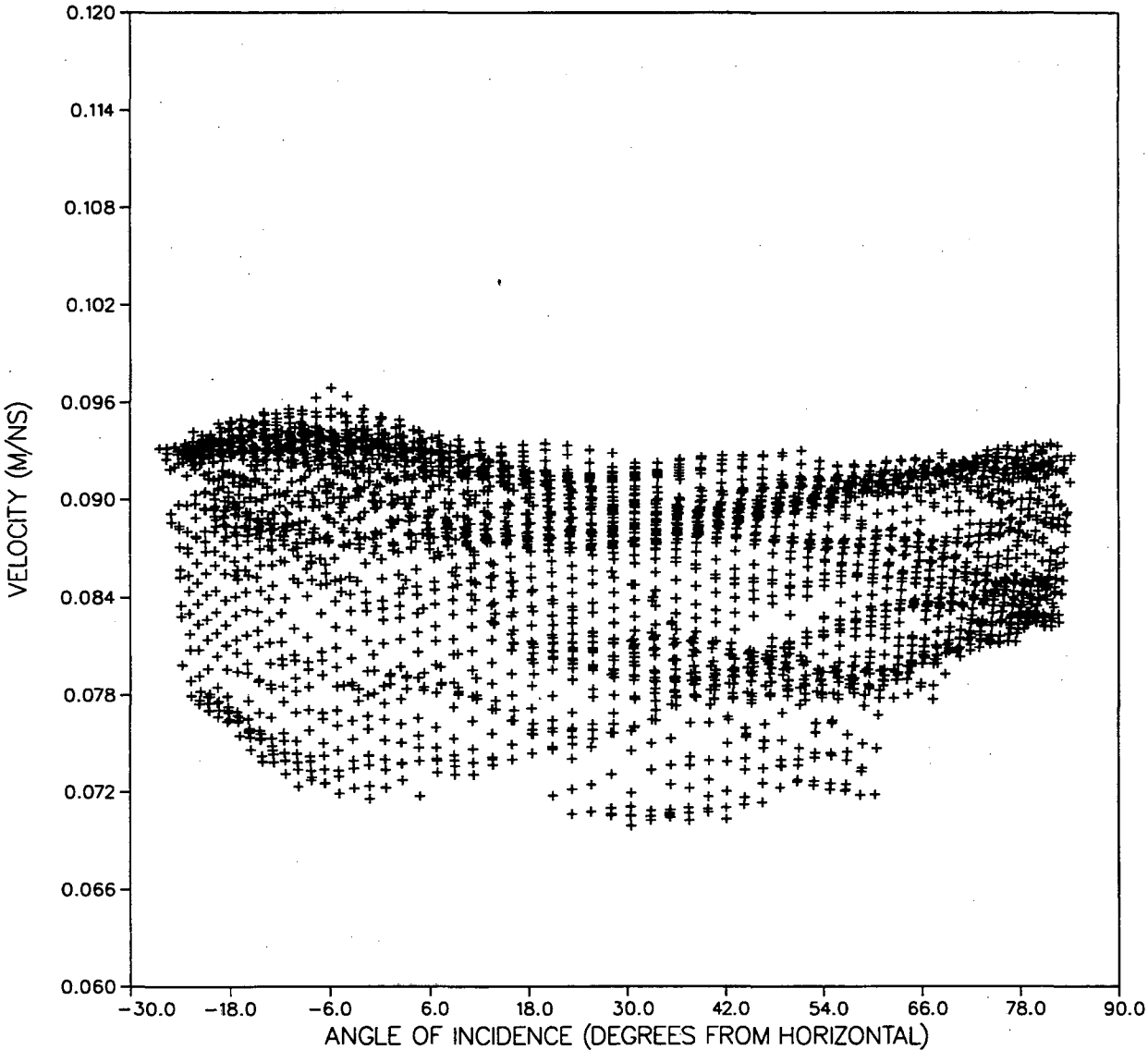

Figure 14b. Same as Figure 14a, but the velocity versus angle of incident values are plotted.

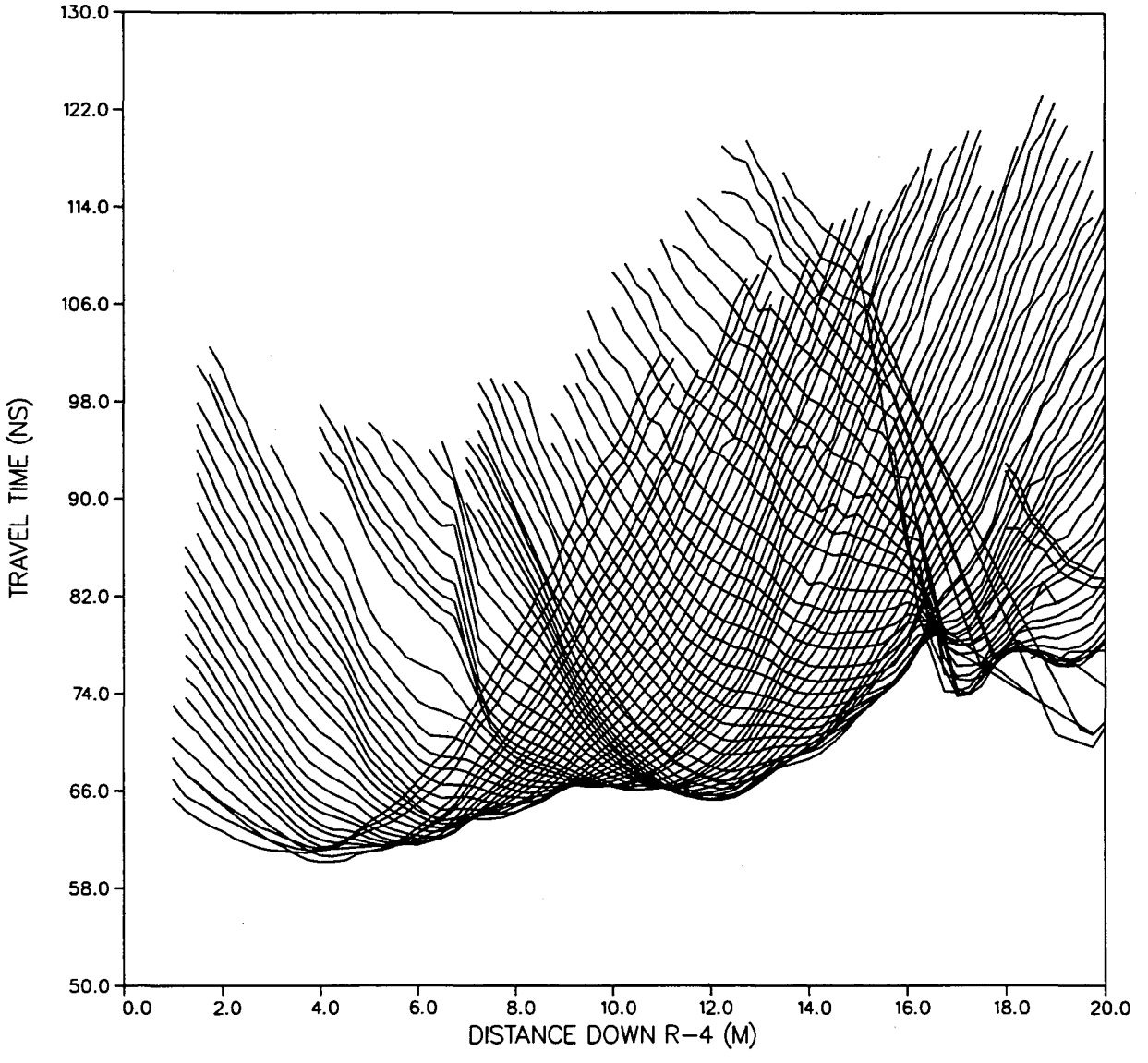

Figure 14c. Travel times for each receiver gather are shown by a single solid line. Values for the DURING data set.

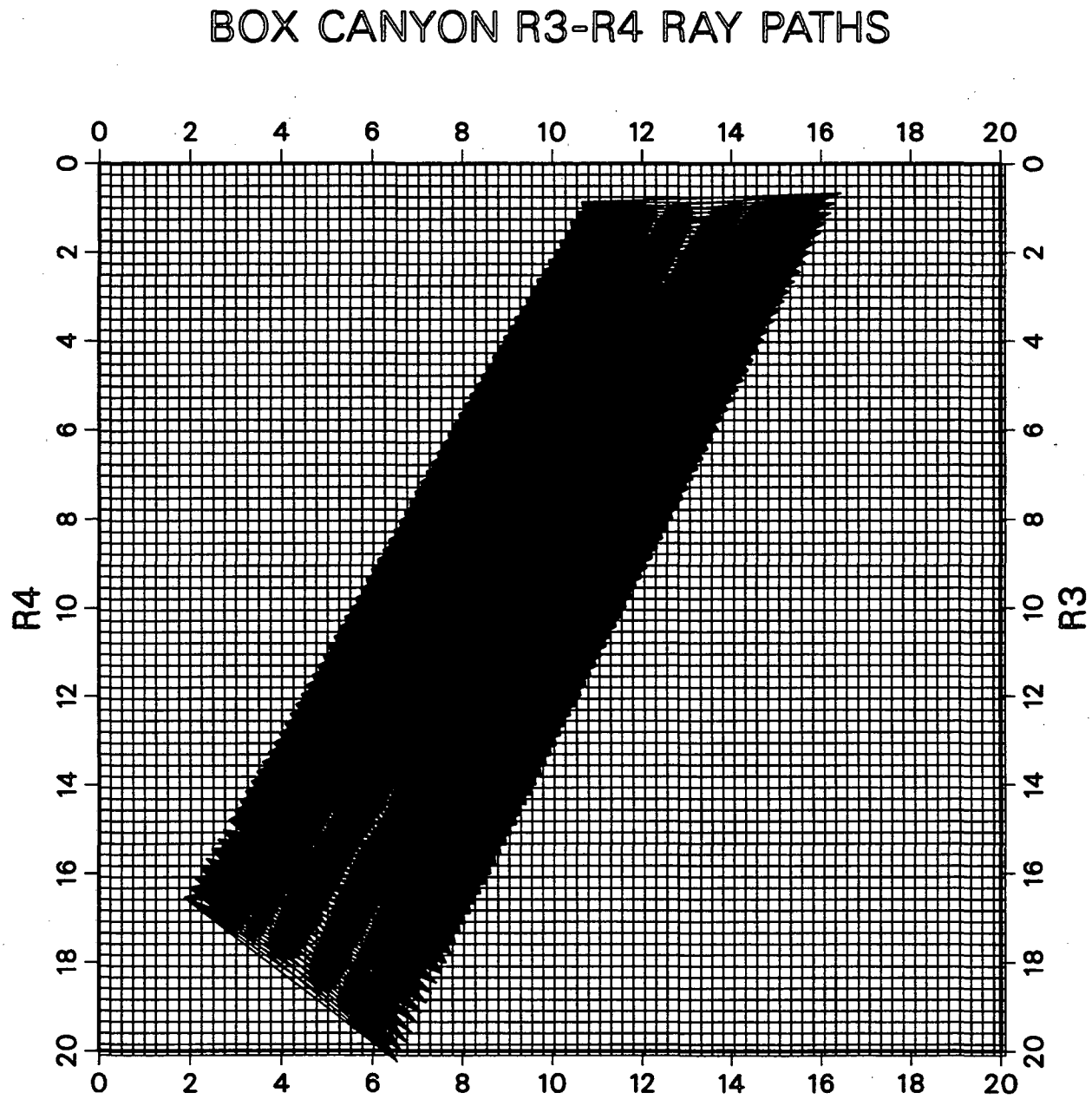

Figure 15. Ray coverage for the DURING travel times superposed on the inversion grid.

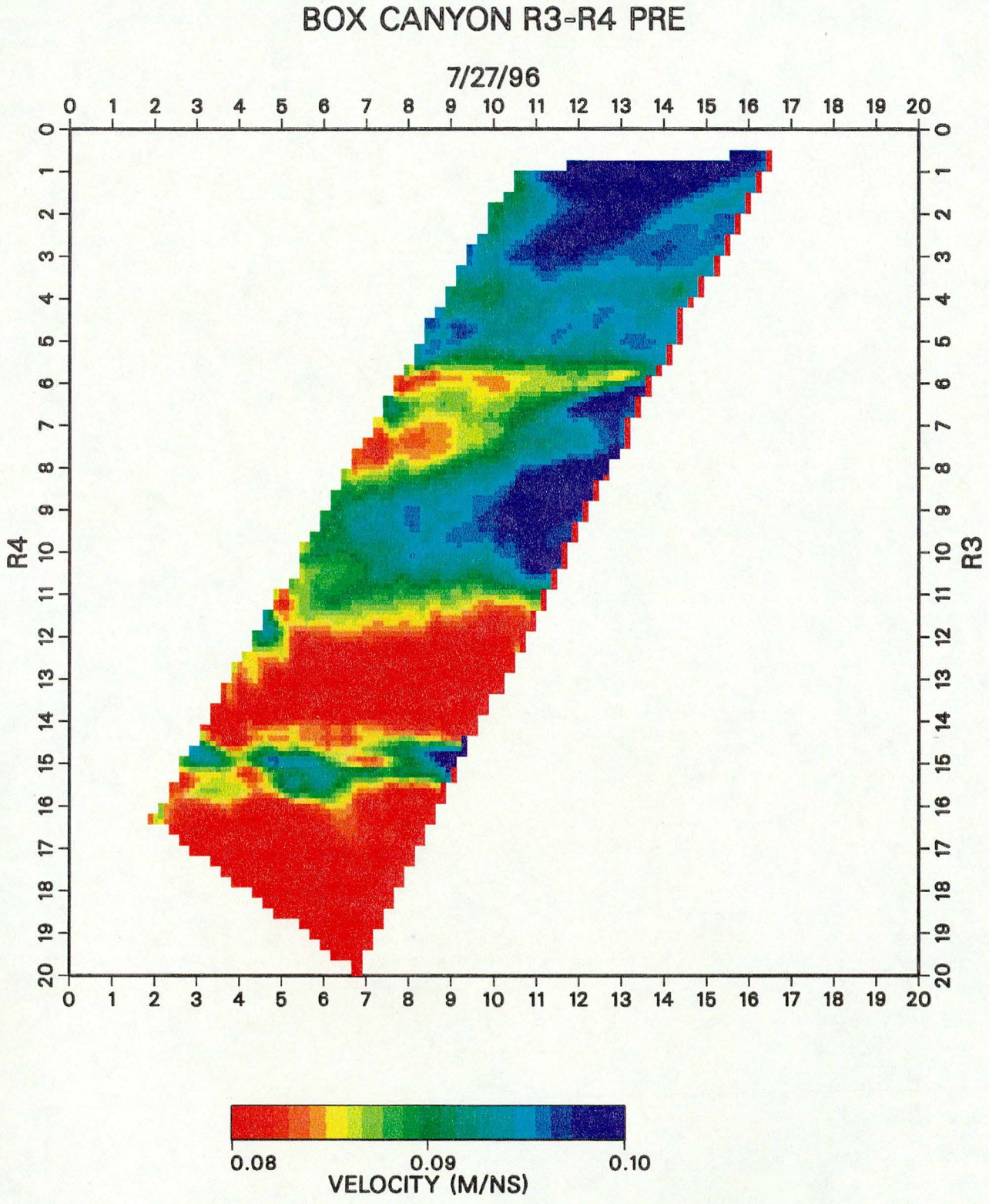

Figure 16a. Velocity tomogram inverted from the PRE R3-R4 travel times.

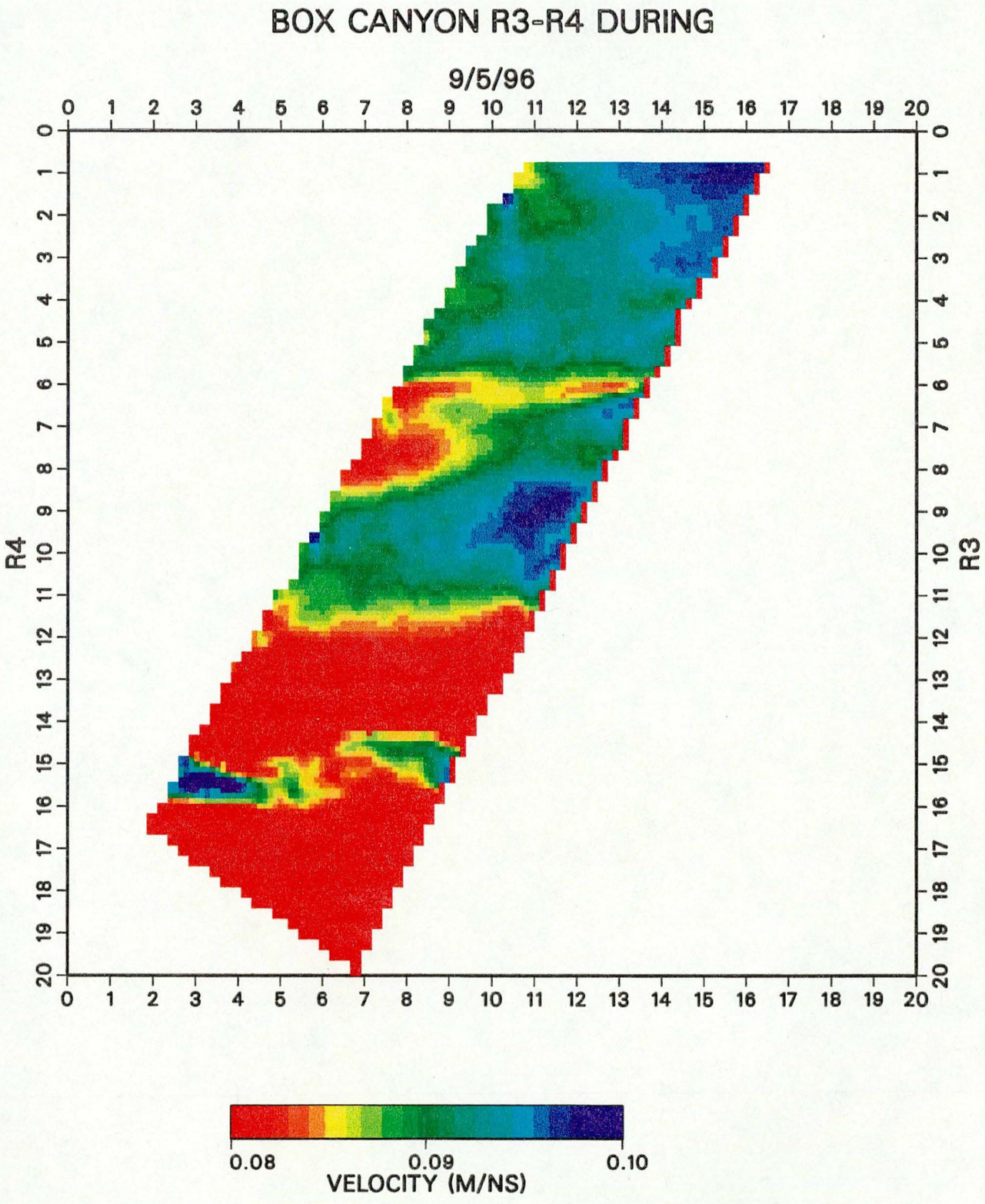

Figure 16b. Velocity tomogram inverted from the DURING R3-R4 travel times.

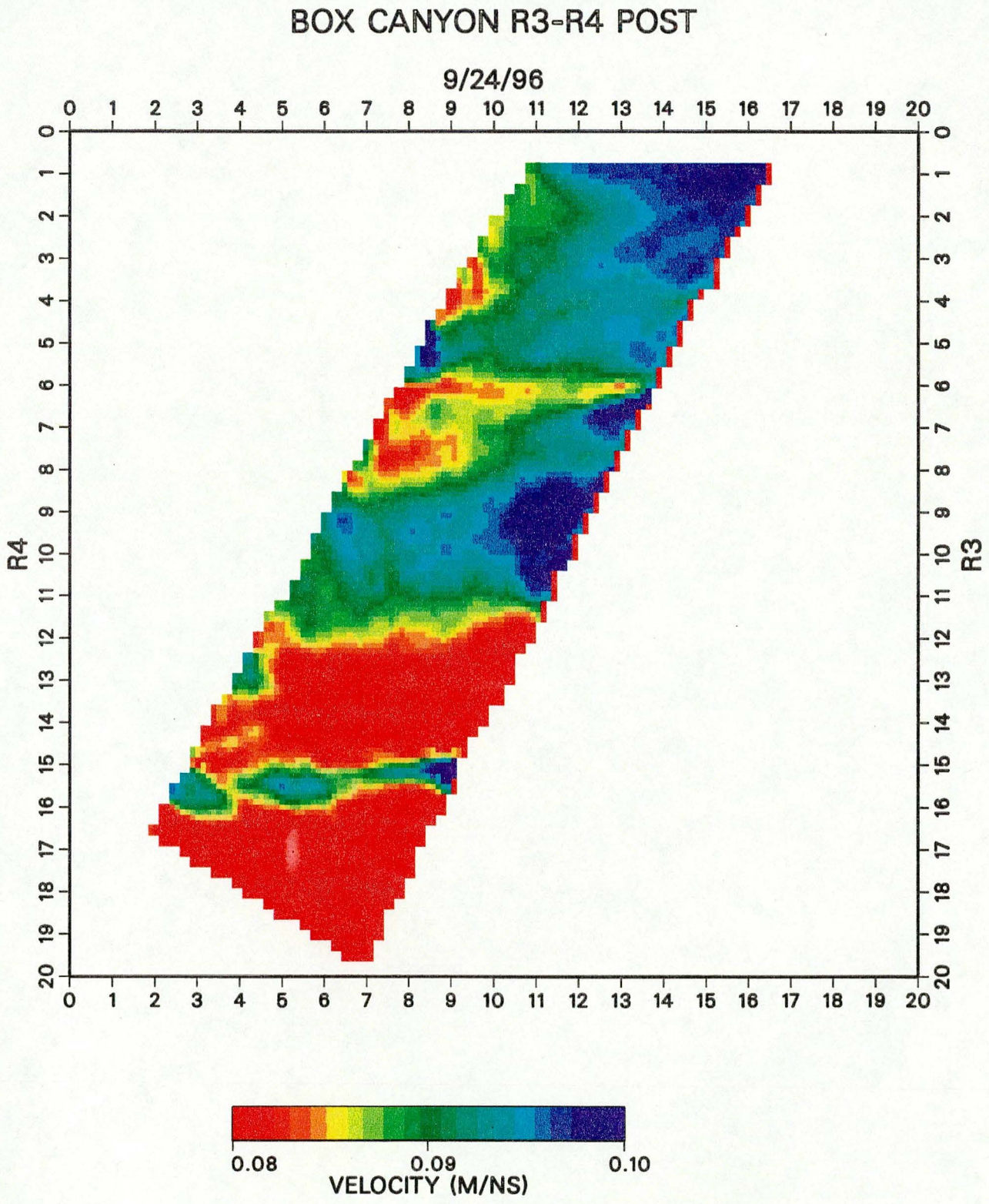

Figure 16c. Velocity tomogram inverted from the POST travel times.

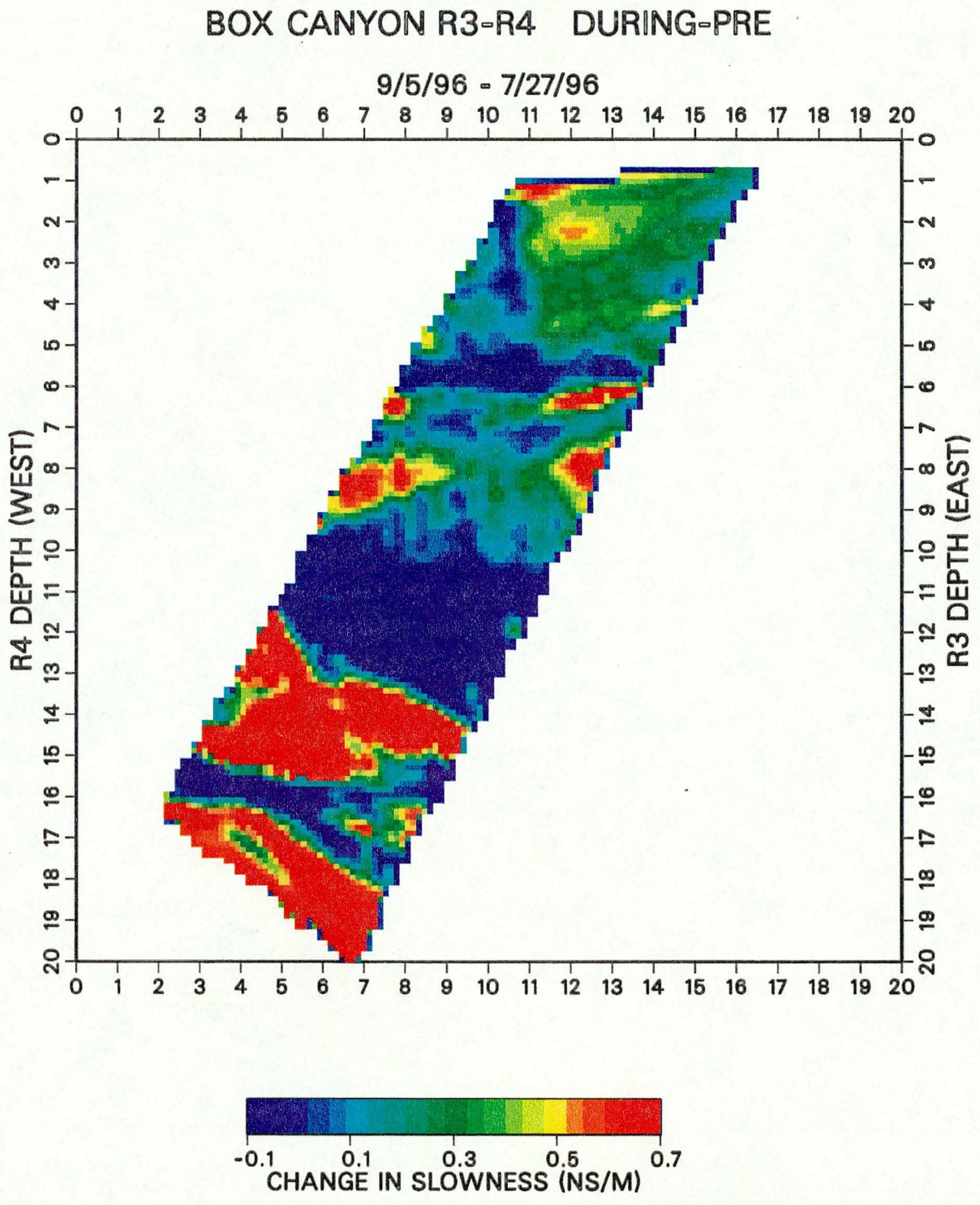

Figure 17a. Slowness difference tomogram determined by inverting the differences in the DURING minus PRE travel times. Note that an increase in slowness corresponds to a decrease in velocity.

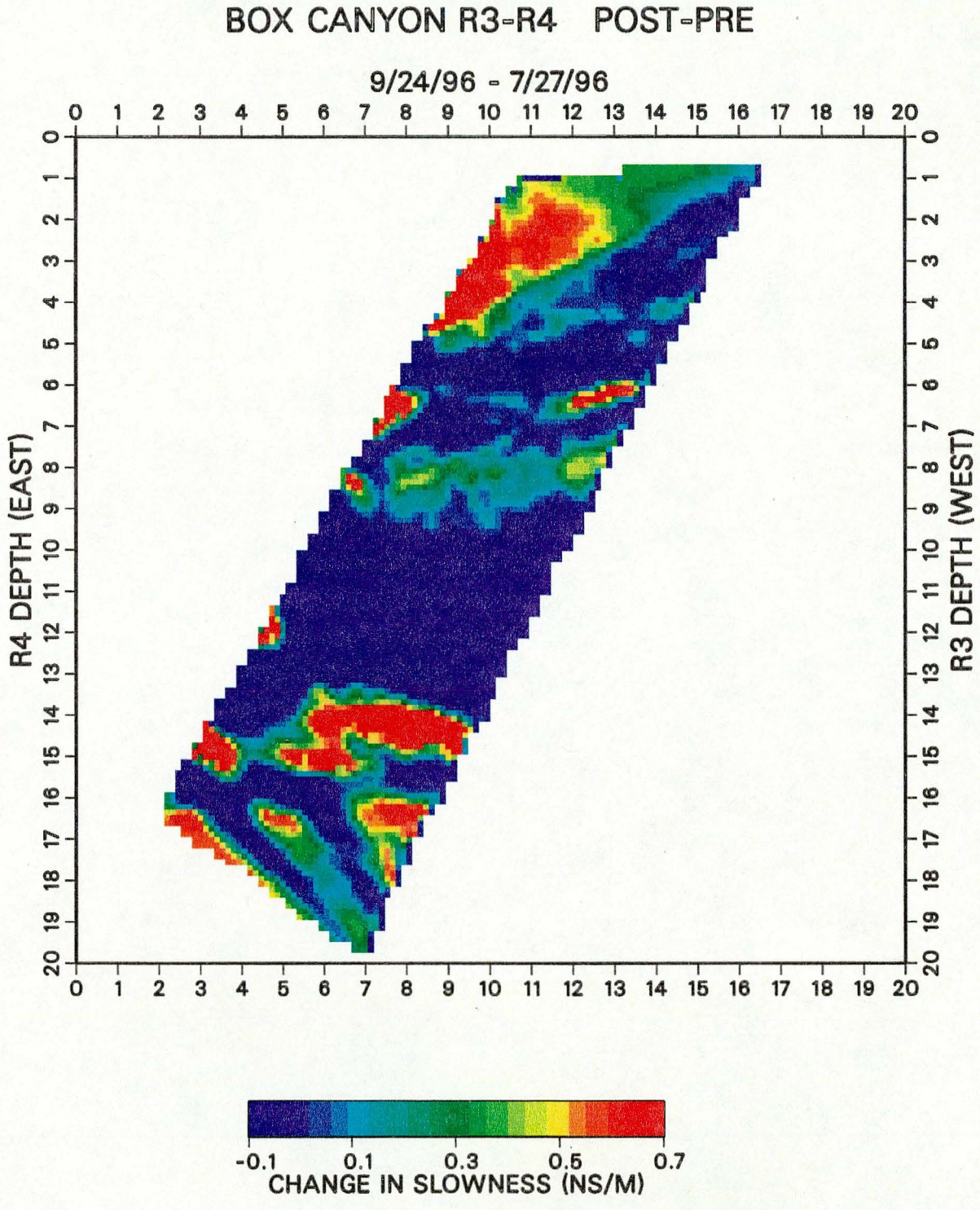

Figure 17b. Slowness difference tomogram determined by inverting the differences in the POST minus PRE travel times. Note that an increase in slowness corresponds to a decrease in velocity.

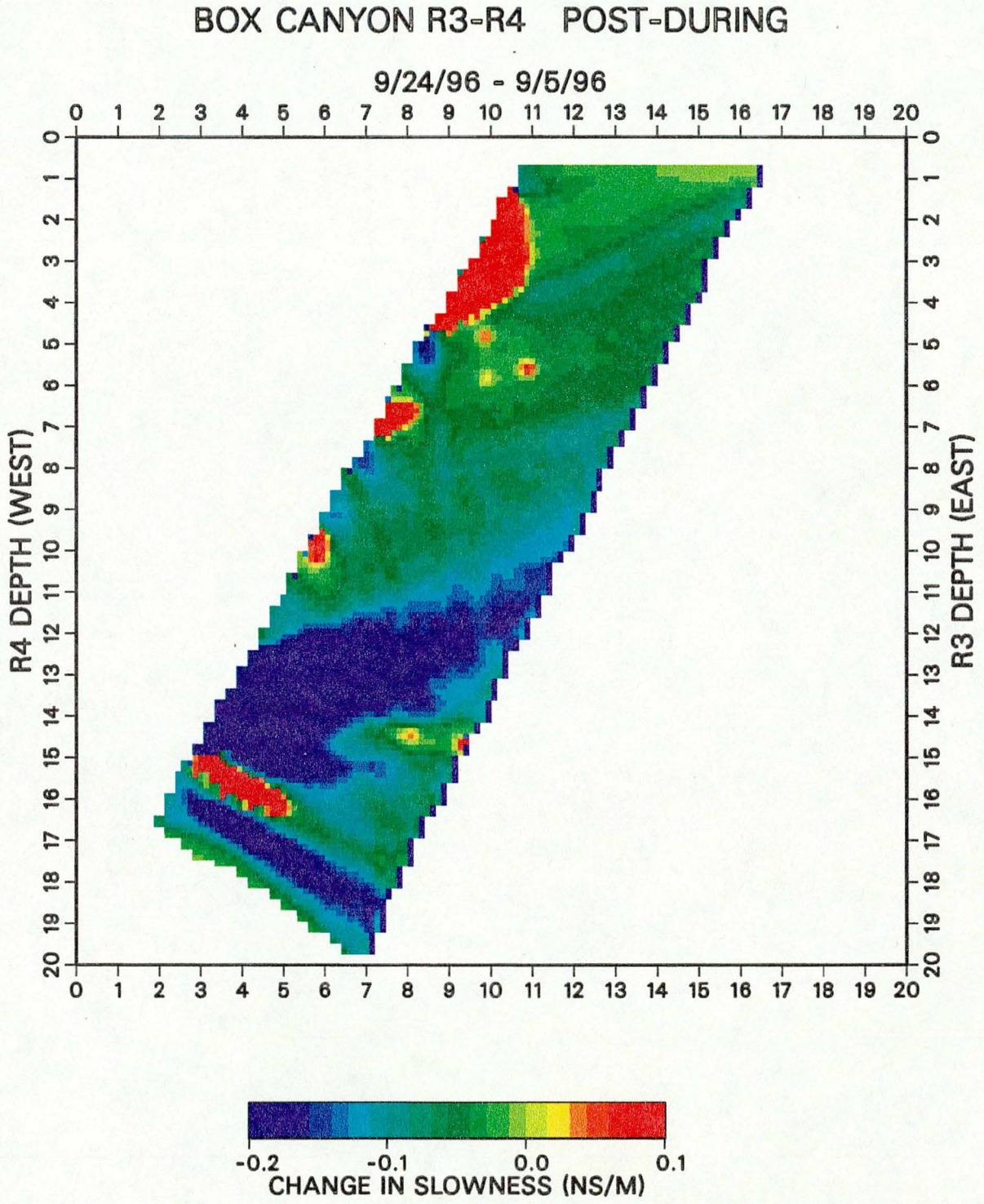

Figure 17c. Slowness difference tomogram determined by inverting the differences in the POST minus DURING travel times. Note that an increase in slowness corresponds to a decrease in velocity.

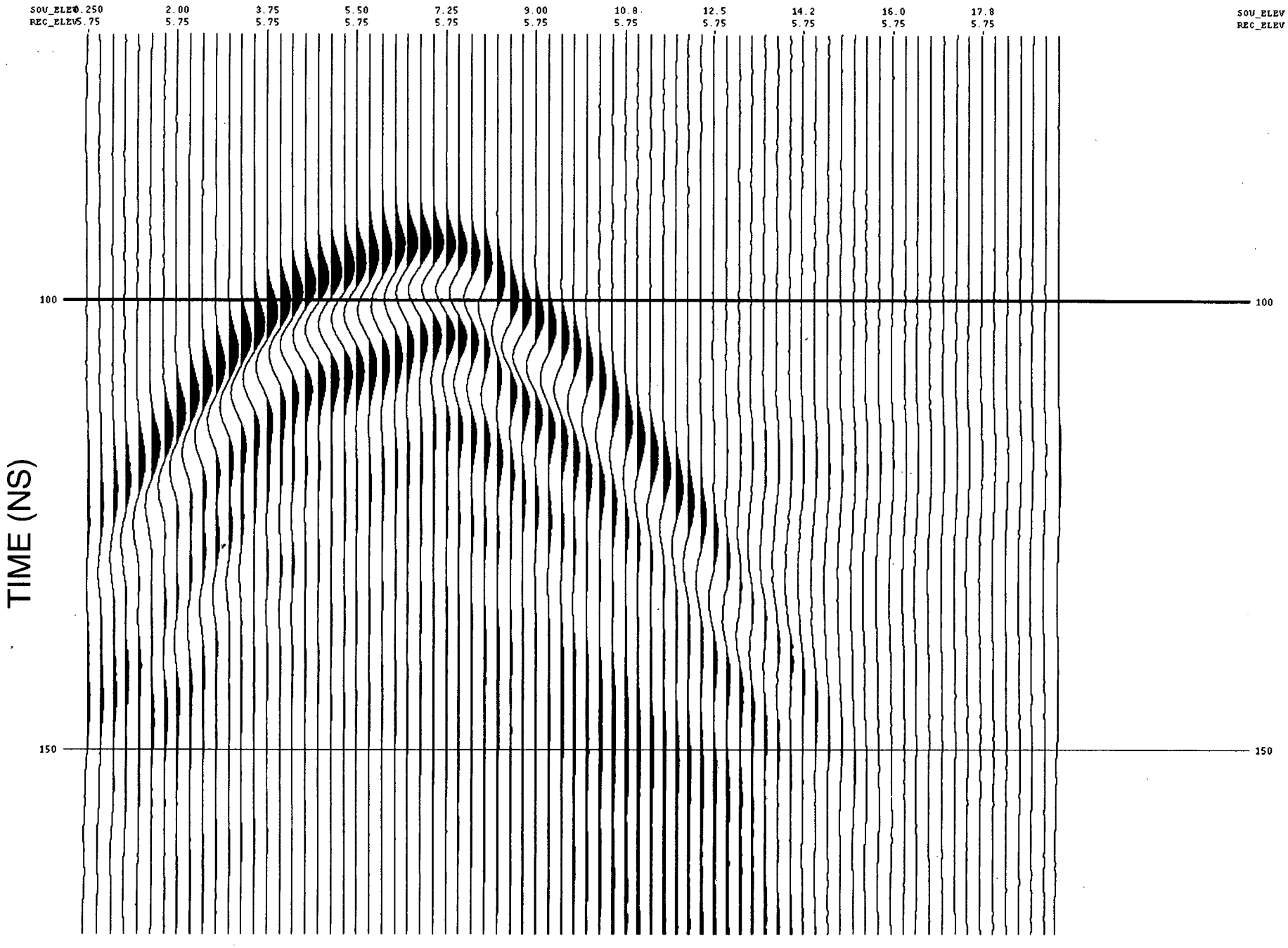

Figure 18. Typical receiver gather for R2-R4 with the receiver at 5.75 meters down R-4.

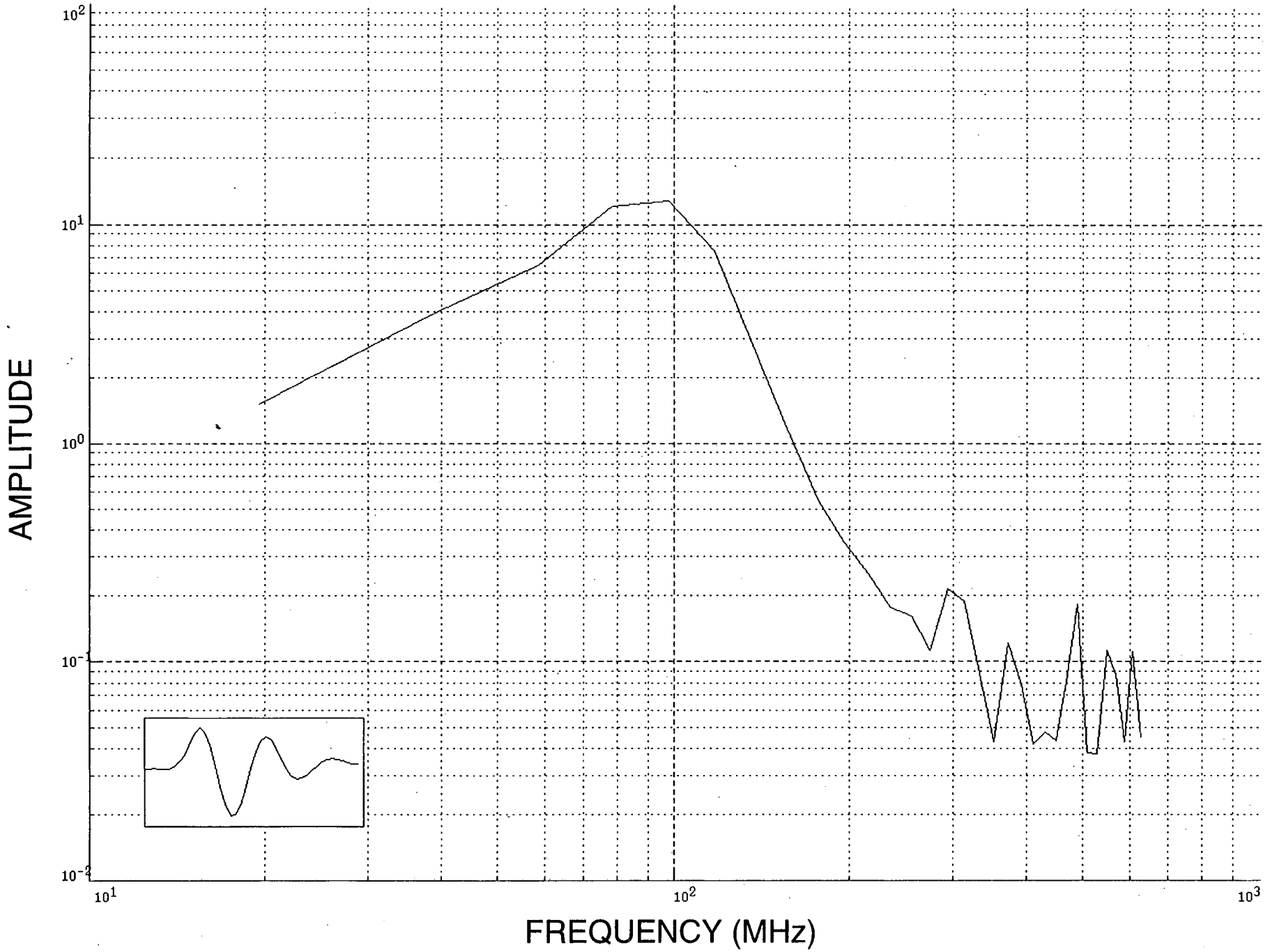

Figure 19. Spectra of a representative trace; receiver 5.75 meters down R-4 and the source 5.75 meters down R-2.

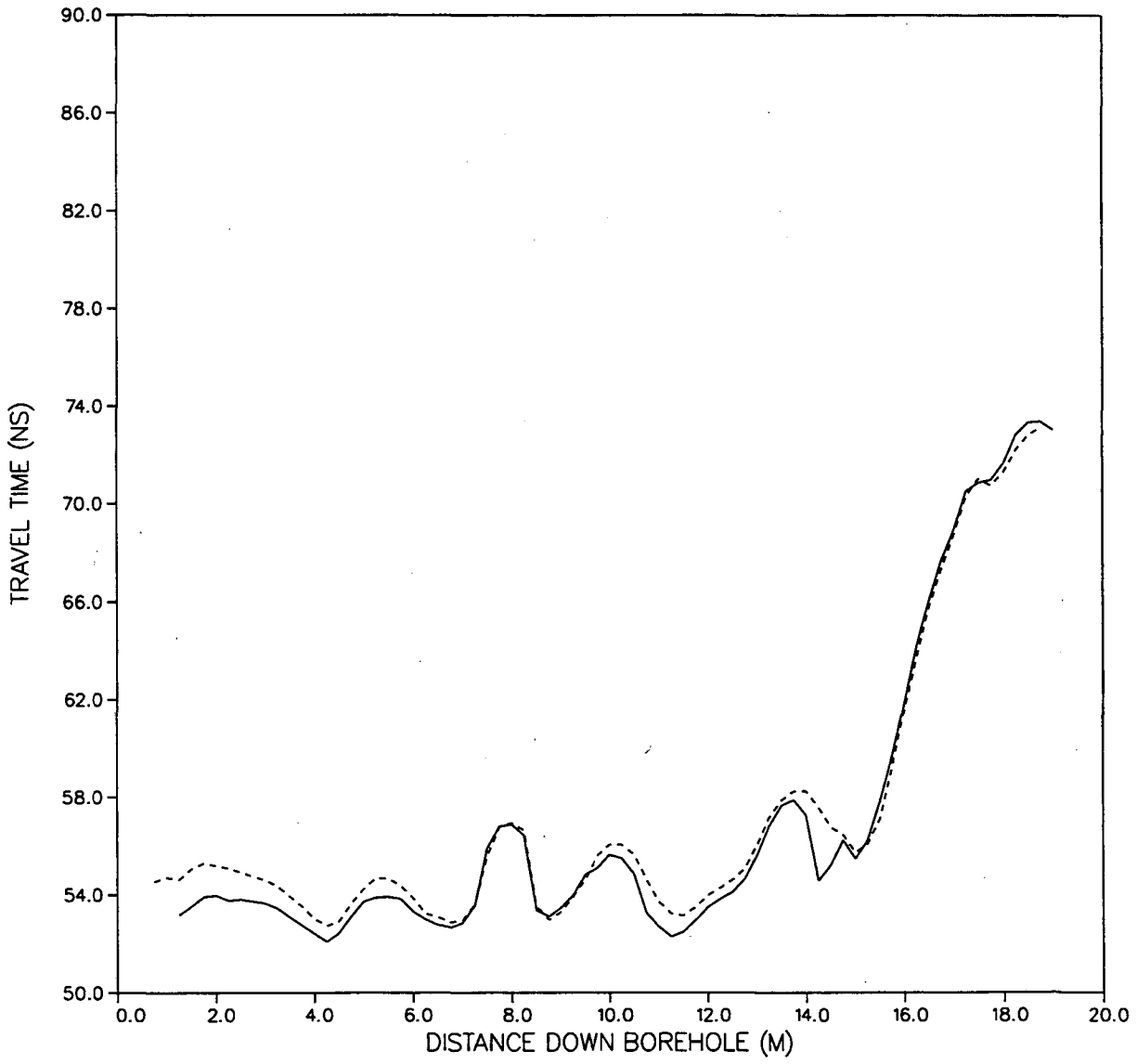

Figure 20a. Zero-offset travel times vs. distance down source/receiver wells for the PRE data set. The solid line is for the zero-offset MOP values; dashed is for ZOP values.

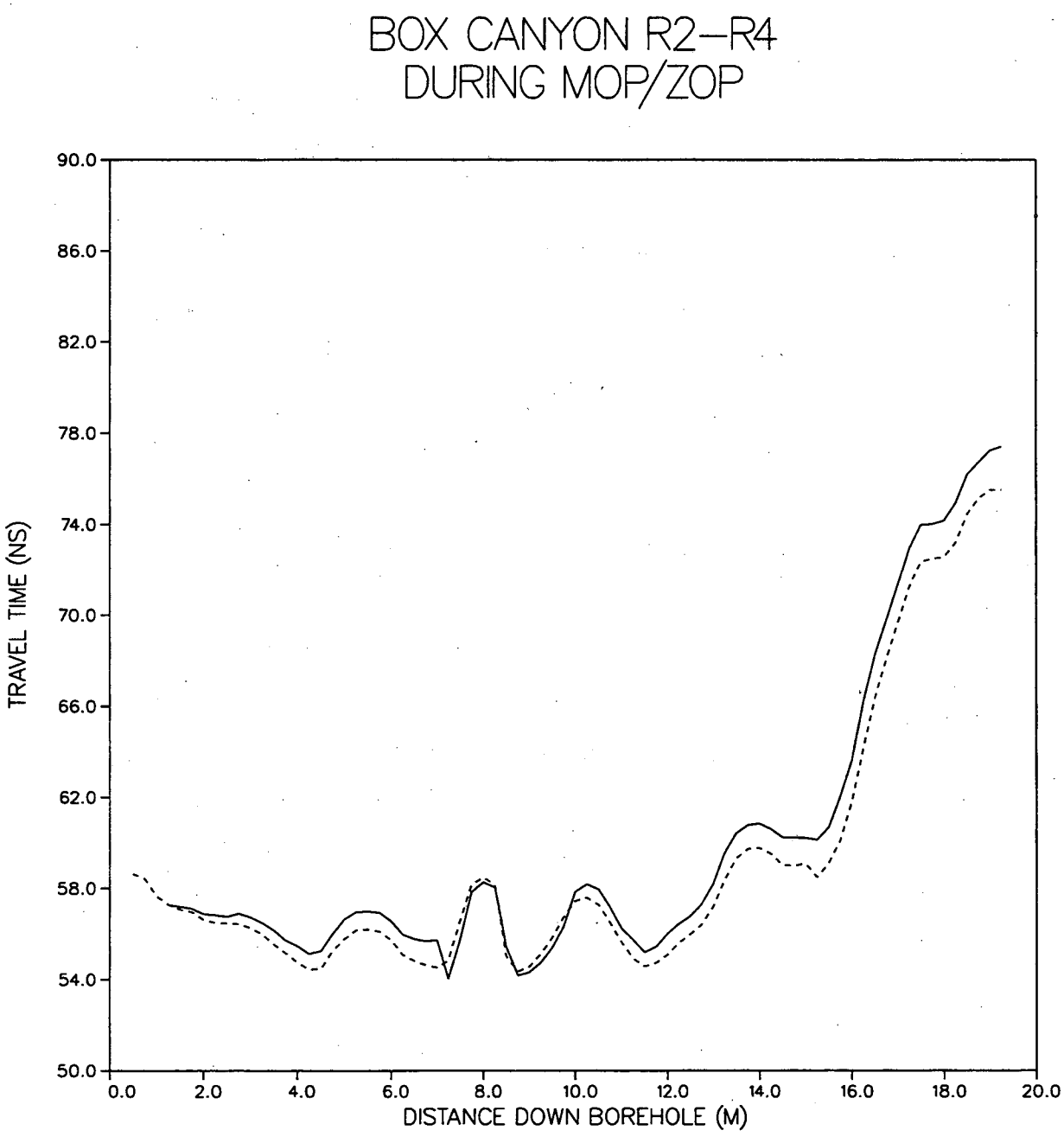

Figure 20b. Same as Figure 20b, but for the DURING data set values.

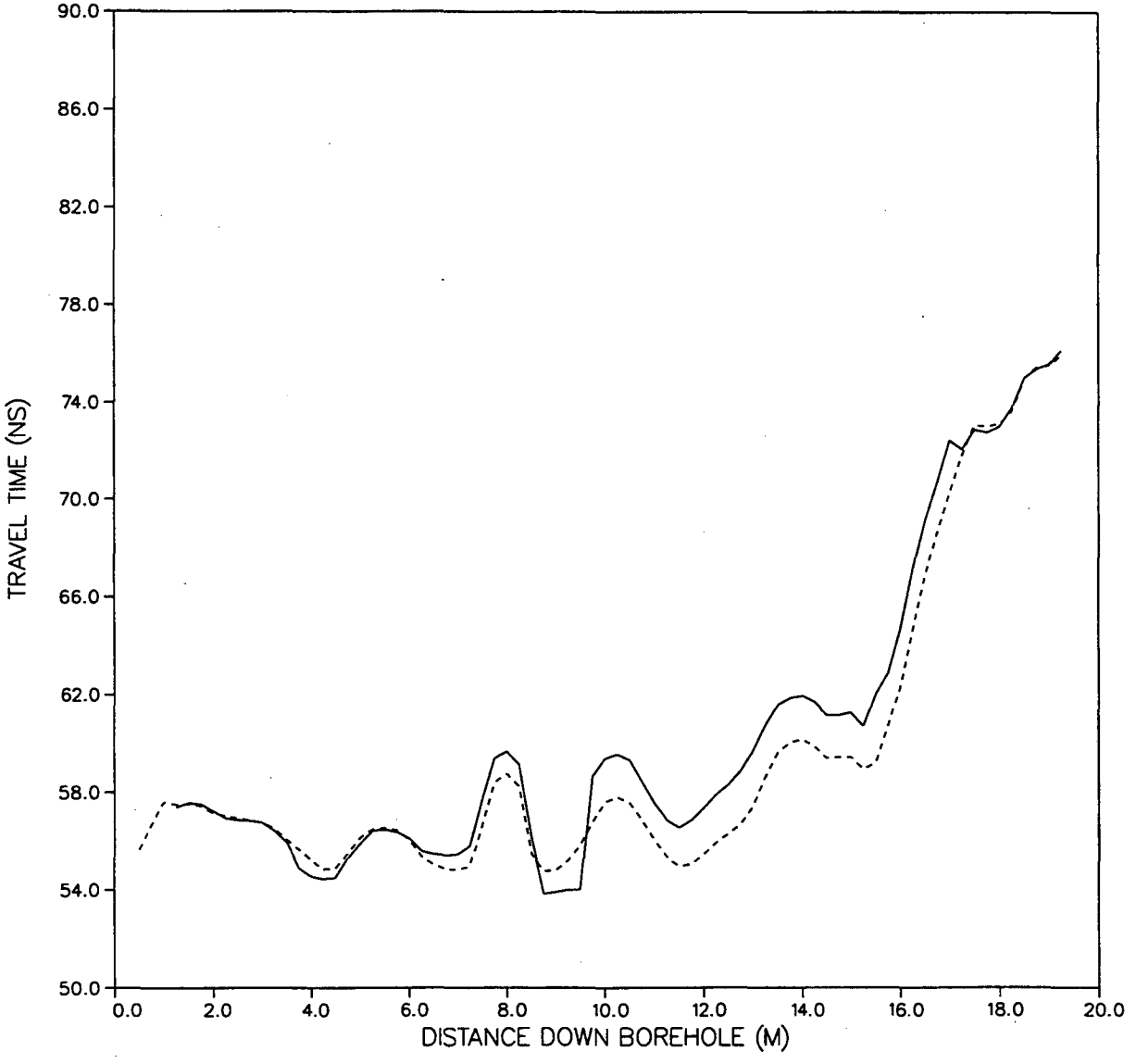

Figure 20c. Same as Figure 20c, but for the POST data set values.

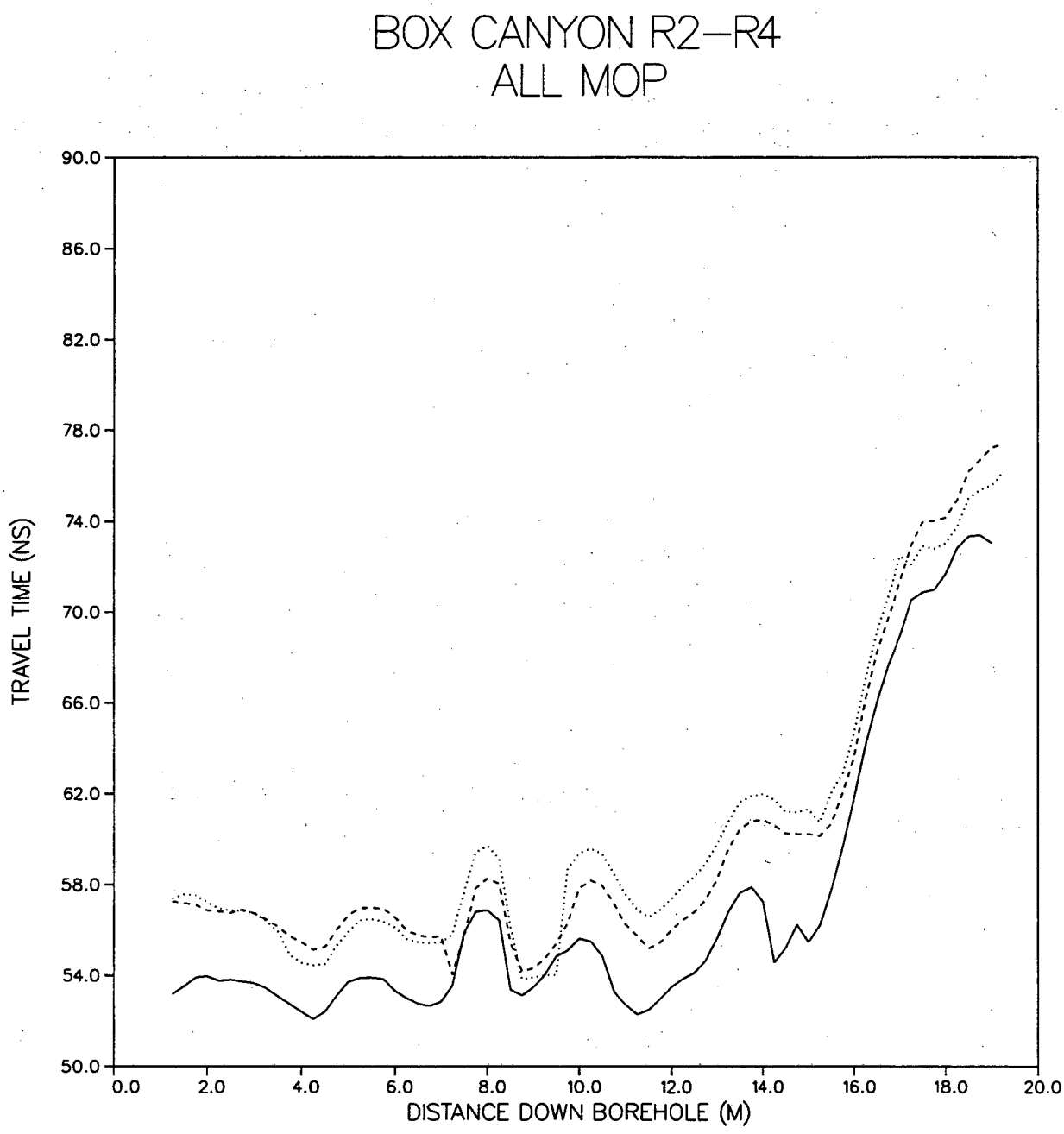

Figure 20d. Zero-offset travel time vs. distance down source/receiver wells for the zero-offset MOP values for the PRE (solid), DURING (dashed), and POST (dotted) data sets.

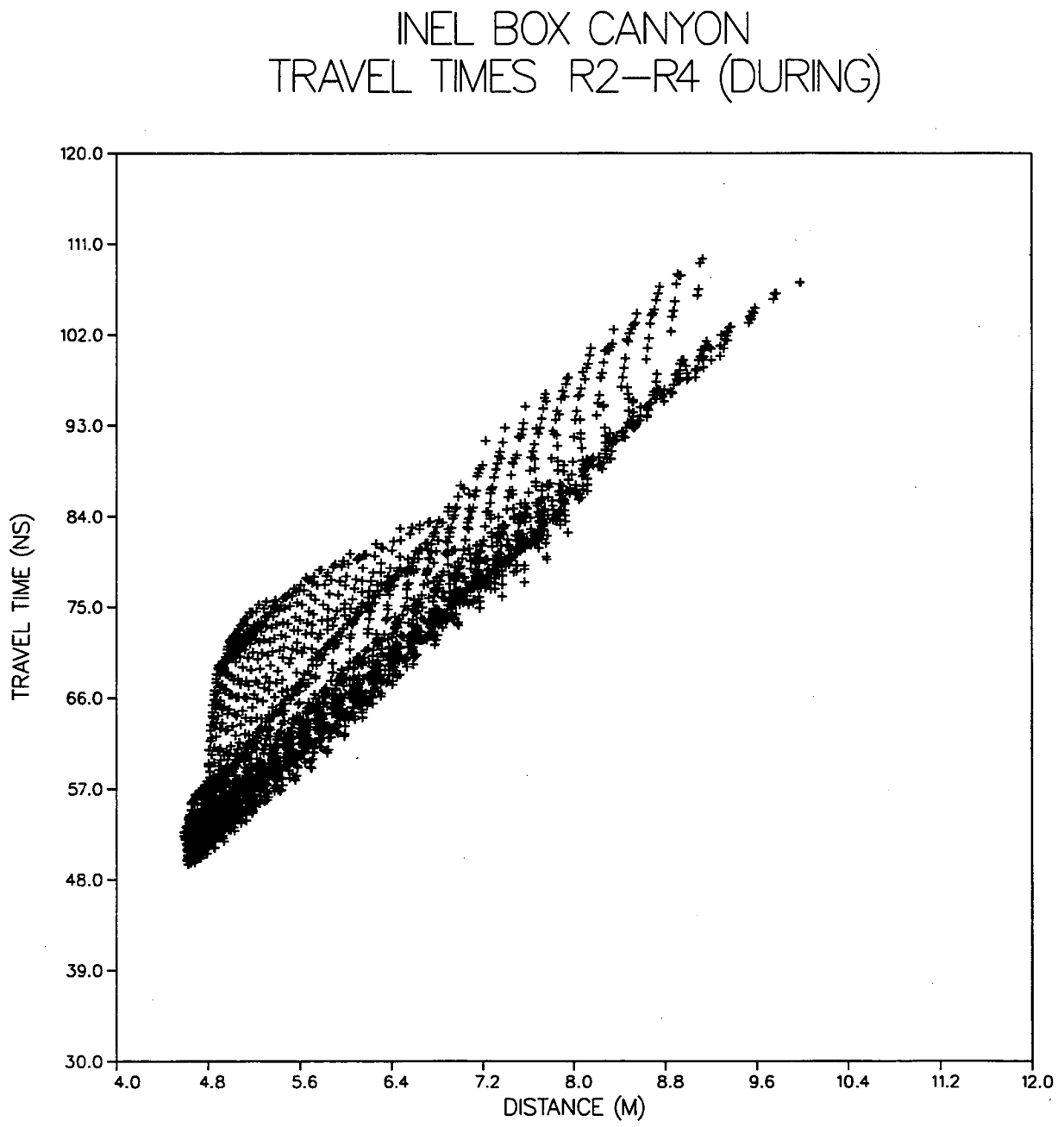

Figure 21a. Travel time vs. distance values for the DURING data set. The difference in travel time values between data sets is relatively small.

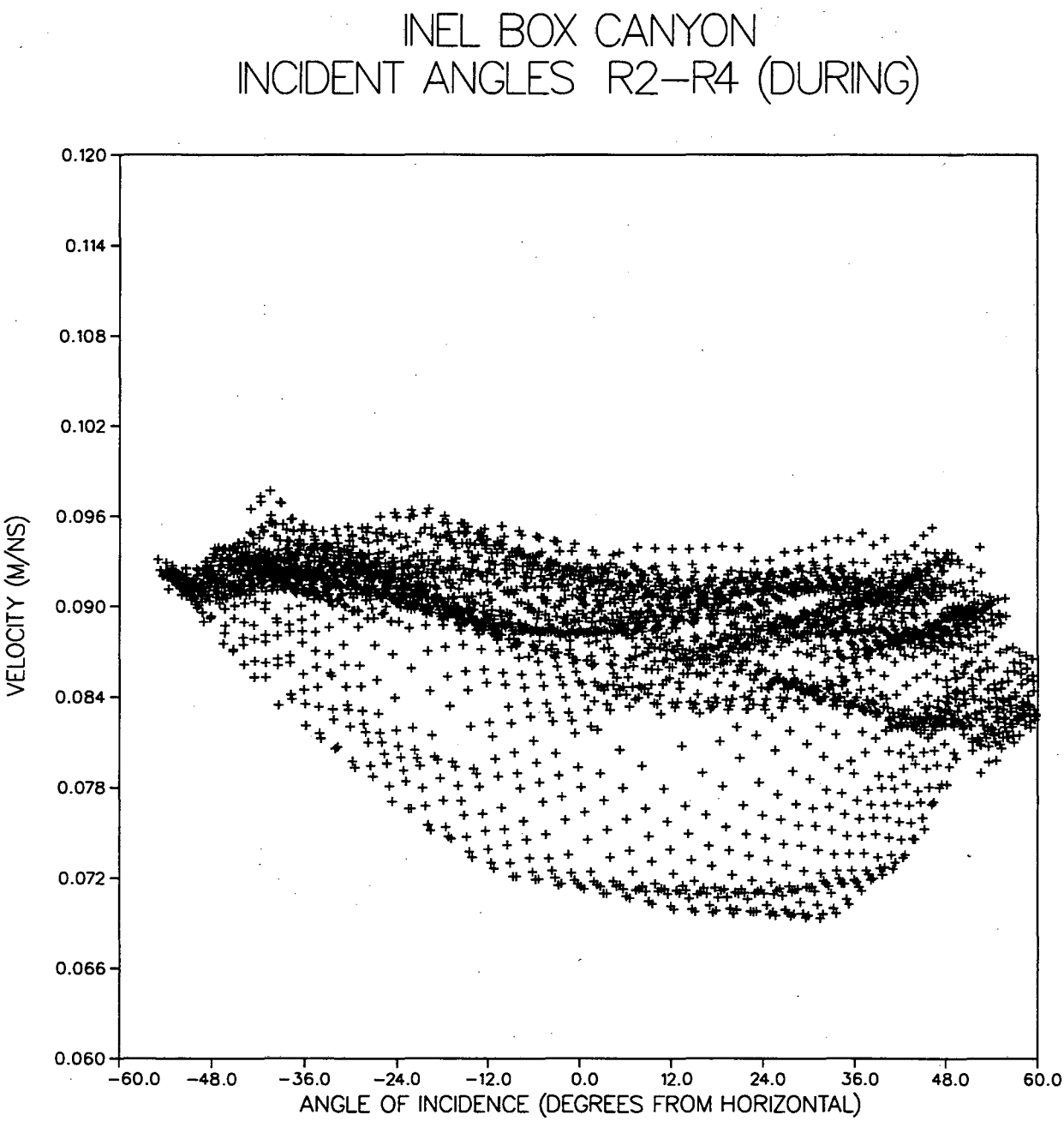

Figure 21b. Same as Figure 21a, but the velocity versus angle of incedent values are plotted.

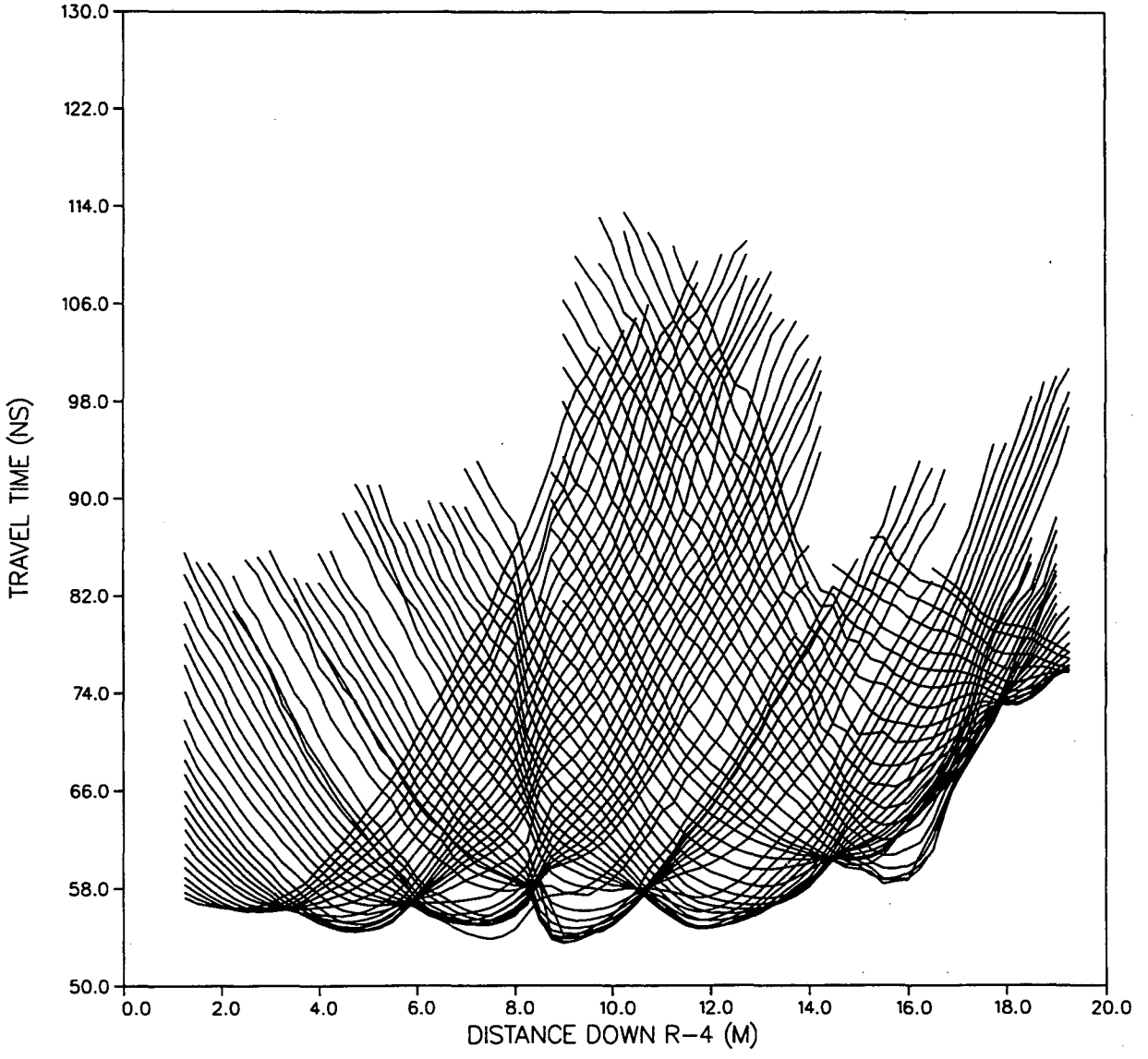

Figure 21c. Travel times for each receiver gather are shown by a single solid line. Values for the DURING data set.

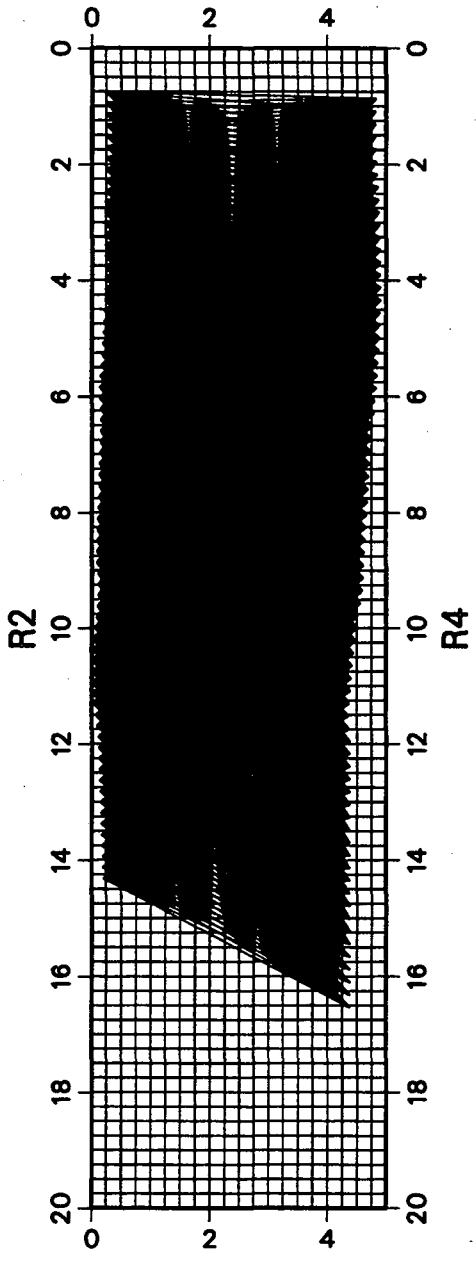

Figure 22. Ray coverage for the DURING travel times superimposed on the inversion grid.

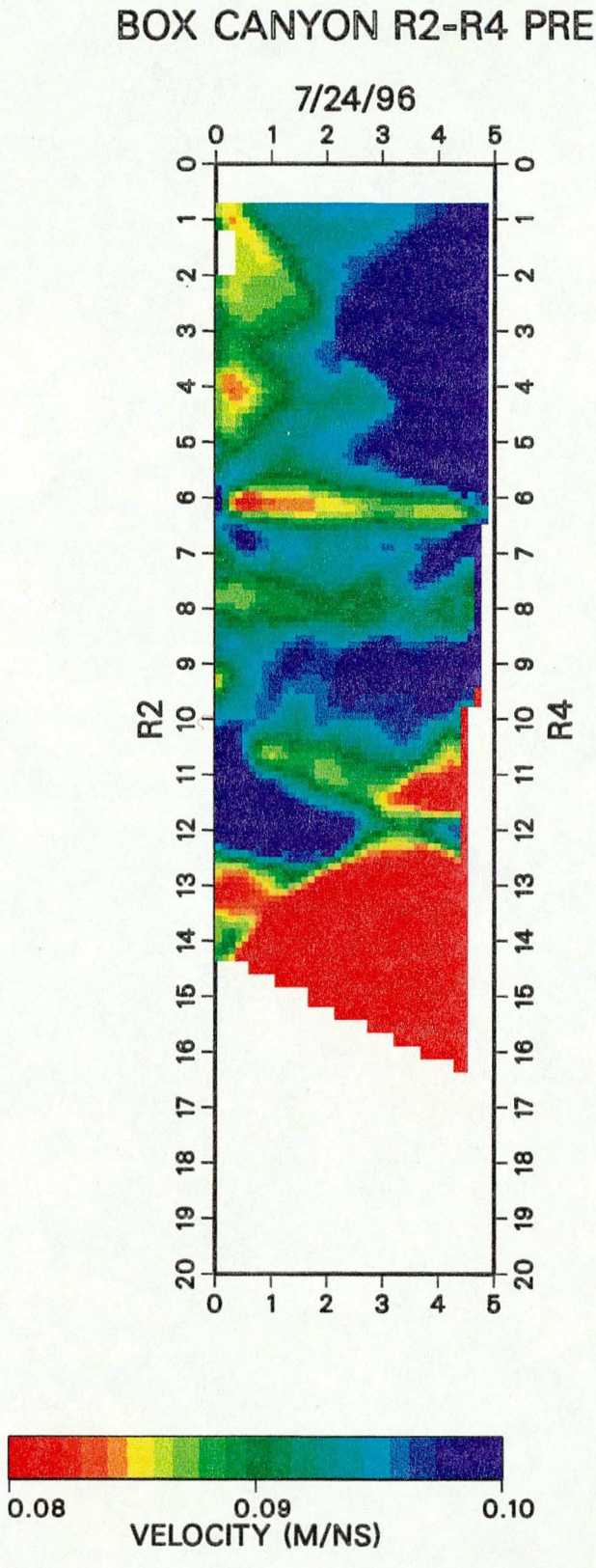

Figure 23a. Velocity tomogram inverted from the PRE R2-R4 travel times.

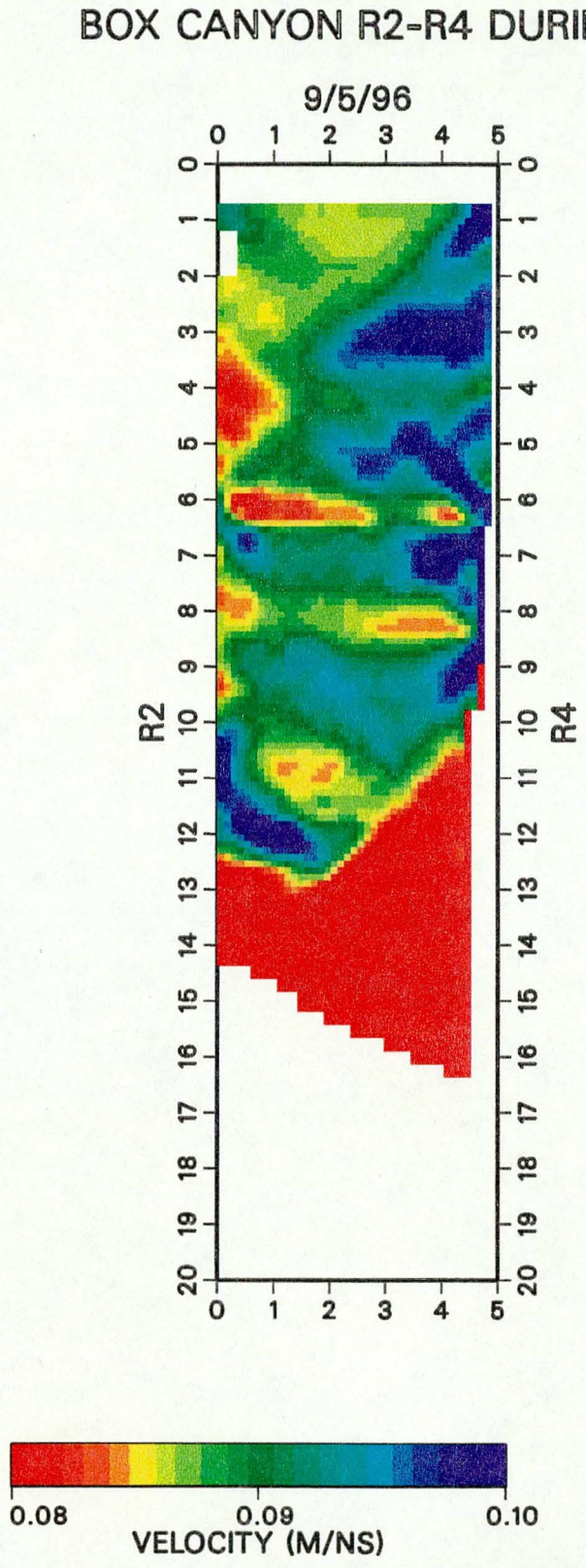

Figure 23b. Velocity tomogram inverted from the DURING R2-R4 travel times.

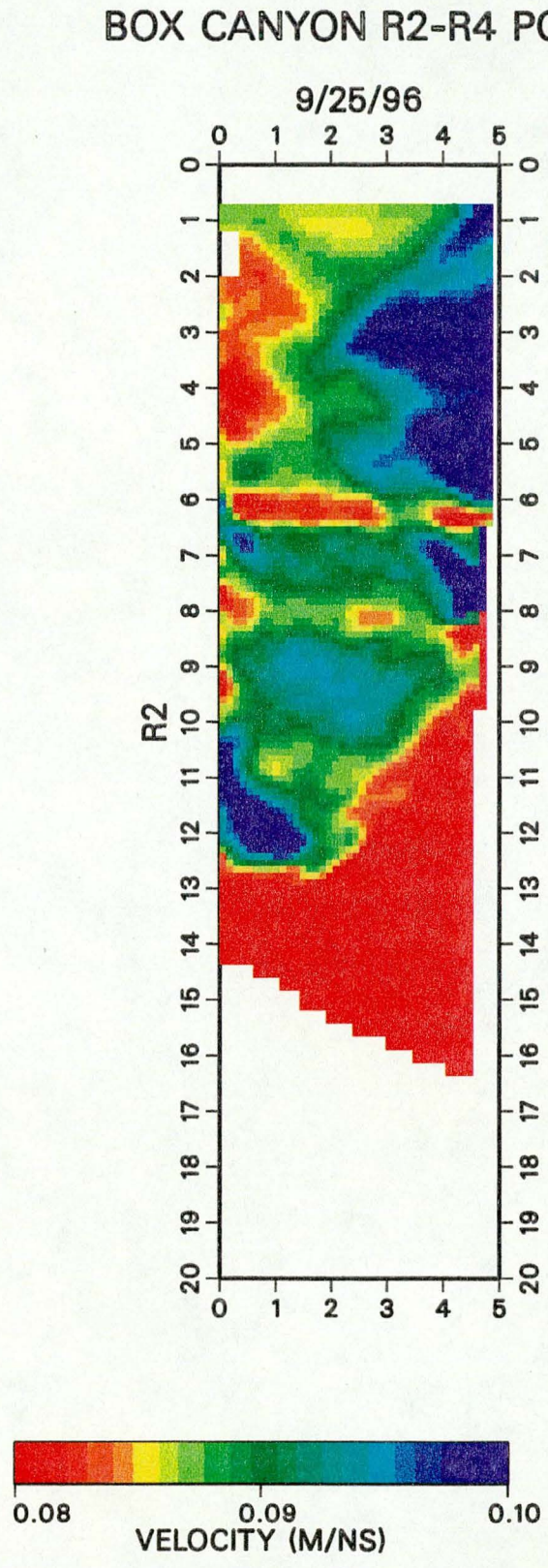

Figure 23c. Velocity tomogram inverted from the POST R2-R4 travel times.

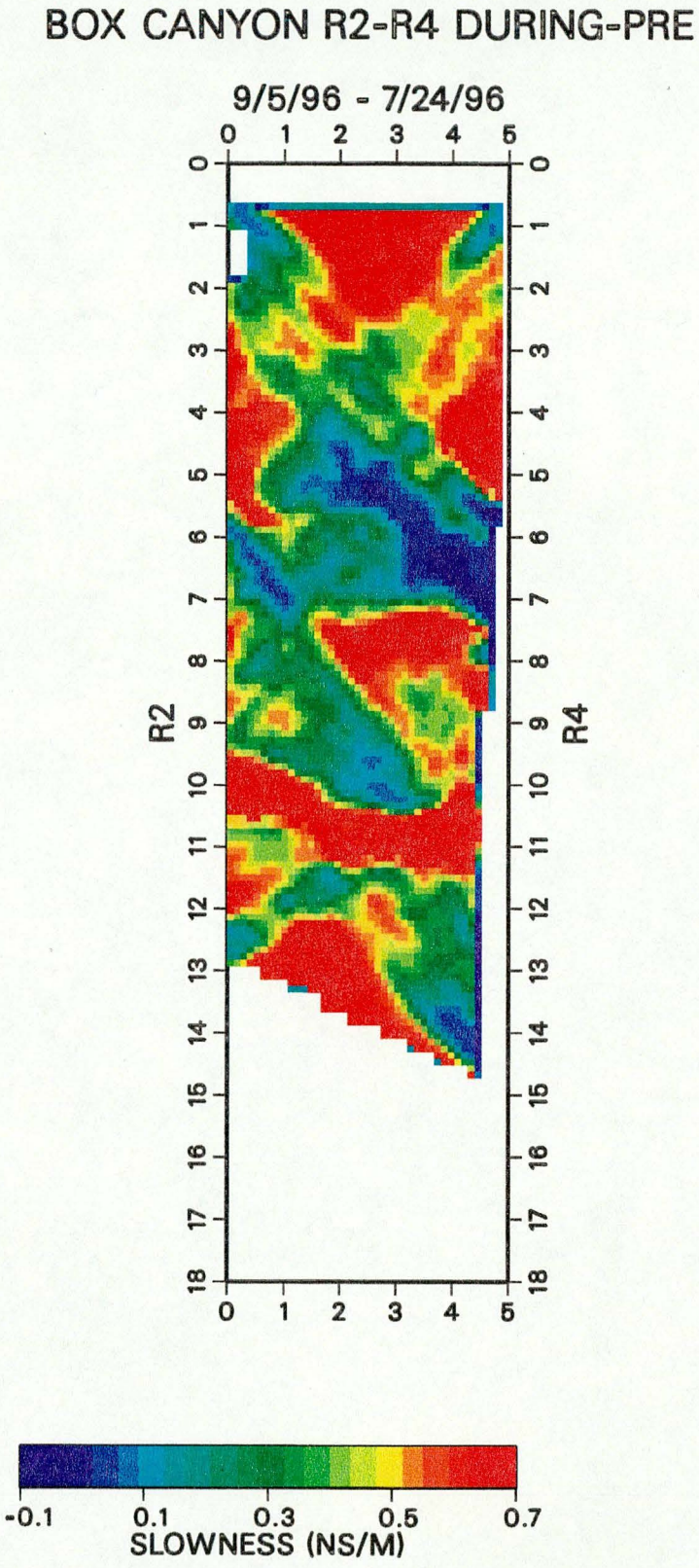

Figure 24a. Slowness difference tomogram determined by inverting the differences in the DURING minus PRE travel times. Note that an increase in slowness corresponds to a decrease in velocity.

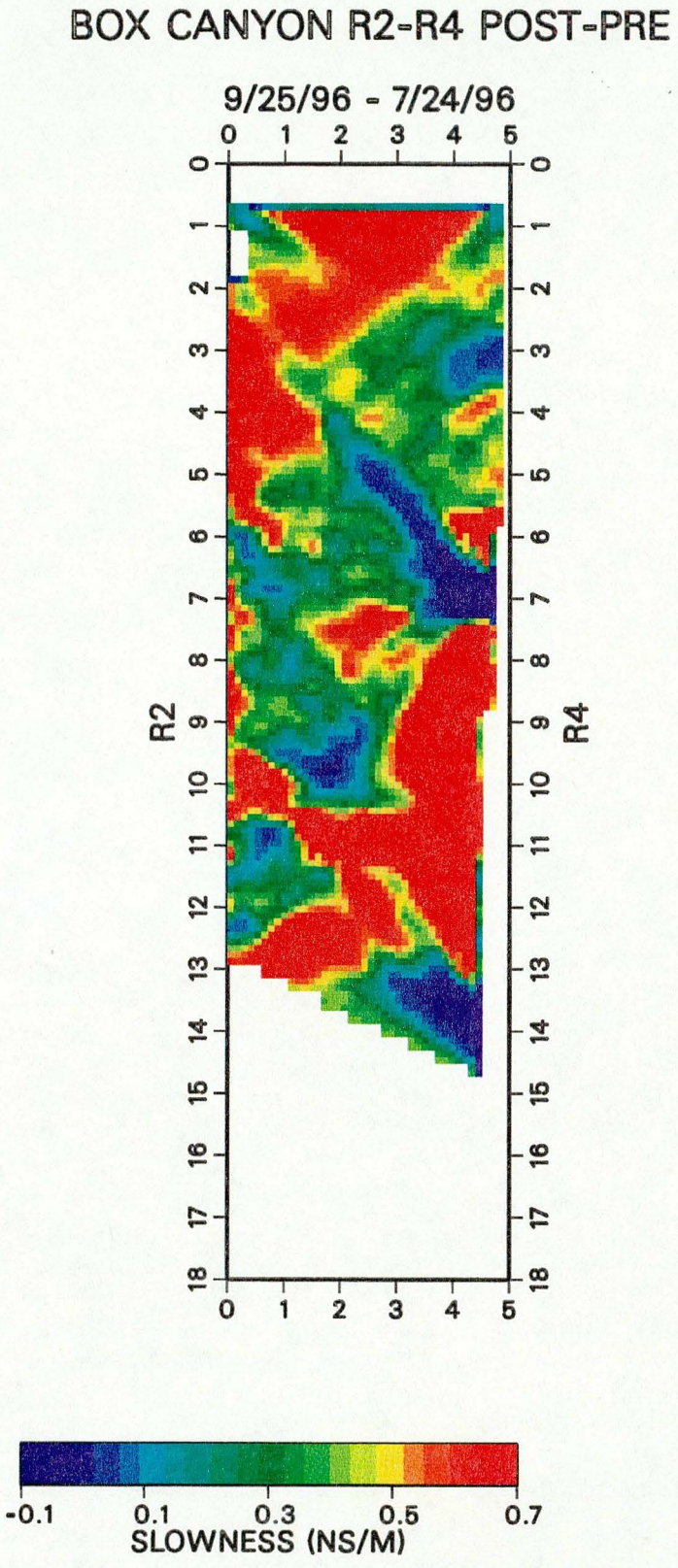

Figure 24b. Slowness difference tomogram determined by inverting the differences in the POST minus PRE travel times. Note that an increase in slowness corresponds to a decrease in velocity.

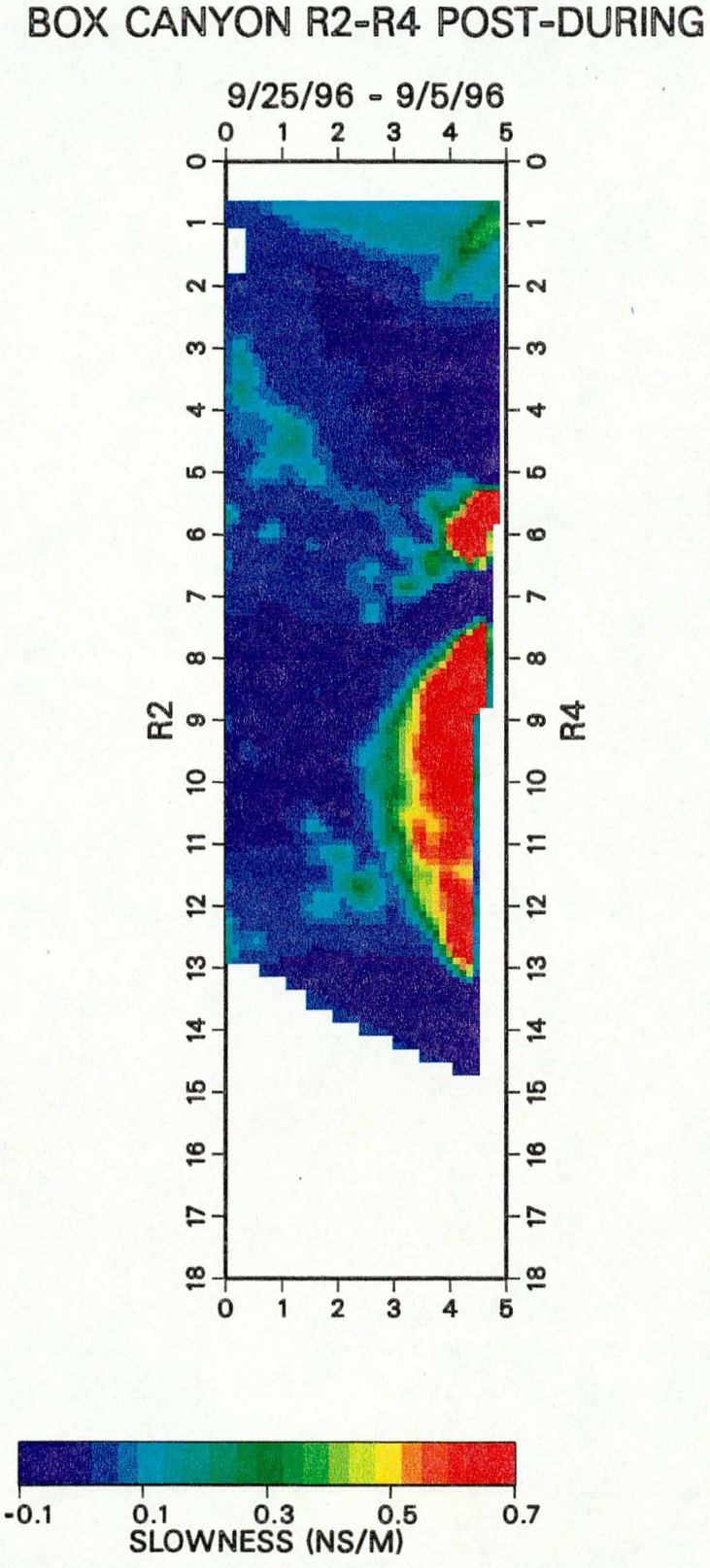

Figure 24c. Slowness difference tomogram determined by inverting the differences in the POST minus DURING travel times. Note that an increase in slowness corresponds to a decrease in velocity.

Ernest Orlando Lawrence Berkeley National Laboratory
One Cyclotron Road | Berkeley, California 94720

Prepared for the U.S. Department of Energy under Contract No. DE-AC03-76SF00098